



Synchrotron Radiation Techniques
for Catalysts and Functional Materials

October 23 - 27 / Novosibirsk

ABSTRACTS

ABSTRACTS

Federal Research Center Boreskov Institute of Catalysis
Synchrotron Radiation Facility SKIF
Budker Institute of Nuclear Physics of SB RAS
Novosibirsk State University

**II International Conference
Synchrotron Radiation Techniques
for Catalysts and Functional Materials**

October 23-27, 2023
Novosibirsk, Russia

УДК 544.47 + 621.384.6
ББК 24.54 + 22.383
S 98

S 98 **«Synchrotron Radiation Techniques for Catalysts and Functional Materials»**
II International Conference, Abstracts
(October 23-27, 2023, Novosibirsk, Russia)
[Electronic resource] / eds.: Prof. V.I. Bukhtiyarov, Prof. O.N. Martyanov,
Prof. Ya.V. Zubavichus
– Novosibirsk : Boreskov institute of Catalysis SB RAS, 2023.
– ISBN 978-5-906376-54-1
– URL: <http://conf.nsc.ru/SRTCFCM-2023/en>

В надзаг.:
Federal Research Center Boreskov Institute of Catalysis
Synchrotron Radiation Facility SKIF
Budker Institute of Nuclear Physics of SB RAS
Novosibirsk State University

Сборник включает тезисы пленарных, устных и стендовых докладов.
Основные темы научной программы конференции:
The collection includes abstracts of plenary lectures, oral and poster presentations.
The main topics of the Conference scientific program are:

- Theoretical and applied aspects of experimental techniques utilizing synchrotron radiation
- Structure-driven design of catalysts and functional materials based on synchrotron diagnostics
- Synchrotron radiation for structural biology
- Development of instrumentation for synchrotron beamlines
- New data processing algorithms, artificial intelligence and machine learning in bulk data analysis

УДК 544.47 + 621.384.6
ББК 24.54 + 22.383

ISBN 978-5-906376-54-1

© Boreskov Institute of Catalysis, 2023

CONFERENCE ORGANIZERS

- Boreskov Institute of Catalysis, Novosibirsk, Russia
- SRF SKIF, Novosibirsk, Russia
- Budker Institute of Nuclear Physics of SB RAS, Novosibirsk, Russia
- Novosibirsk State University, Novosibirsk, Russia



UNDER THE AUSPICES OF



Conference Chair

Valerii BUKHTIYAROV Borekov Institute of Catalysis, Novosibirsk, Russia

SCIENTIFIC COMMITTEE

Chair of the Scientific Committee

Oleg MARTYANOV Borekov Institute of Catalysis, Novosibirsk, Russia

Deputy Chair of the Scientific Committee

Yan ZUBAVICHUS SRF SKIF, Borekov Institute of Catalysis, Novosibirsk, Russia

Scientific Committee

Danil DYBTSEV Nikolaev Institute of Inorganic Chemistry, Novosibirsk, Russia

Dmitry ZHARKOV Institute of Chemical Biology and Fundamental Medicine,
Novosibirsk, Russia

Vasily KAICHEV Borekov Institute of Catalysis, Novosibirsk, Russia

Sergey TSYBULYA Borekov Institute of Catalysis, Novosibirsk, Russia

ORGANIZING COMMITTEE

Andrey BUKHTIYAROV SRF SKIF, Borekov Institute of Catalysis, Novosibirsk, Russia

Andrey SARAEV SRF SKIF, Borekov Institute of Catalysis, Novosibirsk, Russia

Mikhail PLATUNOV SRF SKIF, Borekov Institute of Catalysis, Novosibirsk, Russia

Kristina SHEFER SRF SKIF, Borekov Institute of Catalysis, Novosibirsk, Russia

Marina SHABANOVA Borekov Institute of Catalysis, Novosibirsk, Russia

Marina SUVOROVA Borekov Institute of Catalysis, Novosibirsk, Russia

Svetlana LOGUNOVA Borekov Institute of Catalysis, Novosibirsk, Russia

Daria ALMAEVA Borekov Institute of Catalysis, Novosibirsk, Russia

Plenary Lectures

PL-1 ÷ PL-10

Metal-Organic Frameworks: From Synthesis and Structure to Porous Materials for Separation of Hydrocarbons

Fedin V.P.

*Nikolaev Institute of Inorganic Chemistry SB RAS, Novosibirsk, Russia
cluster@niic.nsc.ru*

In the world's most developed economies, up to 15% of total energy consumption is spent on chemical separation and purification processes. The development of advanced materials for highly efficient and highly selective technologies for the separation of complex mixtures will replace traditional distillation processes and significantly reduce energy costs, including for large-scale production products during the processing of natural gas and oil. Micro- and mesoporous metal-organic frameworks (MOFs) are considered as new promising materials for the separation of hydrocarbons (Fig. 1) [1, 2].

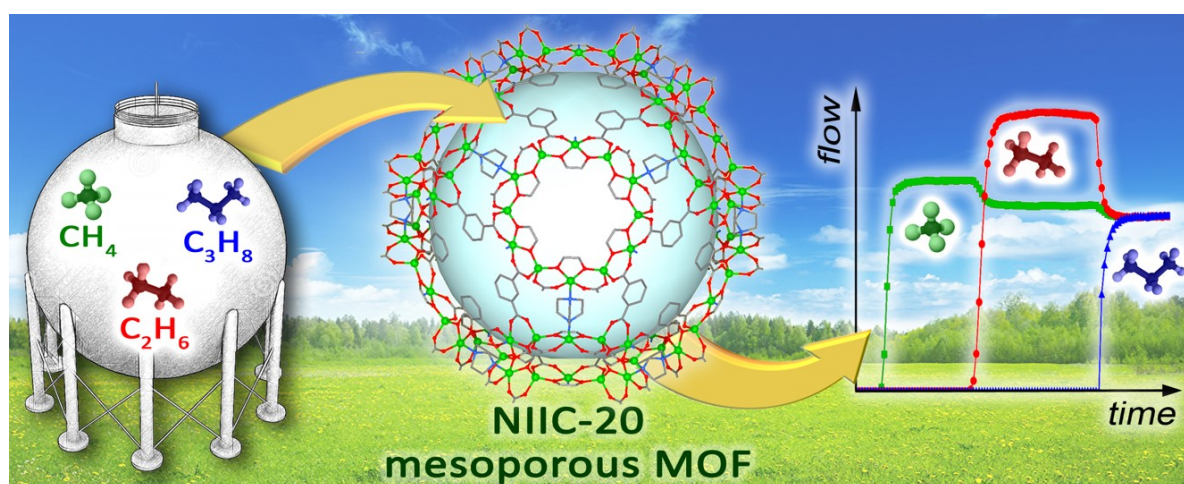


Fig. 1. Mesoporous MOFs as effective adsorbents for the separation of light alkanes

The MOFs under study have a complex structure, so synchrotron radiation is often necessary to perform a complete X-ray diffraction analysis. This makes it possible to fully characterize crystals of small sizes, with large unit cell parameters, often with complex disordering of the positions of ligands and guest molecules. However, complete structural information makes it possible to identify adsorption sites for guest molecules and explain the selectivity of adsorption of components of hydrocarbon mixtures.

The report will discuss our work [3-9] on obtaining new families of metal-organic frameworks NIIC-10, NIIC-20 and NIIC-30, determining their crystal structure and studying the sorption of a number of gases, the selective separation of C2 and C3 hydrocarbons, benzene and cyclohexane (Fig. 2), as well as isomeric xylenes.

The achievements of fundamental research and unsolved problems related to the use of MOFs in industrial separation processes will be critically reviewed.

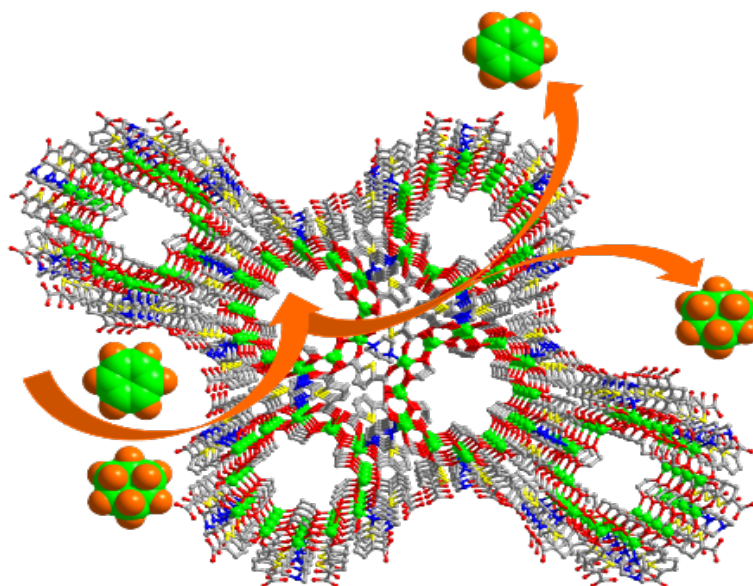


Fig. 2. Microporous MOFs as effective adsorbents for the separation of benzene and cyclohexane

Acknowledgement: The authors are grateful to the Ministry of Science and Higher Education of the Russian Federation for financial support (Agreement No. 075-15-2022-263), providing an access to the large-scale research facility “EXAFS spectroscopy beamline”. This work was partially supported by the Russian Science Foundation, grant 19-73-20087.

References:

- [1] M.A. Agafonov et al, J. Struct. Chem. 63 (2022) 671.
- [2] K.A. Kovalenko, A.S. Potapov, V.P. Fedin, Russ. Chem. Rev. 91 (2022) RCR 5026.
- [3] A.A. Lysova, D.G. Samsonenko, P.V. Dorovatovskii, V.A. Lazarenko, V.N. Khrustalev, K.A. Kovalenko, D.N. Dybtsev, V.P. Fedin, J. Am. Chem. Soc. 141 (2019) 17260.
- [4] A.A. Lysova, D.G. Samsonenko, K.A. Kovalenko, A.S. Nizovtsev, D.N. Dybtsev, V.P. Fedin, Angew. Chem. Int. Ed. 59 (2020) 20561.
- [5] A.A. Sapiyanik, K.A. Kovalenko, D.G. Samsonenko, M.O. Barsukova, D.N. Dybtsev, V.P. Fedin, Chem. Commun. 56 (2020) 8241.
- [6] M.O. Barsukova, K.A. Kovalenko, A.S. Nizovtsev, A.A. Sapiyanik, D.G. Samsonenko, D.N. Dybtsev, V.P. Fedin, Inorg. Chem. 60 (2021) 2996.
- [7] A.A. Sapiyanik, E.R. Dudko, K.A. Kovalenko, M.O. Barsukova, D.G. Samsonenko, D.N. Dybtsev, V.P. Fedin, ACS Applied Materials & Interfaces. 13 (2021) 14768.
- [8] A.A. Lysova, K.A. Kovalenko, D.N. Dybtsev, S.N. Klyamkin, E.A. Berdonosova, V.P. Fedin, Microporous and Mesoporous Materials 328 (2021) 111477.
- [9] A.A. Lysova, K.A. Kovalenko, A.S. Nizovtsev, D.N. Dybtsev, V.P. Fedin, Chem. Eng. J. 453 (2023) 139642.

PL-2

Kurchatov Synchrotron Radiation Source: Current Status, Research and Development Prospects

Svetogorov R.D.

National Research Centre "Kurchatov Institute", Moscow, Russia

rdsvetov@gmail.com

Kurchatov Synchrotron Radiation Source (KISI-Kurchatov) for now is the only specialized source of synchrotron radiation in the post-Soviet space and is the most popular "megascience" facility in Russia. Today, the research infrastructure of "KISI-Kurchatov" includes 14 experimental research beamlines in various fields, from fundamental studies in the fields of physics, chemistry, biology and the study of archeological and cultural heritage objects to applied research in the field of materials science and medicine.

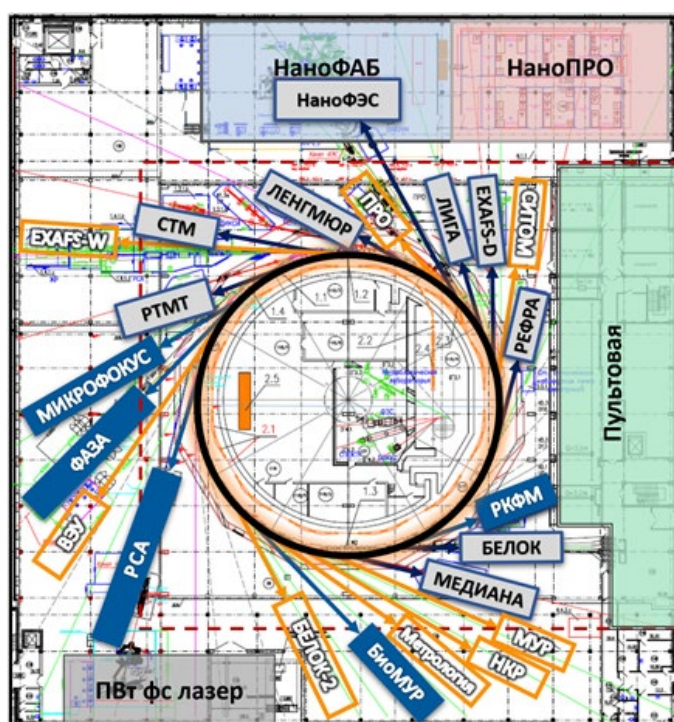


Рис. 1. Исследовательская инфраструктура КИСИ-Курчатов

One of the key activities of the KISI-Kurchatov is research in the field of materials science using complementary techniques available at existing unique scientific facilities. An important task is the structural study of a wide range of functional materials that are useful in many areas of science and industry, from structural chemistry to reactor materials science. Another important goal is the search for new functional materials, nanomaterials, nano-sized heterostructures and promising chemical compounds necessary for the development of modern high-tech industry. The unique capabilities of the experimental beamlines of the KISI-Kurchatov make such research extremely popular for external and internal scientific users.

Synchrotron research in the field of biology and medicine has become extremely popular due to the special functionality of modern experimental beamlines. The development of medical technologies and personalized medicine requires detailed knowledge of the functions

PL-2

of a variety of biological and biomimetic systems. Using techniques based on the interaction of synchrotron radiation with matter, it is possible to obtain qualitatively new information about the structure and state of the biological object under study, be it a protein, a virus, or a model of a cell membrane. This information can serve as a basis for understanding the properties of promising drugs, as well as the processes occurring in biological systems. The combination of unique experimental capabilities with breakthrough scientific tasks makes such research one of the most important and significant.

In total, in 2022, more than 140 research proposals from 44 scientific were completed at the KISI-Kurchatov experimental beamlines. It is important to note that for the third time in a row, KISI-Kurchatov became the most popular research facility in Russia during the Russian Science Foundation competition “Research conducted on the base of the existing world class research infrastructure”, winning the maximum possible 8 projects.

PL-3

**Digital Twin of the Siberian Ring Source of Photons - a Modern Tool
to Support the Life Cycle of a Mega-Science Facility and Manage Big
Scientific Data**

Marchenko M.

*The Institute of Computational Mathematics and Mathematical Geophysics
SB RAS, Novosibirsk, Russia*

Current Progress of the SRF «SKIF» Project

Bukhtiyarov A.V.¹, Zubavichus Y.V.¹, Levichev E.B.¹, Bukhtiyarov V.I.²

1 – Synchrotron Radiation Facility SKIF, Boreskov Institute of Catalysis, Kol'tsovo, Russia

2 – Boreskov Institute of Catalysis, Novosibirsk, Russia
avb@catalysis.ru

The SRF SKIF is a 4th generation synchrotron light source which is being created in the Science town Koltsovo near Novosibirsk. The accelerator complex of the SRF SKIF consists of an electron linear accelerator of 200 MeV, a full-energy synchrotron booster, and a storage ring. The 3-GeV storage ring with a circumference of 476 m and an ultralow theoretical horizontal emittance of 73.2 pm rad will produce synchrotron radiation (SR) beams with the maximum brightness in the photon energy range from 100 eV to 100 keV for 30 experimental beamlines. For a photon energy of ~1.5 keV, the source emittance approaches the diffraction limit, providing a high degree of spatial coherence thus expanding the research capabilities of the facility.

Currently there are six beamlines with different scientific scopes and aims being built in the first phase. The first-phase beamlines of SKIF are as follows: (1-1) "Microfocus," (1-2) "Structural Diagnostics," (1-3) "Fast Processes," (1-4) "XAFS Spectroscopy and Magnetic Dichroism," (1-5) "Hard X-ray Diagnostics and Imaging," and (1-6) "Electronic Structure". In total, the SRF SKIF may accommodate up to 30 beamlines; 14 of them will use the radiation of special insertion devices (wigglers and undulators) in straight sections, and 16 will be located at bending magnets.

The main functional task of the SRF SKIF will be infrastructural support of fundamental and applied research of scientific and educational institutions, as well as industrial companies, acting as users, in order to ensure leadership in the priority lines of scientific and technological development of the Russian Federation.

The SRF SKIF will allow one to perform world-leading studies in different fields of physics, chemistry, materials science, molecular biology, medicine, and other disciplines, with an emphasis placed on the most breakthroughs, economically and socially significant multidisciplinary tasks.

Magnetism as Seen with X-Rays

Platunov M.S.

*Synchrotron radiation facility SKIF, Boreskov Institute of Catalysis SB RAS, Kol'tsovo,
Russian Federation
m.s.platunov@srf-skif.ru*

An emergence of modern synchrotron radiation sources has boosted X-ray spectroscopy, as illustrated by the discovery of a variety of new experimental techniques associated with the exploitation of the polarisation properties of x-rays. It especially concerns x-ray magnetic circular dichroism (XMCD) that is now a workhorse technique in modern magnetism research, leading to a deeper understanding of the microscopic origin of the magnetic state of matter with element and orbital specificity [1]. In this talk, examples of the applications of XMCD to magnetism research with few examples will be given: molecular magnets; ferromagnetic semiconductors; heavy fermion systems, etc. Moreover, the recently discovered x-ray magnetochiral dichroism (XM χ D) [2] which is observable in magnetoelectric systems or chiral molecular magnets, will be described.

Acknowledgement: This work was supported by the Ministry of Science and Higher Education of the Russian Federation within the budget project of SRF SKIF, Boreskov Institute of Catalysis.

References:

- [1] A. Rogalev, F. Wilhelm, *The Physics of Metals and Metallography* 116 (2015) 1285–1336.
- [2] D. Mitcov, M. Platunov, et al. *Chemical science* 11(31) (2020) 8306-8311.

Art in Chemistry: Cage-Like Metallasilsesquioxanes

Khrustalev V.N.

Peoples Friendship University of Russia (RUDN University), Moscow, Russia
khrustalev-vn@rudn.ru

The development of modern science-driven technologies and, first of all, nanotechnologies is based on the study of chemical compounds capable of forming molecular structures of various compositions and diverse structural architecture. Just these compounds potentially contain the possibility of realizing various physical effects aimed at creating materials for various areas of information technologies as well as for use in various catalytic processes. The above-mentioned requirements are fully consistent with the class of organoelement compounds – cage-like metallasilsesquioxanes, which are discussed in the presented report. The lecture is focused on (a) the main methods for the synthesis of these compounds, (b) the regularities that determine the intricate architecture of cage-like metallasilsesquioxanes, (c) modern concepts describing the formation of their structure and (d) the principles of controlling this process.

It is important to note that cage-like metallasilsesquioxanes are aesthetically quite attractive (for example, see Fig. 1): the kaleidoscopic variety of framework structures is complemented by the color-grade of the compounds painted in the bright colors of the inorganic metal ions. The synthesis of such compounds, the study of their structure as well as acquaintance with new results obtained in this field of chemistry are very exciting.

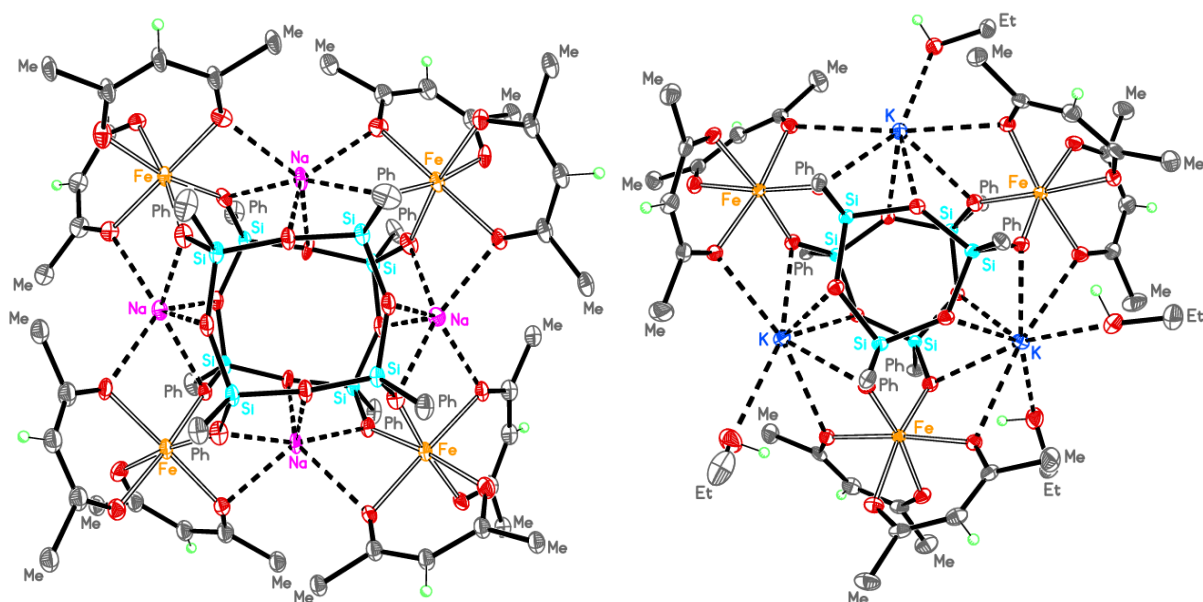


Fig. 1. Fe^{III} -based phenylsilsesquioxane/acetylacetonate complexes: $(Ph_4Si_4O_8)_2Fe_4Na_4(acac)_8$ (left) and $(Ph_3Si_3O_6)_2Fe_3K_3(acac)_6(EtOH)_4$ (right).

Coherent X-Ray Optics and Microscopy for Advanced Material Research Applications

Snigirev A.

Immanuel Kant Baltic Federal University, Kaliningrad, Russia

With the appearance of new Megascience facilities - fourth-generation X-ray sources (synchrotrons and free-electron lasers) materials research will strongly benefit from the increased spectral brightness, small source size, and divergence. New ultimate parameters of the beam provided by the diffraction-limited sources – new synchrotrons with reduced horizontal emittance will open up unique opportunities to build up a new concept of X-ray diagnostics including diffraction, spectroscopy and microscopy techniques based on the beam transport and conditioning systems using in-line refractive optics [1]. The refractive optics can provide various beam conditioning functions in the energy range from 3 to 200 keV: condensers, micro-radian collimators, low-band pass filters, high harmonics rejecters [2], and beam-shaping elements [3-4]. The implementation of the lens-based beam transport concept will significantly simplify the layout of new beamlines, easily expanding their microscopy capabilities in different fields including biomedical science [5-6] and material research under extreme conditions [7-10].

The versatile beam conditioning properties of refractive optics enable to development and implementation of novel X-ray coherence-related techniques including Fourier optics [11-13] and interferometry [14-18]. Further development of phase contrast bright [19-24] and dark field microscopy [25] will benefit by recently proposed light and ultra-compact objectives based on polymer and diamond microlenses made by 3D printing [26-27] and FIB technology [28].

All mentioned achievements and applications based on refractive optics are becoming especially relevant for the new SKIF synchrotron in Novosibirsk.

References:

- [1] A. Snigirev, V. Kohn, I. Snigireva, B. Lengeler, *Nature*, **384**, 49, 1996.
- [2] M. Polikarpov, I. Snigireva, A. Snigirev, *J. Synchrotron Rad.*, **21**, 484, 2014.
- [3] D. Zverev, A. Barannikov, I. Snigireva, A. Snigirev, *Opt. Express*, **25**, 28469, 2017.
- [4] D. Zverev, et al., *Optics Express*, **29**, 35038, 2021.
- [5] M. W. Bowler, D. Nurizzo, R. Barrett, et al., *J. Synchrotron Rad.*, **22**, 1540, 2015.
- [6] M. Polikarpov, et al., *Microsc. Microanal.* **24** (Suppl. 2), 384, 2018.
- [7] N. Dubrovinskaia , L. Dubrovinsky, N. Solopova, et al., *Sci. Adv.*, **2**, e1600341, 2016.
- [8] F. Wilhelm, G. Garbarino, J. Jacobs, et al., *High Pressure Research*, **36**, 445, 2016.
- [9] A. Snigirev et al., *Microsc. Microanal.* **24** (Suppl. 2), 236, 2018).
- [10] T. Fedotenko, et al., *Rev. Sci. Instrum*, **90**, 104501, 2019.
- [11] P. Ershov, S. Kuznetsov, I. Snigireva et al., *Appl. Cryst.*, **46**, 1475, 2013.
- [12] D. V. Byelov, J.-M. Meijer, I. Snigireva et al., *RSC Advances*, **3**, 2013)
- [13] A. Chumakov, et al., *J. Appl. Cryst.*, **52**, 1095, 2019.
- [14] A. Snigirev, I. Snigireva, M. Lyubomirskiy, et al., *Opt. express*, **22**, 25842, 2014.
- [15] M. Lyubomirskiy, I. Snigireva, A. Snigirev, *Optics express*, **24**, 13679, 2016.

PL-7

- [16] M. Lyubomirskiy, I. Snigireva, V. Kohn, et al, *J. Synchrotron Rad.*, **23**, 1104, 2016.
- [17] S. Lyatun, et al., *J. Synchrotron Rad.*, **26**, 1572, 2019.
- [18] O. Konovalov, et al., *J. Synchrotron Rad.*, **26**, 1572, 2019.
- [19] D. Zverev et al., *Microsc. Microanal.* **24** (Suppl. 2), 162, 2018.
- [20] D. Zverev, et al., *Optics Express*, **28** (15), 21856, 2020.
- [21] K. V. Falch, C. Detlefs, M. Di Michiel et al., *Appl. Phys. Lett.*, **109**, 054103, 2016.
- [22] K. V. Falch, D. Casari, M. Di Michiel et al., *J. Mater. Sci.*, **52**, 3437, 2017.
- [23] K. V. Falch, M. Lyubomirskiy, D. Casari, et al., *Ultramicroscopy*, **184**, 267, 2018.
- [24] I. Snigireva et al., *Microsc. Microanal.* **24** (Suppl. 2), 552, 2018.
- [25] H. Simons, A. King, W. Ludwig et al., *Nature Communications*, **6**, 6098, 2015.
- [26] A. K. Petrov, V. O. Bessonov, K. A. Abrashitova et al., *Optics Express*, **25**, 14173, 2017.
- [27] A. Barannikov, et al., *J. Synchrotron Rad.*, **26** (2019) 714.
- [28] P. Medvedskaya, et al., *Optics Express*, **28** (04), 4773, 2020

PL-8

**Synchrotron Radiation Station "Diagnostics in the High-Energy X-Ray Range"
Present and Future**

Kuper K.

SRF SKIF, Koltsovo, Russia

Structural Biology in the Study of Enzyme Catalysis: An Example of DNA Glycosylases

Zharkov D.O.^{1,2}

1 – Novosibirsk State University, Novosibirsk, Russia

2 – SB RAS Institute of Chemical Biology and Fundamental Medicine, Novosibirsk, Russia
dzharkov@niboch.nsc.ru

About 100,000 nucleotides in DNA in each cell of the human body are damaged daily by a variety of endogenous and environmental factors. To prevent mutations and cell death, several enzymatic DNA repair systems had evolved. The most common types of DNA lesions, such as products of oxidation, deamination, and alkylation, are removed by base excision repair. This process is initiated by DNA glycosylases, the enzymes that hydrolyze the *N*-glycosidic bond of the damaged deoxyribonucleotide. All living species have several DNA glycosylases with different substrate specificities; e. g., eleven DNA glycosylases are currently known from human cells, and nine, in *Escherichia coli*. Based on their sequences and three-dimensional structures, DNA glycosylases can be divided into several unrelated superfamilies. However, some DNA glycosylases belonging to different superfamilies can have identical substrate specificities. The question of how DNA glycosylases discriminate between substrate and nonsubstrate nucleobases has not yet been resolved. The structures of many DNA glycosylases and their complexes with DNA has been determined by X-ray crystallography and NMR spectroscopy. A number of modified nucleotides has been synthesized, allowing one to analyze the features of damaged base recognition. Modern approaches to studying the mechanisms of damage recognition by DNA glycosylases are based on a combination of complementary structural, computational and biochemical methods, making it possible to establish the principles of selection of damaged nucleobases among a large excess of normal ones, based on multiple conformational transitions during the recognition process.

Acknowledgement: The work was supported by the Strategic Academic Leadership Priority 2030 Program (NSU) and state assignment No. 12103130056-8 (SB RAS ICBFM).

PL-10

Structure Guided Assistance in Biological Tasks

Boyko K.M.

Research Center of Biotechnology RAS, Moscow, Russia

kmb@inbi.ras.ru

Nowadays, structural studies are a key part of modern biology. Over the last decade alone, the number of macromolecular structures (proteins and their complexes) has increased by more than 120 thousand, which is half of all structures in the PDB data bank. Moreover, the vast majority of these structures (more than 90%) were obtained using X-ray diffraction, which mostly uses synchrotron radiation and is today the major method for the structural study of macromolecules. Here I will demonstrate examples of the use of this method to solve both fundamental and applied biological problems, as well as an example of the use of integrative structural biology approach in case, where the application of the only one structural method is awkward.

Acknowledgements: This work was supported by the Russian Science Foundation (grants 23-74-30004 and 19-74-10099) as well as by the Ministry of Science and Higher education of the Russian Federation in the framework of the Agreement no. 075-15-2021-1354 (07.10.2021).

Oral Presentations

OP-1 ÷ OP-30

Combined Studies of Crystal Structure and Catalytic Properties of Pt and Pd-Based Heterometallics

Yakushev I.A., Smirnova N.S., Vargaftik M.N.

*Kurnakov Institute of General and Inorganic Chemistry, Russian Academy of Sciences,
Moscow, Russia
ilya.yakushev@igic.ras.ru*

Bimetallic functional materials, such as supported catalysts, reveal unique properties in selective hydrogenation processes of triple bonds in alkynes [1]. One of the synthetic methods for the preparation of a supported catalysts is using carboxylate-bridged bimetallic complexes $[M_1M_2(OOCMe)_4]$ (where $M_1 = Pt$ or Pd , $M_2 =$ non-precious metal atom) with “paddlewheel” structure as simple precursors with short M_1 to M_2 interatomic distance. Such shortening together with carboxylate-bridged ligands leads to highly effectiveness of complexes $[PdIn(OOCMe)_5]$ (Fig. 1a) in homogeneous hydrogenation of diphenylacetylene in mild conditions (Fig. 1b) [2]. Structural studies by X-ray diffraction methods of crystal structures and X-ray spectroscopy techniques (EXAFS, XANES) utilizing the synchrotron radiation of reaction media reveal preserving of binuclear moiety Pd-In during the reaction pathway.

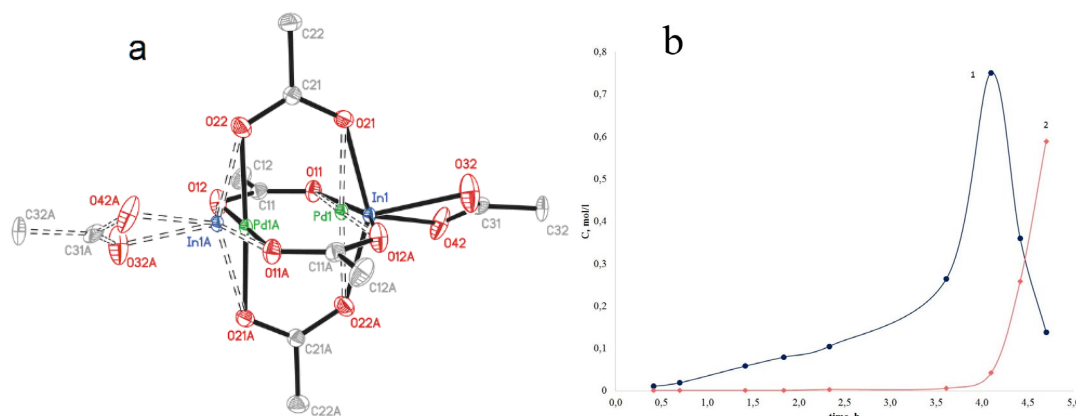


Fig. 1a. Molecular structure of the complex $[PdIn(OOCMe)_5]$. Fig. 1b. Time profile for phenylacetylene hydrogenation styrene accumulation (curve 1) and ethylbenzene accumulation (curve 2).

Analogous perspective Pt-based compounds can be obtained by proposed convenient methods [3] for the synthesis of heterometallic complexes with transition and post-transition metals. These compounds can be easily transformed by thermal decomposition to Pt-based bimetallic catalysts as an advanced alternative to traditional ways of their preparation.

Acknowledgement: The work was carried out in terms of State assignment of the Kurnakov Institute of General and Inorganic Chemistry (Russian Academy of Sciences) in the field of fundamental research.

References:

- [1] Smirnova N.S., Khramov E.V., Stolarov I.P. et al. *Intermetallics* (2021) V. 132. P. 107160.
- [2] Stolarov I.P., Yakushev I.A., Churakov A.V. et al. *Inorg. Chem.* (2018) V. 57. № 18. P. 11482.
- [3] Yakushev I.A., Stolarov I.P., Cherkashina N.V. et al. *Inorganica Chimica Acta* (2020) V. 508. P. 119631.

XANES Investigation of Oxaliplatin Loaded Zr-MOFs for Targeted Drug Delivery

Rud P.A., Burachevskaya O.A., Gritsai M.A., Soldatov M.A.

Southern Federal University, The Smart Materials Research Institute, Rostov-on-Don, Russia
 prud@sfedu.ru

Metal-organic frameworks (MOFs) are the class of compounds that consists of metal ions or clusters coordinated with organic ligands to form a three-dimensional crystal structure. Among the various possible applications, MOFs are also promising candidates for targeted drug delivery systems. For nanocarriers, the requirements for ensuring an efficient therapy are to efficiently entrap drugs with high payloads, control the release and matrix degradation, offer the possibility to easily engineer its surface to control in vivo fate and be detectable by imaging techniques. Currently, for delivery, some materials are being used (for example, liposomes, nanoparticles, or micelles) [1] but, for the most part, unsatisfactory [2]. MOFs allow to overcome such problems as low drug loading, instability, and toxicities due to their high porosity, biodegradability, large BET surface, controlled release of loaded drugs.

Increasing the efficiency of loading of functional nanoparticles or molecular substances into porous particles is a currently central research problem. Solving this problem would allow to improve carriers of bioactive substances for targeted delivery. In this study we estimated the efficiency of various methods for loading oxaliplatin into nanoparticles of Zr-based MOFs UiO-66. They included one of the conventional methods - solution impregnation new method of freezing induced loading (FIL) [3]. Also, the efficiency of the selected methods was studied during the staged loading of platinum drugs using several cycles.

Loading efficiency was assessed by X-ray fluorescence analysis (Zr/Pt ratio). The content of Pt and Zr (in at.%) was recalculated to the weight of drug, that was loaded into MOF (efficient loading) and weight of the loaded drug relative to the weight of the MOF ($\omega_{MOF, \%}$). These parameters were calculated according to the equations 1-2:

$$(1) \text{ Efficient loading} = \frac{m(MOF) \times M(\text{drug}) \times \text{at.}\%(\text{Pt}) \times N(\text{Zr or Fe})}{\text{at.}\%(\text{Zr or Fe}) \times N(\text{Pt}) \times M(MOF)};$$

$$(2) \omega_{MOF, \%} = \frac{\text{eff.load.}}{m(MOF) + \text{eff.load.}} \times 100\%;$$

N - number of atoms in structural formula.

UiO-66-NH₂ turned out to be the best candidate for loading platinum drugs and demonstrated the highest efficient loading, presumably due to the binding of platinum atoms in the drug molecule to the amino groups of MOFs. For both methods, loading of the drug was carried out for 5 cycles, and the effective loading increases with increasing loading cycles. The highest loading was achieved for the modified zirconium MOF UiO-66-NH₂ with mixed linkers (BDC-NH₂/NDC 50/50). In the case of loading by the FIL method, the maximum loading after the 5th cycle was $\omega_{MOF} = 3.2\%$, and for the impregnation method after the 7th cycle - 5.3%.

The release experiments in water and saline were performed and demonstrated no change in platinum content during first 4 h. Due to the ability of UiO-BDC-NH₂-NDC 50/50 nanoparticles prevent oxaliplatin from spontaneous release, they could be very promising for further investigation.

For better understanding the loading mechanism, the loaded samples were studied by X-ray absorption spectroscopy. The Pt L₃-edge data were collected at the Structural Materials Science end-station in the Kurchatov Synchrotron Radiation Center (NRC Kurchatov Institute, Moscow, Russia) [4]. All reference samples were measured in the transmission geometry using conventional sample holder. Pt L₃-edge was measured in fluorescence mode. Si(111) channel-

OP-02

cut monochromator was used for the energy scanning, providing an energy resolution $\Delta E/E \sim 10^{-4}$. Intensities of the X-ray radiation before (I_0) and after (I_1) the samples were measured with ion chambers with appropriate N_2/Ar mixtures. The spectra were processed using standard procedures for subtracting the background and normalizing the magnitude of edge jump in the Demeter software package [5]. Energy calibration was performed using the first derivative maximum point by the reference sample.

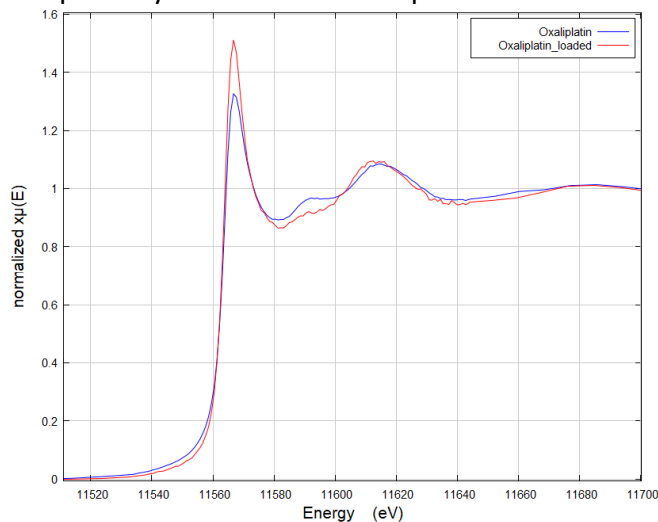


Fig. 1. XANES spectra of oxaliplatin before (blue) and after (red) loading.

Obtained XANES spectra show no pre-edge features and a clear ‘white line’ peak at approximately 11.567 keV (Fig. 1). The white line (WL) is the largest peak associated with absorption edge. The spectrum produced after oxaliplatin loading demonstrates higher intensity of WL, that could be a sign of the oxidation processes. Additionally, some significant changes occur after the edge position. In particular, spectral feature at 11591 eV decreases intensity, indicating significant changes in the local environment of the absorbing atom.

Acknowledgement: Research was financially supported by the Ministry of Science and Higher Education of the Russian Federation (State assignment in the field of scientific activity, № FENW-2023-0019)

References:

- [1] Peer, D. et al. (2007). Nanocarriers as an emerging platform for cancer therapy. *Nature Nanotech.*, 2, 751–760.
- [2] Wilczewska A. Z., Niemirowicz K., Markiewicz K. H., Car H. Nanoparticles as drug delivery systems // *Pharmacological Reports.* – 2012. – T. 64, № 5. – C. 1020-1037.
- [3] German, S. V. et al. (2018). High-efficiency freezing-induced loading of inorganic nanoparticles and proteins into micron- and submicron-sized porous particles. *Scientific Reports*, 8(1).
- [4] Chernyshov, A.A., A.A. Veligzhanin, and Y.V. Zubavichus, Structural Materials Science end-station at the Kurchatov Synchrotron Radiation Source: Recent instrumentation upgrades and experimental results. *Nuclear Instruments and Methods in Physics Research Section A: Accelerators, Spectrometers, Detectors and Associated Equipment*, 2009. 603(1): p. 95-98;
- [5] Ravel, B. and M. Newville, Data analysis for X-ray absorption spectroscopy using IFEFFIT. *Journal of synchrotron radiation*, 2005. 12: p. 537-41

Single-Crystal X-Ray Diffraction for Molecular Crystals at Synchrotron vs. Laboratory Source

Zakharov B.A.^{1,2}

1 – Boreskov Institute of Catalysis, Novosibirsk, Russia

2 – Novosibirsk State University, Novosibirsk, Russia

b.zakharov@yahoo.com

X-ray diffraction experiments using synchrotron radiation (SR) sources has become more accessible during the last decades and used in many fields of research. Due to the advantages of SR including high brightness, high intensity, low divergence of the beam, it become the only probe that can be used for structure determination of some samples. For some research groups it is possible to perform an experiment using SR only without using a laboratory diffractometer due to easy access to SR source, higher speed of experiment and the ability to study much smaller samples or local areas of larger samples. At the same time, many processes in crystals develop in fundamentally different ways, depending on how long the sample is under certain conditions, for example, at high pressure, low or high temperature, and how quickly these conditions change. Due to the fact that the data collection time difference for laboratory and SR diffraction experiments is orders of magnitude, this can influence the kinetics of processes, the formation of phases completely different to obtained in laboratory conditions can be observed. An additional influence on the samples can be caused by X-ray radiation effect leading even to radiation damage of the sample at SR, which is different for laboratory source experiments. In the title contribution I shall illustrate this effects with examples of X-ray diffraction studies of molecular crystals at variable temperatures and pressures, including L-alanine, L-serine, β -alanine, polymorphic modifications of chlorpropamide, glycine, glyciniun phosphite and other examples.

Acknowledgement: This work was supported by the Ministry of Science and Higher Education of Russia; the work was carried out jointly by Boreskov Institute of Catalysis (project AAAA-A21-121011390011-4) and Novosibirsk State University (strategic academic leadership program “Priority 2030”). The equipment of MDEST laboratory at NSU was used for in-house diffraction experiments.

Application of *In Situ* XRD to Study of MnOx-CeO₂-ZrO₂ Catalysts Formation

Bulavchenko O.A.¹, Vinokurov Z.S.^{1,2}, Konovalova V.P.¹, Mishchenko D.D.^{1,2}

1 – Boreskov Institute of Catalysis, Novosibirsk, Russia

2 – SKIF Synchrotron Radiation Facility, BIC, Kol'tsovo, Russia

obulavchenko@catalysis.ru

The development of new technologies requires a deep understanding of the processes occurring at all stages of catalyst synthesis and operation. Modern *in situ* methods for the analysis of materials make it possible to monitor the state of the catalyst under various conditions. *In situ* XRD assists in the characterization of the active catalyst, the behavior of the catalyst during activation/deactivation, the characterization of catalyst precursor materials, the study of some steps in the preparation of the catalyst, in the reaction medium. *In situ* diffraction was used to follow the evolution of phases and their crystal size, the formation of both stable phases and intermediates during the reaction, and rapid monitoring processes and kinetics of chemical reactions. This work illustrates the mechanism of MnOx-CeO₂-ZrO₂ catalyst formation using *in situ* XRD.

Manganese based oxides are active catalysts in several oxidation reactions. Their catalytic properties arise from the ability of Mn to form oxides with wide range of oxidation states and from their oxygen storage capacity in the crystalline lattice. Interaction with Ce/Zr oxides improves in the catalytic properties due to the formation of "reactive" oxygen species, which are formed both in MnOx nanoparticles and Mn_yCe(Zr)_{1-y}O₂ solid solutions. *In situ* and *operando* XRD was used for study two ways to develop an active catalyst: (1) formation of solid solution from low-temperature precursor; (2) decomposition of Mn_yCe(Zr)_{1-y}O₂ solid solution. During the first step, the mechanism of Mn_yCe(Zr)_{1-y}O₂ solid solution formation depends on the Mn content, treatment conditions. The second way includes decomposition of solid solution by the introduction of a topochemical reduction-reoxidation stage. The main idea is that under reducing medium, the surface of the mixed oxide is enriched with Mn²⁺. With further reoxidation, the oxidation of Mn cations is observe leading to the formation of active states of MnOx. To determine the activation conditions, the temperature of reduction and oxidation, the concentration of the reducing agent, the composition of the mixture during reoxidation, the flow rates, and the treatment mode were varied. For the first time, the processes of exolution of manganese oxides MnOx are studied in detail by *operando* XRD. XPS and TEM methods detect the segregation of manganese cations on the surface of the solid solution. Thus, by adjusting the pretreatment conditions, it is possible to control the phase state and dispersion of the crystalline modifications of Mn oxides, promote the decomposition of the solid solution with the formation of a new type of active states.

Acknowledgement: This work was supported by the Russian Science Foundation, project 21-73-10218

Middle-Range Atomic Order in Glasses of $\text{La}_2\text{O}_3\text{-Nb}_2\text{O}_5\text{-B}_2\text{O}_3$ and $\text{BaO-Nb}_2\text{O}_5\text{-P}_2\text{O}_5$ Systems

Avakyan L.A.¹, Alexeev R.O.², Firsova J.A.^{2,3}, Shakhgildyan G.Yu.², Sukharina G.B.¹,
Sigaev V.N.², Bugaev L.A.¹

1 – Southern Federal University, Rostov-on-Don, Russia

2 – Mendeleev University of Chemical Technology of Russia, Moscow, Russia

3 – Corporation «Lytkarino Optical Glass Plant», Lytkarino, Russia

laavakyan@sfnedu.ru

The non-silica oxide glasses are intensively studied as a high-refraction index lead-free materials perspective for optics, photonics, laser and solid state energy storage applications [1-3]. The lanthanum, barium and niobium oxides are promising high refraction index materials, but their glass-forming ability is limited [4], so that the addition of glass forming agent (boron or phosphate oxide) is required for the application of convenient glass-production technologies [5].

In this study we consider the glass samples of two series: $\text{La}_2\text{O}_3\text{-Nb}_2\text{O}_5\text{-B}_2\text{O}_3$ (in the following – LNB) and $\text{BaO-Nb}_2\text{O}_5\text{-P}_2\text{O}_5$ (in the following – BNP). The nominal fraction of niobium oxide is denoted with number in the sample notation. Despite of the practical importance of non-silica glass systems, their atomic structure is not well established. In particular, the spatial arrangement of NbO_6 octahedra in glass systems is debated. Masuno *et al* [4] proposed that NbO_n polyhedra are connected by corners and by edges, while the last connections are doubtful for low-density glass structures. Jordanova *et al* [6] stated that both octahedral NbO_6 and tetrahedral NbO_4 groups are present in glass. Aronne *et al* [7] insisted on the high static disorder of the first coordination shell Nb-O with absence of NbO_4 groups.

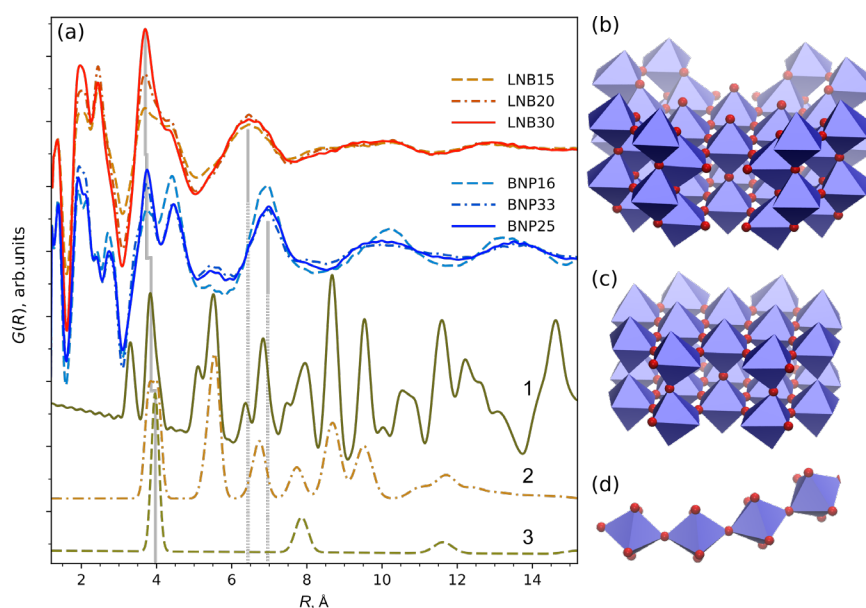


Fig. 1. (a) The comparison of experimental PDFs for LNB and BNP samples with theoretical PDFs obtained from model structures. (b-d) Illustration of model structures (blue – Nb, red – oxygen).

OP-05

In order to reveal the atomic structure of the considered LNB and BNP glasses we applied the X-ray total scattering (PDF analysis) and Nb K- and La L₃-XAFS spectroscopy methods. Figure 1 presents the experimental pair distribution functions (PDF) extracted from the experimental data measured at the beamline P02.1 within the rapid access program 2021A of PETRA III (DESY, Hamburg). The experimental curves are compared with the theoretical functions (curves 1-3 in Figure 1) calculated for the atomic models based on the crystal structures of bulk Nb₂O₅ (I4/mmm, COD ID 1528723).

The peaks at low distances (< 3 Å) correspond to metal-oxygen bonds with bond lengths, which agree well with the reference data and with XAFS results [5]. However, the nature of middle-range order peaks at Figure 1 (> 3 Å) is puzzling. The peak at ~ 4 Å can be explained by Nb – Nb atom pairs bridged by oxygen, which can be noticed in bulk niobium oxide. However, the more distant peaks (~ 6.5, ~ 10, ~ 13 Å) can not be explained by any motif presented in bulk oxide, including any flexible chain of NbO₆ groups (curve 3 at Figure 1). Also we see no signal from NbO₆ octahedra connected by edges, with expected distance of ~ 3.1 Å.

This means that NbO₆ octahedra are connected only by corners with the average length of the chain of less than 5 Å. The consideration of PDFs of bulk oxides of La and Ba (not presented) indicates on the possibility of the formation of Ba- and La- polyhedra chains able to explain the experimental peaks. The analysis of XANES and EXAFS spectra (not presented) show the sensitivity of oxygen coordination number of La from the amount of boron oxide in the glass.

Acknowledgement: This work was supported by the Russian Science Foundation, grant 22-12-00106.

References:

- [1] T. T. Fernandez, S. Gross, K. Privat, B. Johnston, M. Withford *Advanced Functional Materials*, 32 (2021) 2103103
- [2] T. Komatsu, T. Honma, T. Tasheva, V. Dimitrov *J. Non-Cryst. Solids*, 581 (2022) 121414
- [3] Zou K., Dan Y., Xu H., et al. Recent advances in lead-free dielectric materials for energy storage *Materials Research Bulletin*. 113 (2019) 190-201
- [4] A. Masuno, H. Inoue, K. Yoshimoto, Y. Watanabe *Opt. Mater. Express*, 4 (2014) 710
- [5] R. Alekseev, L. Avakyan, G. Shakhgildyan, G. Komandin, V. Savinkov, N. Romanov, A. Veligzhanin, S. Lebedev, A. Ermakova, G. Sukharina, L. Bugaev, V. Sigaev *J Alloy Compd*, 917 (2022) 165357
- [6] R. Iordanova, M. Milanova, L. Aleksandrov, K. Shinozaki, T. Komatsu *J. Non-Cryst. Solids*, 543 (2020) 120132
- [7] A. Aronne, E. Fanelli, P. Pernice, M. Malvestuto, P. Bergese, E. Bontempi, P. Colombi, L. Depero, L. Bignardi, C. Giannetti, et al. *J. Non-Cryst. Solids*, 357 (2011) 1218
- [8] G.B. Sukharina, A.M. Ermakova, R.O. Alekseev, G.Yu. Shakhgildyan, A.A. Veligzhanin, L.A. Avakyan, L.A. Bugaev, V.N. Sigaev, *J. Non-Cryst. Solids*, 616 (2023) 122454

Interatomic Auger Transitions End Excitations in Photoemission from Cu_2SnS_3

Grebennikov V.I., Kuznetsova T.V.

Mikheev Institute of Metal Physics UB RAS, Ekaterinburg, Russia

vgrebennikov@list.ru

The interatomic Auger transitions in Cu_2SnS_3 are studied by XPS spectroscopy using a synchrotron source. $\text{CuL}_3\text{CuM}_{2,3}\text{SnN}_{4,5}$ and $\text{CuL}_3\text{SnN}_{4,5}\text{V}$ lines with kinetic energies 23 eV lower than the corresponding $\text{CuL}_3\text{M}_{2,3}\text{V}$ and CuL_3VV copper Auger lines were found experimentally. They are formed due to the shaking of Sn 4d electrons into the valence band under the action of the dynamic field of core-level holes arising in the process of photoexcitation and autoionization of the copper atom shown in Fig.1.

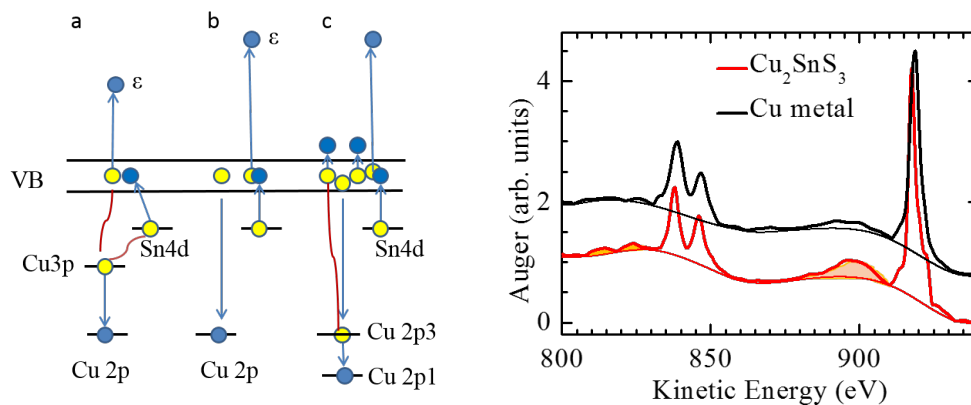


Fig. 1. Diagrams of the interatomic Auger process: (a) $\text{CuL}_3\text{CuM}_{2,3}\text{SnN}_{4,5}$; (b) $\text{CuL}_3\text{SnN}_{4,5}\text{V}$; (c) $\text{CuL}_3\text{SnN}_{4,5}\text{V}$ Auger transition following formation of the inner Cu L₂ core hole.

Fig. 2. Auger spectrum of the Cu_2SnS_3 compound, obtained at a photon energy of 950 eV.

The absorption of an X-ray quantum in matter leads to a photoelectron ejection from the core level of the atom, and the resulting photo-hole is then filled with an electron from the overlying shell with the emission of a second electron from the atom due to the Coulomb interaction and conservation of energy (the so-called Auger transition). Usually the whole process takes place within one central atom. We intend to tackle the unusual - to get an answer to the fundamental question: is the photo effect possible with the ejection of electrons from the core levels of neighboring elements surrounding the atom that has absorbed the quantum? There are certain reasons to believe that such an interatomic photo effect exists and has a significant probability, especially in compounds with elements containing highly localized 4d shells with binding energy 15-50 eV [1]. These states experience an anomalously strong effect of the dynamic field of the photo hole, forming long-lived excited atomic states.

Fig. 2 shows the CuL_3 Auger spectra obtained at a photon energy of 950 eV, which is above the L₃ edge but below the L₂ edge of the spin-orbit doublet. The background of inelastic electron scattering is drawn by a thin smooth line. The figure also shows the corresponding spectrum of pure metallic copper for comparison. Both curves are formed mainly by intra-atomic Auger lines CuL_3VV (kinetic energy of the maximum is 917.7 eV) and by $\text{CuL}_3\text{M}_{2,3}\text{V}$ line

split into two peaks 837.9 and 846 eV. However, the main difference between the curves is that an additional extended line is observed at the compound. Its maximum has an energy 22 eV below the peak of the main Cu L₃VV line. In addition, two more maxima appear in the compound at 23 eV below the Cu L₃M_{2,3}V Auger line. These are interatomic CuL₃ SnN_{4,5} V and CuL₃ CuM_{2,3} SnN_{4,5} Auger excitations.

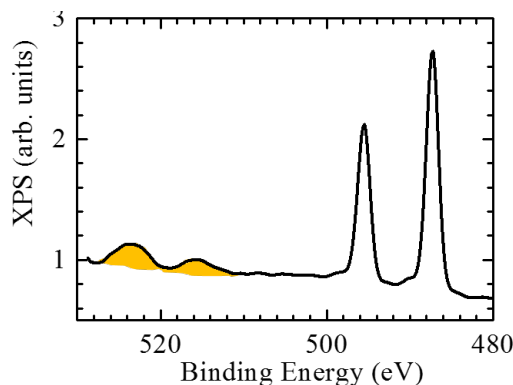


Fig. 3. XPS spectra of the Sn 3d spin-orbital doublet and intrinsic loss on excitation of a Sn 4d electron to the valence band during photoemission from Cu₂SnS₃.

The interatomic Auger transition occurs as a result of the shaking of Sn 4d electrons. Therefore, let us look for similar processes in other spectra, in particular, in the direct photoemission spectrum. Fig. 3 shows the XPS spectra of the Sn 3d doublet in Cu₂SnS₃. The main lines are accompanied by 28.5 eV satellites arising due to the transfer of additional 4d electrons into unoccupied valence states during the sudden creation of a 3d photohole. The energy shift is determined by the binding energy of the Sn 4d level and the energy of intraatomic repulsion of two holes $U = 1.8$ eV. The Sn 4d electron is shaken by one photo hole in direct photoemission.

The obtained experimental XPS spectra of the Cu₂SnS₃ compound show intense interatomic CuL_{2,3} CuM_{2,3} SnN_{4,5} and CuL_{2,3} SnN_{4,5} V Auger transitions. The sudden appearance of holes in the photo and Auger emission creates a dynamic field with a wide frequency spectrum, which causes the shaking of electrons in the neighboring atoms. This process substantially increases the probability of the interatomic Auger transition. In compounds with a narrow valence band (for example, 3d or 4d type) a strong Coulomb interaction arises between electrons and holes on the neighboring atoms, which creates the favorable conditions for the appearance of intense interatomic transitions in the soft x-ray range.

Acknowledgement: This work was supported by the Russian Science Foundation, grant 23-72-00067

References:

[1] V.I. Grebennikov, T.V. Kuznetsova, *Physica Status Solidi (A)*, 216 (2019) 1800723.

Improper Ferrielectric Phase Transitions in the PMN-PSN Solid Solutions

Vakhrushev S.B.¹, Bronwald Iu.A.¹, Petroukhno K.A.^{1,2}, Filimonov A.V.^{1,2}, Raevski I.P.³

1 – Ioffe Institute, St.Petersburg, Russia

2 – Peter the Great St.Petersburg Polytechnic University, St.Petersburg, Russia

3 – Southern Federal University, Rostov-on-Don, Russia

s.vakhrushev@mail.ioffe.ru

Relaxor ferroelectrics constitute large, scientifically interesting and practically important class of dielectric compounds. Despite these extensive studies the microscopic nature of the relaxors remains questionable. Relaxors show very complicated hierarchical structure, that is the key point of their physics. One of the major obstacles is the difficulty in the control of chemical order in relaxors. Such control, albeit not complete, can be achieved in the 1:1 compounds like $\text{PbSc}_{1/2}\text{Nb}_{1/2}\text{O}_3$ (PSN), however in more physically and practically interesting 1:2 ($\text{PbMg}_{1/3}\text{N}_{2/3}\text{O}_3$ (PMN) - like) compounds is quite difficult. The most direct way of controlling is by solid solution of 1:1 and 1:2 compounds, $\text{PMN}_{1-x}\text{PSN}_x$ serves as an example.

We performed comprehensive study of the short-range and long-range structure evolution in the PMN-PSN with $x=0.35$ and 0.8 solid solutions and in pure PSN. We have determined the long-range compositional order parameter and have followed the temperature evolution of the lattice constant demonstrating the similarity with the pure PMN. Temperature dependence of the diffuse scattering near the Brillouin Zone (BZ) centre was studied and was found to be similar to the pure PMN for the $x=0.35$ and to the PMN-PT for $x=0.8$.

Asymmetric diffuse scattering was observed near the M-point of the BZ ($h+1/2, k+1/2, l$) extinct for $h=k$. It was described in the frames of the earlier developed mode coupling model [1,2] with M_3 oxygen octahedra rotation relevant mode. On cooling the lock-in transition was identified resulting in the cancelling of the extinction rules and creation of the symmetric peaks at all M-points. It can be concluded that the antiferroelectric order parameter is aroused. Considering this observation together with the data at around the BZ centre related to the polarization fluctuations and taking into account the fact that the primary relevant mode is the non-polar oxygen rotation mode we can describe the low temperature phase transition as the improper transition to the ferrielectric phase.

Acknowledgement: This work was supported by the Russian Science Foundation, grant № 22-12-00328, <https://rscf.ru/project/22-12-00328/>.

References:

- [1] Vakhrushev, S. B., et al. Physics of the Solid State (2021): 1-7.
- [2] Vakhrushev, S. Et al. Materials. 2022 Jan; 15(1):79.

Application of High-Energy X-Rays and Atomic Pair Distribution Function Analysis to Structural Diagnostics of Ni/Ce_{0.75}Zr_{0.25}O₂ Catalysts for Methanation of Carbon Oxides

Pakharukova V.¹, Kharchenko N.^{1,2}, Vinokurov Z.¹, Stonkus O.¹, Saraev A.¹, Gorlova A.^{1,2}, Rogozhnikov V.¹, Potemkin D.^{1,2}

1 – Borekov Institute of Catalysis, Novosibirsk, Russia

2 – Novosibirsk State University, Novosibirsk, Russia

verapakh@catalysis.ru

The development of catalysts for methanation of carbon oxides attracts a great attention. CO selective methanation is a promising method for a deep purification of hydrogen gas designed for fuel cells. CO₂ methanation is considered as a way of CO₂ utilization with methane production [1]. Nickel-based catalysts exhibit a good performance in these processes. Supported Ni/Ce_{1-x}Zr_xO₂ catalysts and mixed Ni-Ce_{1-x}Zr_xO₂ materials are considered as promising systems [2, 3]. It is believed that their high activity is related to the reducibility of Ce_{1-x}Zr_xO₂ surface and synergetic metal-support interaction [4]. However, there is still insufficient information about structural organization of these catalysts and nature of metal-support interaction.

This work was devoted to study on structural organization of supported Ni/Ce_{0.75}Zr_{0.25}O₂ and mixed Ni-Ce_{0.75}Zr_{0.25}O₂ catalysts. A wide range of methods for structure diagnostics were used: X-ray diffraction (XRD) studies, high resolution electron microscopy (HRTEM) studies. To reveal the structure of highly dispersed nickel species and organization of metal-support interface, total X-ray scattering method, namely atomic pair distribution-function (PDF) was used. This method gives information on short-range arrangement of atoms in materials. The structural evolution of the catalyst at standard activation in H₂ atmosphere was studied by in situ XRD and pseudo in situ X-ray photoelectron spectroscopy (XPS).

X-ray scattering data for the PDF analysis were obtained using synchrotron radiation. The experiments were performed at the precision diffractometry and anomalous scattering beamline at the Siberian Synchrotron and Terahertz Radiation Centre (SSTRC, Institute of Nuclear Physics, Novosibirsk). In situ XRD experiments were performed at the Precision Diffractometry-2 station at SSTRC.

Acknowledgement: This work was supported by the Russian Science Foundation, grant 21-73-20075.

References:

- [1] S.Rönsch, J. Schneider et al. Fuel 166 (2016) 276.
- [2] S. Tada, T. Shimizu, et al. Int. J. Hydrogen Energy 37 (2012) 5527.
- [3] B. Nematollahi, M. Rezaei et al. Int. J. Hydrogen Energy 40 (2015) 8539.
- [4] N. Martin, F. Hemmingsson et al. Catal. Sci. Technol.9 (2019) 1644.

Influence of Alloying Elements on the Retention of $\text{Al}_{11}\text{Ti}_5$ at Room Temperature

Lazurenko D.V.¹, Lozanov V.V.², Dovzhenko G.D.^{1,3}

1 – Novosibirsk State Technical University, Novosibirsk, Russia

2 – Institute of Solid State Chemistry and Mechanochemistry SB RAS, Novosibirsk, Russia

*3 – Synchrotron Radiation Facility - Siberian Circular Photon Source «SKIF», Boreskov Institute of Catalysis SB RAS, Novosibirsk, Russia
pavlyukova_87@mail.ru*

TiAl_3 -based alloys are in the focus of attention of many research groups due to the high specific properties. However, they have not yet found wide application due to the poor ductility and fracture toughness [1]. Alloying of TiAl_3 allows solving this problem. Addition of transition elements results in modification of its crystal structure from D0_{22} to L1_2 , which possesses reasonable ductility. However, the alloy formation is accompanied by precipitation of other phases, namely TiAl_2 or $\text{Ti}_5\text{Al}_{11}$. It is worth noting that $\text{Ti}_5\text{Al}_{11}$ is a high-temperature compound in the binary Ti-Al system and its precipitation was previously observed only in the Ti-Al-Ag [2], Ti-Al-V [3], and Ti-Al-Zn [4] ternary alloys. In this study, we carried out a systematic investigation of Ti-Al-Me (Me = Mn, Au, Pt, and Pd) samples to estimate the possibility of $\text{Ti}_5\text{Al}_{11}$ stabilization at room temperature and understand the nature of this phenomenon.

The temperature ranges in which $\text{Ti}_5\text{Al}_{11}$ exists in Ti-Al-Me systems were experimentally found using in situ synchrotron X-ray diffraction. The influence of alloying elements on stability of $\text{Ti}_5\text{Al}_{11}$ phase was also estimated theoretically using density functional theory (DFT) simulation. For the experimental investigations, Ti, Al, and Me powders were mixed and heated in the induction furnace. The transformations occurring in the samples during heating were registered every 4 seconds. It was found that the L1_2 phase forms in all the systems under investigation and further participates in the formation of $\text{Ti}_5\text{Al}_{11}$ at the temperatures above 900 °C, which is evidenced by the presence of about 1.5 – 2 at. % transition metal in the $\text{Ti}_5\text{Al}_{11}$ composition. The type of alloying element influenced the temperature range of $\text{Ti}_5\text{Al}_{11}$ stability and its retention at room temperature. In samples with Au and Pd, $\text{Ti}_5\text{Al}_{11}$ transformed to TiAl at temperatures 1100 – 1250 °C, while in samples with the addition of Mn and Pt, $\text{Ti}_5\text{Al}_{11}$ was stable up to the maximum heating temperature (1250 °C) and retained after cooling (Fig. 1). Also, alloying elements affected the cell parameters of $\text{Ti}_5\text{Al}_{11}$ and its tetragonality upon heating. $\text{Ti}_5\text{Al}_{11}$ formed in binary system lost its tetragonality with temperature, while $\text{Ti}_5\text{Al}_{11}$ alloyed with a transition element better retained c/a ratio. Pt and Mn had the highest effect on the unit cell tetragonality preserving.

To explain this behavior, DFT calculations were performed. According to the simulation results of the $\text{Ti}_5\text{Al}_{11}$ unit cell with 2 at. % Me, Pt and Mn decrease the unit cell volume of the compound and, consequently, the bond length. It probably limits the diffusion of Ti into $\text{Ti}_5\text{Al}_{11}$ and prevents the $\text{Ti}_5\text{Al}_{11}$ to TiAl phase transformation. This idea is in accordance with the

experimental data since the decrease in the Ti amount leads to the decrease in the c/a ratio. In addition, Ti_5Al_{11} alloyed with Mn and Pt had the lowest total DFT energy, which corresponds to the higher stability.

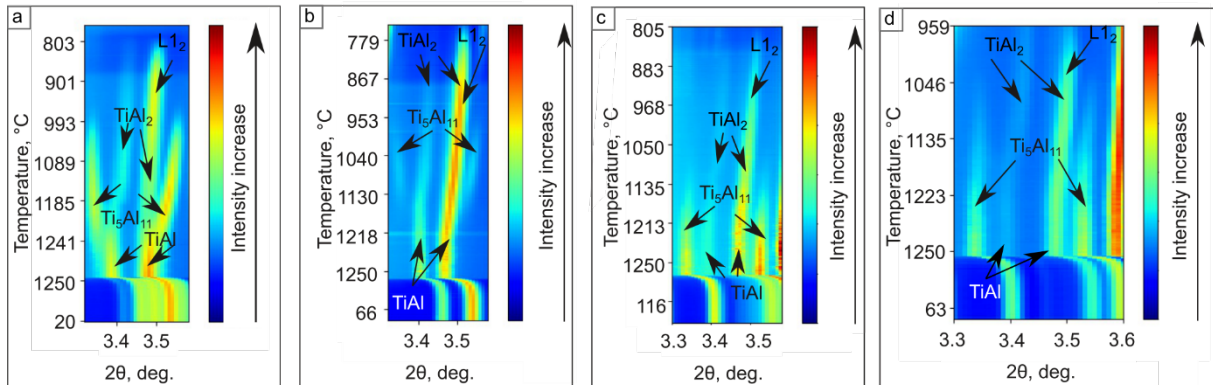


Fig. 1. The sections of the Ti-Al-Au (a), Ti-Al-Pd (b), Ti-Al-Mn (c), and Ti-Al-Pt (d) intensity maps at high temperature ranges.

Acknowledgement: The study was conducted within the framework of Federal Task of Ministry of Education and Science of the Russian Federation (project FSUN-2020-0014) “Investigations of Metastable Surfaces and Interfaces under Extreme External Impacts”.

The structural research was carried out at core facility "Structure, mechanical and physical properties of materials", NSTU.

Synchrotron measurements were implemented at the P07 beamline of German Electron Synchrotron (DESY) in April 2019.

References:

- [1] M. Yamaguchi et al, Mater. Res. Soc., 81 (1986) 275.
- [2] W.H. Tian, M. Nemoto, Intermetallics, 7 (1999) 1261-1269.
- [3] W.S. Chang, B.C. Muddle, Mat. Sci. Eng. A, 192-193 (1995) 233-239.
- [4] J. Pratt, Al-Ti-Zn Ternary Phase Diagram Evaluation · Phase diagrams, crystallographic and thermodynamic data: Datasheet from MSI Eureka in SpringerMaterials, MSI Materials Science International Services GmbH.

Current Experimental Capabilities of the “XSA/Belok” Beamline of the Kurchatov Synchrotron Radiation Source for Single Crystals X-Ray Diffraction Analysis and 2022/2023 Highlight Results

Lazarenko V.A., Dorovatovskii P.V., Svetogorov R.D.

NRC “Kurchatov institute”, Moscow, Russia

Vladimir.a.lazarenko@gmail.com

Single-crystal diffraction remains the most popular and widespread method for solving different structures of varying complexity for tasks of coordination chemistry and biology. The use of a synchrotron radiation source for carrying out such type of experiments makes it possible to achieve high resolution and quality of the data obtained in the shortest possible time.

Research in structural chemistry and biology is part of the vast amount of scientific research in the modern world, due to the fact that knowledge of the structure of a substance helps to confirm the correctness of the synthesis, and also makes it possible to better perform calculations when studying the properties of a substance. Despite the daily increase in demand for solving problems of coordination chemistry and, accordingly, work with small molecules, the number of synchrotron beamlines for single-crystal diffraction on small molecules in the world is quite small, which makes each of them a unique scientific instrument.

To make it easier for Russian users and provide an additional opportunity for foreign users to access this type of synchrotron beamline and to quickly collect high-resolution diffraction data from a wide range of samples, one of the installations of the Kurchatov synchrotron radiation source was optimized for working with crystalline samples in mass flow measurements, which allowed it to become a device that has no analogues in Russia for conducting this type of experiment [1]-[2]. For now, “Belok/XSA” beamline allows to investigate the structures of single crystals of simple organic compounds (with a cell in the region of 5-15 angstroms) and up to complex macromolecular complexes (with a cell of up to 200 angstroms).

At presentation I will talk about the current capabilities of the experimental beamline, the parameters of the focused beam after the upgrade of the magnet system of the accelerator of the Kurchatov synchrotron radiation source, and also demonstrate the main experimental results obtained in 2022/2023.

References:

[1] Lazarenko V.A., Dorovatovskii P.V., Zubavichus Y.V., Burlov A.S., Koshchienko Y.V., Vlasenko V.G., Khrustalev V.N., *Crystals*. 2017. V. 7. P 325-1-19.

[2] Roman D. Svetogorov, Pavel V. Dorovatovskii, Vladimir A. Lazarenko, *Crystal Research & Technology*, 2020, in press

Application of Resonant X-Ray Photoemission Spectroscopy for Studying the Local Electronic Characteristics of Multicomponent Functional Materials, Including Localized and Itinerant Aspects of the Behavior of f- and d-Electrons

Kuznetsova T.V., Grebennikov V.I., Ponomareva E.A.

Mikheev Institute of Metal Physics UB RAS, Ekaterinburg, Russia

kuznetsova@imp.uran.ru

We investigated the interplay of d- and f-elements and effect on the formation of the electronic structure in different multicomponent R-T compounds. The method of resonant x-ray photoemission spectroscopy allows to selecting the contributions of the various components in the valence bands (VB). We discuss about possibility of study not only the ground state, but also the lifetime of the excited (a core-level hole – VB electron) state, determine energies of the VB single-particle states and two-hole states at selected atoms, reactions to appearance of the core-level photo-hole. The VB XPS spectra obtained at different photon energies $h\nu$ crossing the core-level excitation thresholds. A comparative analysis is gave for the two enhancement channels (elastic and Auger electron) of the valence band photoemission under resonant excitation of the 2p core-level. For example, on Gd $N_{4,5}$ edges (148 eV) the 8.5 eV peak in valence band increases in GdNi₄Cu. The Gd 4d core-level electron transfers to a long-lived Gd 4f-state, and then the reverse transition occurs, accompanied by emission of an electron detected. Note that the peak is enhanced much more (350 times) on the Gd M_5 absorption edge (1184 eV). The nickel and copper spectra behave otherwise. The VB signal (0 – 9 eV) in GdNi₃Cu₂ does not change at the Cu L_3 excitation edge $h\nu = 932$ eV, but the Auger line appears with a starting binding energy of 14 eV. This means that the Cu 2p – 3d excited state very quickly leaves the parent atom and then the Auger decay occurs, forming two holes in the Cu 3d-states. Subtracting energy of two single-hole states (2·3.5 eV) from 14 eV, we find experimentally the interaction energy for two holes on the copper atom 7 eV. Nickel behaves the same as copper, but its Auger line is significantly broader than the appropriate copper line. Broadening is due to shaking or the multiple creation of electron-hole pairs near the Fermi energy upon the sudden occurrence of the photo-hole. The probability of this process on a nickel atom is very high, since the Ni has high density of 3d-states at the Fermi level. Shaking on the copper atom is much smaller, since the Cu 3d-states are deepened by 3.5 eV.

Acknowledgement: This work were supported by the Russian Science Foundation grant #23-72-00067

High Pressure and Low Temperature Study of Purine Nucleobases Salt Crystals

Gaydamaka A.A.^{1,2}, Arkhipov S.G.^{1,2}, Zakharov B.A.^{1,2}, Bogdanov N.E.^{1,2}, Rashchenko S.V.^{2,3}, Semerikova A.I.^{2,3}, Smirnova E.S.⁴, Ivanova A.G.⁴, Boldyreva E.V.^{1,2}

1 – Boreskov Institute of Catalysis, Novosibirsk, Russia

2 – Novosibirsk State University, Novosibirsk, Russia

3 – Sobolev Institute of Geology and Mineralogy SB RAS, Novosibirsk, Russia

4 – FSRC “Crystallography and Photonics” RAS, Moscow, Russia

a.gaidamaka@g.nsu.ru

Crystals consisting of small fragments of DNA and RNA can be considered as model objects for studying the effect of pressure on nucleic acids and oligonucleotides, as amino acid crystals are used to model the properties of proteins.

In the present contribution, comparative structural study of guanine, adenine, xanthine salts at cooling and hydrostatic compression will be summarized.

Purine nucleobase salts were studied by single crystal X-ray diffraction and Raman spectroscopy: hydrates of sodium and potassium salts of guanine (samples 1, 2), lithium salt of xanthine (sample 3), adenine salts with 3,5- and 2,6-dihydroxybenzoic acids (samples 4, 5). All the studied objects are able to withstand high pressures by the standards of biological systems (3 GPa or more), most of them undergo phase transitions of various types: with crystal destruction (1), with the formation of an incommensurately modulated phase (2); single crystal-single crystal (3), with reversible amorphization (4); for (5) no phase transitions were detected in the studied pressure range. Potassium guaninate was studied using synchrotron radiation as well as laboratory diffractometer. When cooled to 100 K, the structures of all studied compounds were preserved.

Acknowledgement: This work was supported by the Ministry of Science and Higher Education of Russia; the work was carried out jointly by Boreskov Institute of Catalysis (project AAAA-A21-121011390011-4) and Novosibirsk State University (strategic academic leadership program “Priority 2030”). The equipment of MDEST laboratory at NSU was used for in-house diffraction experiments. Part of the work was carried out using the equipment of the FSRC "Crystallography and Photonics" of the Russian Academy of Sciences. ThetaToTensor [1] was used to calculate thermal expansion and compressibility tensors, as well as to graphically represent their characteristic surfaces

References:

[1] Bubnova R. S., Firsova V. A., Filatov S. K. *Glass Physics and Chemistry*, 39(3) (2013), 347–350.

OP-13

Structural Investigation of Layered Ammonia Polyuranates

Gerber E.^{1,2}, Krot A.^{1,2}, Chernyshev V.^{1,2}, Trigub A.³, Sobolev N.², Averin A.², Maksimov S.², Svetogorov R.³, Nevolin I.^{1,2}

1 – Frumkin Institute of Physical Chemistry and Electrochemistry, Moscow, Russia

2 – Lomonosov Moscow State University, Department of Chemistry, Moscow, Russia

3 – National Research Centre “Kurchatov Institute”, Moscow, Russia

Chem.gerber@gmail.com

Ammonium polyuranates play an important role in the nuclear power, as they are actively involved in the nuclear fuel cycle in the course of UO₂ pellets preparation. However, neither the chemical composition, nor structure of such compounds have not been uniquely determined. Though properties of ammonium polyuranates have been actively investigated in the previous century[1–3], its nature is still an open question. It is still debated, whether ammonium polyuranates are compounds of individual phases with certain stoichiometry or a homogeneous system in which NH₃:U (and H₂O:U) ratio can be varied continuously. Fortunately, the advancement of the characterization techniques, including synchrotron-based methods of X-ray diffraction (XRD) and extended x-ray absorption fine structure (EXAFS) spectroscopy, makes it possible to investigate structure of ammonium uranates even though only polycrystalline samples can be synthetically obtained. It is not surprising, that technical achievements resumed scientific interest to this problem[4,5].

This contribution will show the results of structural characterization of ammonia uranate system. All samples were synthesized by adding ammonia aqueous solution to solid UO₃ with various ratio of UO₃/NH₃. The mixture has been stirred at 40 °C for 28 and 166 days. The precipitates were washed and investigated with a bunch of methods, including XRD, transition electron microscopy (TEM), elemental analysis, infrared, Raman and EXAFS spectroscopies.

Table 1. Results of the structure solution for ammonium polyuranates.

	3UO ₃ ·NH ₃ ·5H ₂ O	2UO ₃ ·NH ₃ ·3H ₂ O
Crystal system	Orthorombic	Orthorombic
Space group	Pnnn	I2 ₁ 2 ₁ 2 ₁
Formula units	6	6
a, Å	12.229(1)	12.175(1)
b, Å	15.012(1)	14.421(1)
c, Å	7.1327(8)	7.0691(7)
V, Å ³	1309.43	1241.16
Rp	0.0280	0.0441
Rwp	0.0366	0.0498

It was found, that UO₃/NH₃ ratio and synthesis time have a significant effect on the product properties, resulting in monophasic or polyphasic samples. The chemical composition of monophasic samples have been revealed and found to be 3UO₃·NH₃·5H₂O and 2UO₃·NH₃·3H₂O. All samples possess a layer structure similar to uranium oxohydroxide

OP-13

(schoepite), with interlayer water partially substituted with ammonium NH_4^+ . Diffraction data have been used for structure solution, additional crystallographic information have been obtained (Table 1).

It is worth to note that despite ammonia polyuranates have similar to schoepite local structure, the layer topology of each compound is different and has some peculiarities.

Acknowledgement: This work was supported by the Russian Science Foundation grant No. 21-73-00138.

References:

- [1] Cordfunke E.H.P., J. Inorg. Nucl. Chem. 24 (1962) 303–307.
- [2] Stuart W.I., Whateley T.L., J. Inorg. Nucl. Chem. 31 (1969) 1639–1647.
- [3] Lloyd M.H. et al., J. Inorg. Nucl. Chem. 38 (1976) 1141–1147.
- [4] Schreinemachers C. et al. Nucl. Eng. Technol. 52 (2020) 1013–1021.
- [5] Leinders G. et al., Inorg. Chem. 62 (2023) 9807–9817.

X-ray Absorption Spectroscopy Study on Spin-Orbit Interaction in Osmium Compounds

Fedorenko A.D.¹, Asanov I.P.¹, Asanova T.I.¹, Nikolenko A.D.²

1 – Nikolaev Institute of Inorganic Chemistry, Novosibirsk, Russia

2 – Budker Institute of Nuclear Physics, Novosibirsk, Russia

fedorenko@niic.nsc.ru

Compounds of 5d transition metals have been the subject of increasing study because they exhibit unique magnetic properties that can be attributed to strong spin-orbit coupling (SOC). In 5d metals, the energy associated with SOC is comparable to the Coulomb energy and the energy of crystal field stabilization. The correlation between these interactions can have an impact on various physical properties, such as the metal-dielectric transition of the Mott-Hubbard type, abnormal and spin Hall effects, the Rashba effect, the formation of skyrmions, and other effects related to Kitaev coupling

The influence of the Jahn-Teller effect and spin-orbit coupling on the spatial and electronic structure of isolated octahedral complexes $\{MX_6\}^{n-}$ (M = Rh, Pd, Re, Os, Ir, Pt, X = F, Cl, Br) and osmium compounds with realized exchange interactions (including $OsCl_4$, OsO_2 , Li_2OsO_3 , $KOsO_4$, and $K_2OsO_2(OH)_4$) was thoroughly investigated using quantum chemical calculations and X-ray absorption spectroscopy. The Os L_3/L_2 edge XANES spectra provided valuable information about the magnitude of the spin-orbit interaction by measuring the intensity ratio of the absorption edge lines. Moreover, the Cl and Br K-edge XANES spectra of transition metal compounds proved to be effective in studying the interaction between ligands and the central metal atom. Theoretical analysis of XANES spectra for Os compounds with different combinations of ligands and outer-sphere cations revealed that the electronic structure and magnetic properties are dependent on various factors, including the spin-orbit interaction, crystal field magnitude, electron pairing energy, and noncubic distortions of the Os environment.

Acknowledgement: This work was supported by the Russian Science Foundation, grant 22-22-00683. This work was performed on equipment at the Siberian Center of Synchrotron and Terahertz Radiation based on the VEPP-4–VEPP-2000 Complex at the Budker Institute of Nuclear Physics. Our quantum chemical calculations were made using the resources of the Siberian Supercomputer Center at the Institute of Computational Mathematics and Mathematical Geophysics.

XMCD and XANES Study of Double Manganite $\text{NdBaMn}_2\text{O}_6$

Titova S.G.¹, Yi-Ying Chin², Pei-Ci Lai², Shu lun Chang², Kuzhetsova T.V.³, Grebennikov V.I.³, Sterkhov E.V.¹, Trigub A.L.⁴

1 – Institute of Metallurgy UB RAS, Ekaterinburg, Russia

2 – National Chung Cheng University, Taiwan

3 – Mikheev Institute of Metal Physics UB RAS, Ekaterinburg, Russia

4 – SRC Kurchatov Institute, Moscow, Russia

sgtitova@mail.ru

Double manganites of rare earth elements (R) attract much attention due to high temperatures of magnetic and electric phase transitions. At room temperature varying R -element leads to charge-order insulating state for small elements $R = \text{Ho} - \text{Sm}$ and to ferromagnetic state for large elements $R = \text{Pr}$ and La . Since $R=\text{Nd}$ is at the boundary between those phases, $\text{NdBaMn}_2\text{O}_6$ is interesting due to competing of different types of interactions.

We performed X-ray magnetic circular dichroism (XMCD) and X-ray absorption near edge structure (XANES) study of magnetic and valence state for Nd and Mn atoms. XANES data were obtained at the Structural Material Science station of KSRS (Kurchatov Synchrotron Radiation Source). All spectra were collected in the transmission mode using a Si (111) channel-cut monochromator. The powder samples were spread over adhesive Kapton tape folded into several layers to achieve an appropriate combination of total absorption and absorption edge jump. Both XMCD and XANES measurements were performed at beam line BL11A of Taiwan Light Source at National Synchrotron Radiation Research Center (NSRRC) by the total-electron-yield method; the circular polarization of the incident photons was fixed and the direction of the applied magnetic field 0.5 T was changed during the measurements.

Nd L-edge and Mn K-edge XANES do not show any change by temperature and demonstrate sharp symmetric line typical for single uniform charge state Nd^{3+} , it means neodymium does not change the valence state during magnetic and electric phase transitions. The spectra for Mn K-edge demonstrate the features attributed with Mn^{2+} and a mixture of Mn^{3+} and Mn^{4+} .

XANES data for Mn L-edge and Nd M-edge have a small change by temperature while XMCD curves change significantly. We estimated spin and orbital contributions for Mn and Nd magnetic moments at different temperatures via the XMCD sum rule. Near metal-insulator phase transition at ~ 280 K the fluctuations of orbital moment for Nd ($\mu_+ - \mu_-$) increase and reach $\sim 1.4 \mu_B$ per formula unit, spin moment for Mn ($\mu_+ + \mu_-$) increases as well.

Acknowledgement: The research was carried out within the state assignment of Ministry of Science and Higher Education of the Russian Federation (122013100200-2 and “Spin” No. 122021000036-3). This work was supported by the National Science and Technology Council of the Republic of China (grant numbers NSTC 109-2112-M-194 -004 -MY3 and 112-2112-M-194 -003).

EXAFS Study of Actinide Complexes with N,O-Donor Polydentate Ligands

Gutorova S.V.¹, Trigub A.L.^{1,2}, Novichkov D.A.¹, Matveev P.I.¹

1 – Lomonosov Moscow State University, Chemistry Department, Moscow, Russia

2 – National Research Centre “Kurchatov institute”, Moscow, Russia

svetlana.gutorova@chemistry.msu.ru

The complexation of organic ligands with actinides is the basis of nuclear technologies used for the whole nuclear fuel cycle. Worldwide, new solvent extraction systems for the separation of the transuranium elements from spent nuclear fuel are under development. The key to finding the «perfect» extractant seems to be in purposeful search for selectivity drivers, which are hidden in complexation specifics of *f*-elements with extractants of interest. Pyridine- and phenanthroline- based ligands (Fig. 1) with a combination of a “soft” aromatic nitrogen atom and a “hard” oxygen atom seem to be promising for separation of actinides. The aim of our work was to investigate complexes of U(VI) and Th(IV), as the less hazardous analogue for Pu(IV), with a set of extractants based on pyridine and phenanthroline.

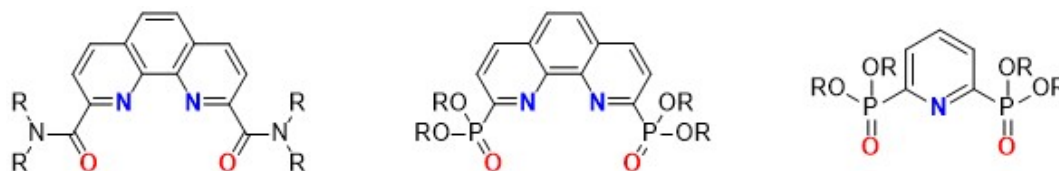


Fig. 1. Structures of ligands used in the research

First, complex structures directly in the organic phase after extraction of $\text{UO}_2(\text{NO}_3)_2$ with phenanthroline diamides **L1-L3** (Fig. 2) in ligand excess over metal were studied. EXAFS analysis combined with XRD showed that all studied extractants form with U(VI) complexes with a stoichiometry 1:1 and a structure of solvate-separated ion pair $\{[\text{UO}_2\text{L}(\text{NO}_3)]^+(\text{NO}_3)^-\}$, which confirms results by Zhang X. et al [1].

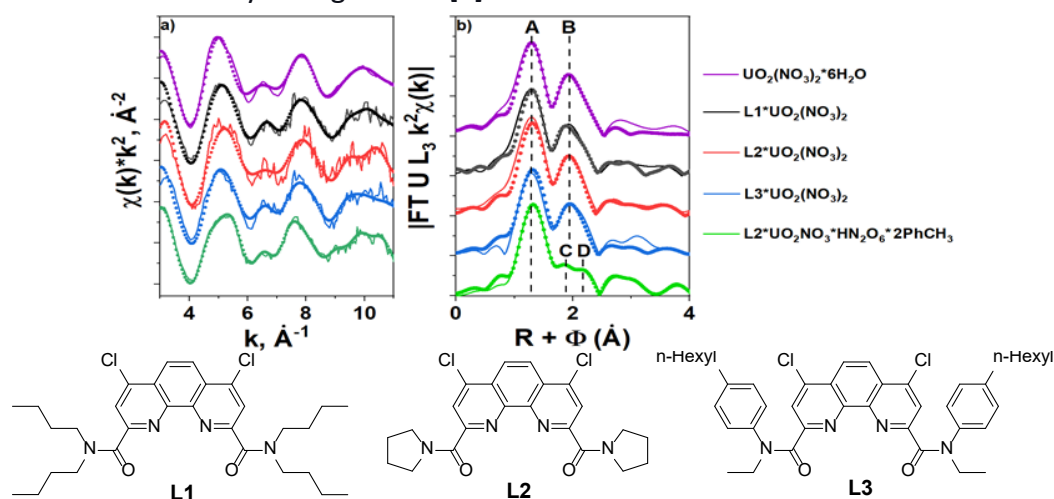


Fig. 2. U L_3 -edge EXAFS results. (a) k^2 -weighted EXAFS spectra, (b) Fourier transform (FT) magnitude of experimental EXAFS data (full lines) and fit (dots) for complexes $\text{L}^*\text{UO}_2(\text{NO}_3)_2$ and $\text{L}2^*\text{UO}_2\text{NO}_3^*\text{HN}_2\text{O}_6^*2\text{PhCH}_3$ and structures of corresponding ligands. k -range of 3-11 \AA^{-1} , R -range 1.1-4.5 \AA , s_0^2 0.90.

OP-16

Then the composition and structure of complexes during extraction from highly concentrated industrial solutions ($>0.1 \text{ mol}\cdot\text{L}^{-1}$) in metal excess over ligand were also studied. Phenanthroline- based ligands demonstrated a high U(VI) capacity providing an U:L1 concentration ratio in the organic phase up to 2:1. A combination of spectroscopic methods (UV-vis, EXAFS, XRD) and DFT was used to demonstrate formation of $\{[\text{UO}_2\text{L1NO}_3]^+[\text{UO}_2(\text{NO}_3)_3]^{-}\}$ complexes both in organic and solid phases (Fig. 3).

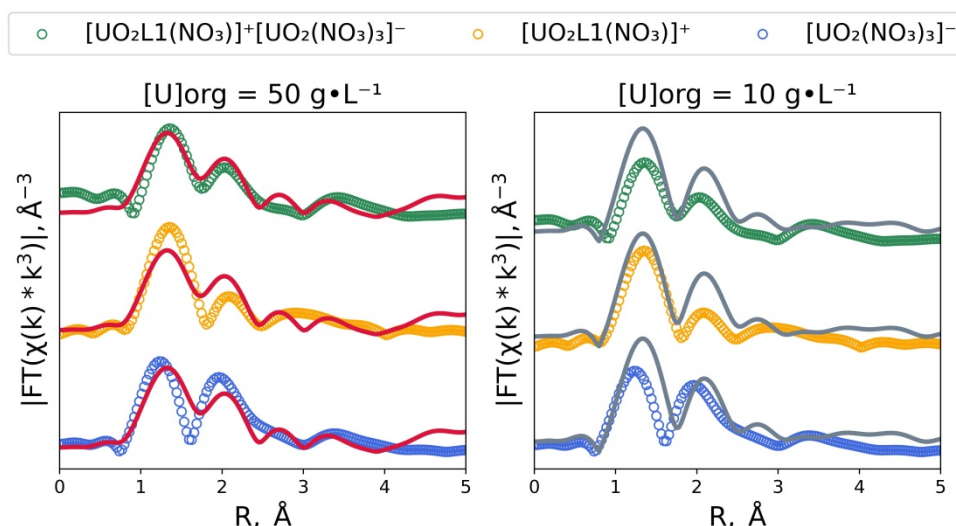


Fig. 3. FT magnitude of experimental EXAFS spectra of U-L samples, containing U(VI) $\sim 50 \text{ g}\cdot\text{L}^{-1}$ (Left panel, solid red line) and $10 \text{ g}\cdot\text{L}^{-1}$ (Right panel, solid grey line), compared to $[\text{UO}_2\text{L3}(\text{NO}_3)]^+[\text{UO}_2(\text{NO}_3)_3]^-$ (green dots), $[\text{UO}_2\text{L3}(\text{NO}_3)]^+[2]$ (orange dots) and $[\text{UO}_2(\text{NO}_3)_3][3]$ (blue dots). k -range of $2.5\text{-}9.5 \text{ \AA}^{-1}$.

Moreover, it was shown that large-volume tetradentate ligands extract actinyl-cations via solvation-anionic exchange mechanism which is a combination of two already well-known mechanisms: solvation and ion-pair anion exchange mechanisms. Whereas, tridentate pyridine-based ligands extract actinides (U(VI), Th(IV)) via solvation mechanism with formation of complexes with stoichiometry 1:1.

Acknowledgement: This work was supported by the Russian Science Foundation, grant 23-73-30006.

References:

- [1] X. Zhang, L. Yuan, Z. Chai, W. Shi, *Sci. China Chem.* 61 (2018), 1285–1292
- [2] S. V. Gutorova, P. I. Matveev, P. S. Lempert et al., *Inorg. Chem.* 61(2021) 384–398.
- [3] A. Ikeda, C. Hennig, A. Rossberg, S. Tsushima, A. C. Scheinost, G. Bernhard, *Anal. Chem.* 80 (2008) 1102–1110.

Lanthanide-Doped Solid Solutions Based on α -MnS with Thermoelectric Properties: XANES Investigation

Syrovkashin M.M., Korotaev E.V.

Nikolaev Institute of Inorganic Chemistry, Novosibirsk, Russia
syrovkashin@niic.nsc.ru

Thermoelectric materials (TEMs), capable of directly converting waste heat into electrical energy, are gaining increasing attention as an alternative to traditional power generation sources. The development and optimization of these high-efficiency thermoelectric materials are considered as one of the trends in modern material science. Thermoelectric Generators (TEGs) based on the highly efficient TEMs could provide potential solutions to global electricity demand growth by exploiting waste-heat. The application of TEMs ranges from power sources in various electronic devices to more specialized uses such as powering wearable smart devices using body heat or in hybrid electric vehicles. Cation-substituted solid solutions based on $4f$ - or $3d$ -metal chalcogenides exhibit a wide range of the electrophysical, magnetic and optical properties. The functional properties of these compounds could be modified by the variation of both type and concentration of the doping atoms. The lanthanide-doped solid solutions $\text{Ln}_x\text{Mn}_{1-x}\text{S}$ based on α -MnS are considered as promising functional materials with the thermoelectric and magnetic properties. The Seebeck coefficient is one of the main characteristics of the TEMs. The electrophysical properties, including the Seebeck coefficient, of semiconductor compounds largely depend on the electronic structure features. For instance, the distribution of the density of states (DOS) in the Fermi-level region is one of the key aspects in the interpretation, prediction and further optimization of the electrophysical properties of TEMs. In this regard, current work involved of the study of the electronic structure features of the lanthanide-doped solid solutions $\text{Ln}_x\text{Mn}_{1-x}\text{S}$ ($\text{Ln} = \text{Dy}, \text{Tm}, \text{Yb}$; $x = 0.01; 0.05$). The data on the conduction band structure of $\text{Ln}_x\text{Mn}_{1-x}\text{S}$ was studied using the X-ray absorption edge near edge structure spectroscopy (XANES). The experimental data were compared to the theoretical XANES spectra of the matrix elements (Mn, S) and lanthanides (Dy, Tm, Yb) calculated using the finite-difference methods (FDMNES software package). The combination of the experimental and calculated data allowed one to determine the partial contributions of DOS in the absorption edge structure and, thereby, to study the conduction and formation features during the cationic substitution of manganese atoms with lanthanides in $\text{Ln}_x\text{Mn}_{1-x}\text{S}$.

Acknowledgement: The authors are grateful to the Ministry of Science and Higher Education of the Russian Federation.

Wavelet Analysis and Machine Learning. New Methodology for XAS Spectrum Analysis

Abrosimov S.V., Guda A.A., Guda S.A., Shapovalova S.O.

*The Smart Materials Research Institute at the Southern Federal University, Rostov-on-Don,
Russia*

sergeyabrosimoov@gmail.com

The XAS spectrum mainly carries information about the geometry of the material and its composition. There are traditional methods of spectrum analysis based on Fourier analysis. In this case, we decompose our “complex” spectrum into the sum of simple trigonometric functions. The frequencies included in the decomposition carry useful information and have a physical meaning. In the Fourier transform, peaks are traced that fade with distance. The physical meaning of these peaks lies in the fact that each peak corresponds to the coordination number of the sample under study: a photoelectron, falling on an atom, is scattered to other atoms in its environment. Neighbors located at approximately the same distance from the atom being dispersed give a signal in the Fourier transform.

Thus, we can indirectly judge the geometry of the sample in general and the density of the distribution of atoms in particular. But as noted earlier, the XAS spectrum carries information not only about geometry, but also about composition. The Fourier transform does not allow us to make a conclusion about the type of atoms (their mass, for example) that give a signal to the final picture.

In order to determine which atoms are present in the sample, you can use a more “tricky” transformation called a Wavelet. As a result, the Wavelet analysis will give a 3-dimensional graph, which can later be applied to machine learning.

The relevance of this method is that it is possible, for example, to study binuclear catalysts. Obtaining exactly binuclear catalysts and their research is one of the priority tasks of chemistry, since it is such substances that are economically profitable.

PDF and XRD Analysis of Promoted Layered Double Ni-Al-O Catalysts for Oxidative Dehydrogenation of Propane

Kardash T.Yu., Cherepanova S.V., Stonkus O.A., Ivanova A.S., Bondareva V.M.
Boreskov Institute of Catalysis, Novosibirsk, Russia
kardash@catalysis.ru

NiO-based mixed oxides are the perspective catalytic materials for various processes; among which oxidative dehydrogenation of ethane and propane to ethylene and propylene attract scientific attention. According to the literature data [1], one of the best results are obtained for NiO catalysts promoted by acidic dopands (Nb^{5+} , W^{6+} , Mo^{6+}). Ni-Al layered double hydroxides (LDH) having hydrotalcite-like structure are the promising precursors of NiO-based oxidative dehydrogenation catalysts.

To promote Ni-Al oxide, it is possible to introduce doping element into the initial hydroxide structure. We are studying the influence of the nature of the interlayer anion $\{A = [\text{H}_2\text{W}_{12}\text{O}_{40}]^{6-}, [\text{Mo}_7\text{O}_{24}]^{6-}, \text{VO}_3^-, [\text{NbO}(\text{C}_2\text{O}_4)_3]^{3-}\}$ in Ni-Al-hydroxides on structural, textural, redox and catalytic properties of calcined Ni-Al samples in the propane oxidative dehydrogenation reaction. Catalytic testing in the propane oxidative dehydrogenation revealed the difference in catalytic properties for different modifiers.

Modified dried Ni-Al samples obtained by introducing an anion $[A]^{n-}$ in the interlayer space retain the layered hydrotalcite-like structure, but more distorted. Thermal treatment of the samples at 450–600°C promotes the formation of a solid solution with NiO basis of the parameter a value which is lower than that of pure NiO, and after calcination at 900°C - a mixture of phases NiO, NiAl_2O_4 and $\text{Ni}_x\text{M}_y\text{O}_z$ ($M = \text{W}, \text{Mo}, \text{V}, \text{Nb}$).

For a structural analysis both PDF and XRD methods were applied. Experimental data were measured at ID15a station at ESRF (Grenoble, France), $\lambda = 0.1428 \text{ \AA}$ and Dectris Pilatus3 X 2M detector utilising a CdTe sensor. In order to study the process of thermal decomposition of modified hydrotalcite-like structure, in-situ XRD measurements of Ni-Al samples during isothermal annealing was performed.

X-ray diffraction and PDF analysis showed that when heated, the destruction of Ni-Al- CO_3 hydrotalcite does not occur, but a gradual transformation of the structure occurs due to local reorganization of atoms after the removal of water molecules (dehydrated phase) and subsequent removal of CO_3 and OH groups (Ni-Al oxide). The mixed oxide has a lamellar shape and consists of NiO octahedral layers and mixed spinel layers. In the structure of NiO there are cations in tetrahedral positions ordered, as in the structure of spinel, i.e. the structure of NiO contains spinel clusters of the NiAl_2O_4 type.

References:

[1] Sanchis R., Delgado D., Agouram S., Applied Catalysis A 536 (2017) 18.

Nature of Pd Sites Supported on Covalent Triazine Frameworks

Bulushev D.A.¹, Golub F.S.¹, Trubina S.V.², Zvereva V.V.²

1 – Boreskov Institute of Catalysis, Novosibirsk, Russia

2 – Nikolaev Institute of Inorganic Chemistry, Novosibirsk, Russia

dmitri.bulushev@catalysis.ru

The main components of covalent triazine frameworks (CTFs) are carbon, nitrogen, hydrogen and sometimes oxygen. The specific surface areas of CTFs and their thermal stability are very high. Their surface sites can stabilize deposited metals in the form of nanoparticles, molecular complexes, and single atoms. This could be the basis for their use as supports for catalysts. Formic acid is a known liquid organic hydrogen carrier. The present work was focused to the development of single-atom Pd catalysts supported on CTFs for hydrogen production from gas-phase formic acid. Catalysts with single-atom metal sites often exhibit a higher activity in this reaction than catalysts with nanoparticles and, therefore, are of interest to researchers [1].

In this work, five CTFs materials were prepared from various organic precursors containing nitrile groups. Pd (1 wt%) was deposited by the impregnation method, and the resulting materials were investigated in hydrogen from formic acid. The materials treated in a 2.5 vol% HCOOH/Ar flow at 573 K were characterized by EXAFS/XANES, HAADF/STEM, XPS, BET, DRIFTS, CHNS, and XRD methods [2,3].

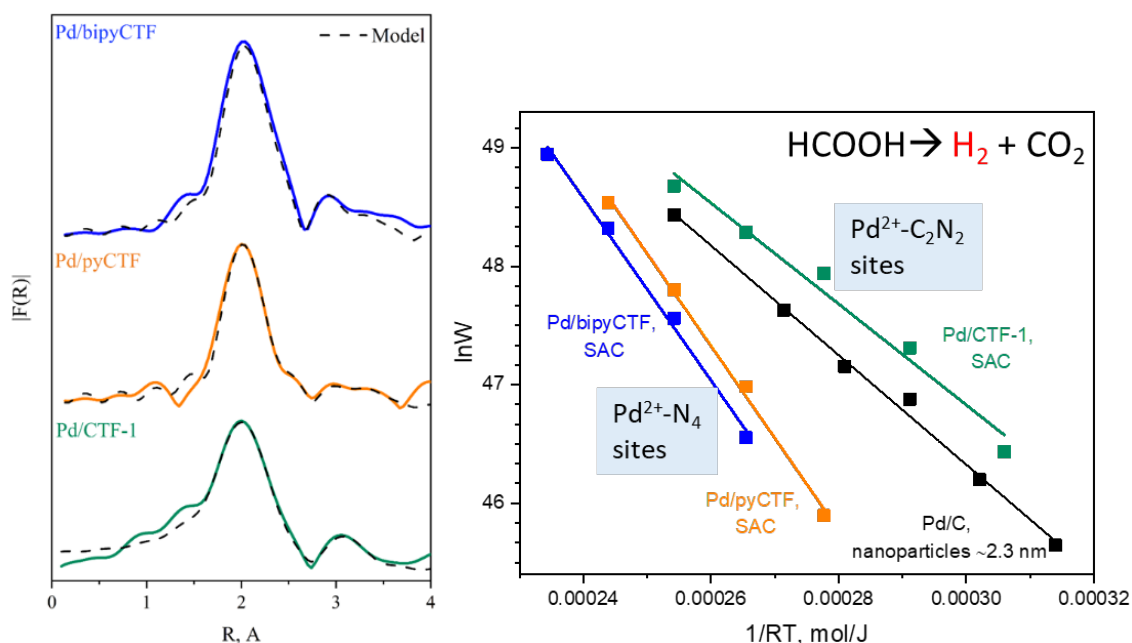


Fig. 1. EXAFS spectra and Arrhenius plots for the single-atom Pd catalysts

It has been shown that the activity and selectivity of the catalysts are determined by the molecular structure of the active Pd sites. Catalysts with Pd²⁺-N₄ and Pd²⁺-O₄ sites showed low activity, while the catalysts with Pd²⁺-C₂N₂ and Pd²⁺-CN₃ sites showed a significantly higher

OP-20

activity which exceeded the activity of metal particles (1-5 nm) deposited on porous carbon and graphitic carbon nitride. Therefore, it seems promising to use CTFs as catalyst supports.

Acknowledgement: This work was supported by the Russian Science Foundation, grant 22-23-00608.

References:

- [1] D.A. Bulushev, L.G. Bulusheva, *Catal. Rev.* 64 (2022) 835.
- [2] D.A. Bulushev, et al. *ACS Appl. Nano Mat.* 5 (2022) 12887.
- [3] D.A. Bulushev, et al. *ACS Appl. Nano Mat.* (2023) submitted.

2-1 “High Energy for Structural Materials Research” Beamline Concept for the Synchrotron Radiation Facility “SKIF”

Dovzhenko G.D.^{1,2}, Emurlaev K.I.¹, Kutkin O.M.¹, Burdilov A.A.¹, Nasyrova A.K.¹, Zverev D.A.³, Snigirev A.A.³, Bataev I.A.¹

1 – Novosibirsk State Technical University, 20 Prospekt K. Marksa, Novosibirsk, 630073, Russian Federation

2 – Siberian Circular Photon Source “SKIF” Boreskov Institute of Catalysis of Siberian Branch of the Russian Academy of Sciences (SRF “SKIF”), 1 Nikol’skii pr., Kol’tsovo, 630559, Russian Federation

*3 – Immanuel Kant Baltic Federal University, 14A Nevskogo ul., Kaliningrad, 236016, Russian Federation
g.d.dovjenko@srf-skif.ru*

SRF “SKIF” is a generation 4+ synchrotron radiation (SR) source being built in Koltsovo city near Novosibirsk [1]. Its storage ring will have the circumference of 476 m and the stored electron energy will be 3 GeV. SRF “SKIF” will be launched with 6 operational “first-stage” beamlines, and then new ones will be added until the storage ring capacity of 30 beamlines is reached.

This work describes the concept of a “second-stage” beamline designed in collaboration between Novosibirsk State Technical University (NSTU), Immanuel Kant Baltic Federal University (IKBFU), and SRF “SKIF”. The technical specifications of the beamline are planned to be established by the end of 2023, and the production, installation, and launch will follow according to the SRF “SKIF” timeline.

The scientific domain of the presented beamline is structural and functional materials science, specifically diffraction and imaging-based techniques. Typical science cases include:

1. Materials performance under thermomechanical processing, including additive manufacturing;
2. Fracture mechanics;
3. Radiation damage;
4. Materials synthesis technologies, e.g. Spark Plasma Sintering (SPS), dealloying, etc.

Since structural materials science often deals with both large and strongly absorbing samples (Ti- or Ni-based alloys, etc.), high photon energy and high brilliance are required, especially for timing resolution sensitive in situ and operando experiments. Hence, a superconducting wiggler was chosen as the beamline’s insertion device, and the main goal of the beamline optics is to focus the wiggler’s radiation in a sub-millimetre sized spot.

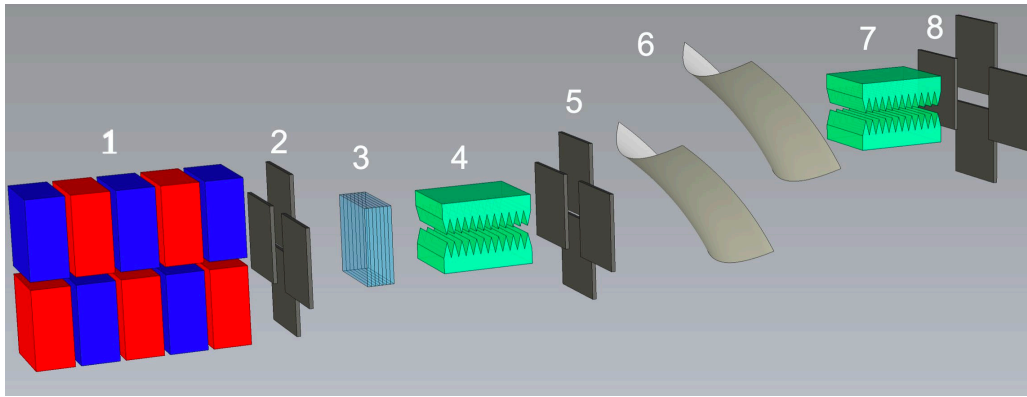


Fig. 1. HESMR optical layout

Fig. 1 shows the beamline's optical layout. A superconducting wiggler (1) developed by Budker Nuclear Physics Institute (BNPI) will be used as an insertion device. While it will provide the necessary high photon energy (30-90 keV) flux on a 3 GeV ring, its downsides are high thermal load, large source size, and high beam divergence. To moderate the thermal load, a set of diamond and SiC filters (3) will be installed in the front-end after the fixed mask (2). In order to focus the beam vertically and decrease the thermal load on the monochromator, a set of alligator-type lenses developed by IKBFU (4) will be installed after the front-end. The lenses coupled with the slits (5) will perform beam pre-monochromatization. A sagittally bent double-crystal Laue monochromator (SBDCLM) developed by Technological Design Institute of Scientific Instrument Engineering (TDIoSIE) (6) will focus the beam horizontally. And finally, a second set of alligator lenses (7) will focus the beam vertically and produce a beam spot on the exit slits (8) around 100-300 μm horizontally by 10-30 μm vertically. The expected photon flux of the order 10^{11} ph/s at 90 keV and 10^{13} ph/s at 30 keV should provide enough flux for 100 kHz diffraction experiments and ~ 10 kHz imaging experiments. The beamline layout was optimised using ray-tracing software package XRT [2].

Since the beamline's most important feature will be in situ and operando experiments, a set of various sample environments will be available for the future users, as well as a possibility to install their own. A graphite dome vacuum furnace and a tensile testing machine will allow standardised materials performance testing with an additional insight into the microscopic scale evolution, and a custom designed Selective Laser Melting (SLM) 3D printer will help enable in-depth investigations of modern manufacturing processes.

References:

- [1] Bukhtiyarov A. V. et al. Synchrotron Radiation Facility "Siberian Circular Photon Source"(SRF SKIF) //Crystallography Reports. – 2022. – T. 67. – №. 5. – C. 690-711.
- [2] Klementiev K., Chernikov R. Powerful scriptable ray tracing package xrt //Advances in Computational Methods for X-Ray Optics III. – SPIE, 2014. – T. 9209. – C. 60-75.

Radiation-Resistant Luminescent Diamond Composites Based on Polycrystalline Diamond with Embedded Oxide and Fluoride Nanoparticles

Kuznetsov S.V.¹, Ermakova Yu.A.¹, Sedov V.S.¹, Boldyrev K.N.², Batygov S.Ch.¹,
Alexandrov A.A.¹, Drobysheva A.R.¹, Martyanov A.K.¹, Rezaeva A.D.¹, Voronov V.V.¹,
Tiazhelov I.A.¹, Tarala V.A.³, Vakalov D.S.³

1 – Prokhorov General Physics Institute of the Russian Academy of Sciences, Moscow, Russia

2 – Institute of Spectroscopy of the Russian Academy of Sciences

*3 – Scientific and Laboratory Complex Clean Room, North Caucasus Federal University
kouznetzovsv@gmail.com*

The development of studies of biomolecules, crystal structure of bulk materials and micro/nano-objects requires the use of high-power sources of X-ray radiation. Their efficient operation requires detectors (scintillators) and visualizers with high thermal conductivity, hardness and stable characteristics under intense, long-term exposure to ionizing radiation. One of the most robust materials for these applications is diamond. Single-crystal diamonds with nitrogen-vacancy color centers (NV), which are grown by the high-pressure high-temperature method (HPHT) or chemical vapor deposition (CVD), are limited in size to few millimeters in thickness and sub-inch range laterally. An alternative is polycrystalline diamond (PCD) films, that can reach up to 7-inch in diameter with a thickness reaching few millimeters. The further development of the approach to form new diamond-based scintillating materials lies in the synthesis of composite films consisting of a transparent CVD-grown PCD matrix and embedded X-ray luminescent nanoparticles [1]. A search for the best-suited composition for the material of such luminescent nanoparticles is ongoing.

Here, $Y_3Al_5O_{12}:Ce$, $SrF_2:Eu$, $SrF_2:Eu:Ba$ and $\beta-NaGdF_4:Eu$ nanopowders were synthesized by precipitation from aqueous solutions with following thermal treatment and embedded inside the diamond. The conditions for the embedded of nanoparticles into the diamond are determined. The requirements for nanoparticles for their successful embedding into diamond with a subsequent luminescent response are determined. The processes occurring during the embedding of nanoparticles under the influence of methane-hydrogen plasma during the growth of a diamond film by chemical vapour deposition technique are revealed. The concentration dependence of the X-ray and photoluminescence intensity has revealed, and the most optimal composition with the brightest luminescence response was determined. The obtained type of nanoparticles has potential applications for the fabrication of new scintillating and visualizing composites.

Acknowledgement: This work was supported by the Russian Science Foundation, grant 22-13-00401.

References:

[1] V. Sedov, S. Kuznetsov, A. Martyanov, V. Ralchenko. *Functional Diamond* (2022) 2:1 (2022) 53.

Composite Diamond Thin Film with Embedded Fe-Based Nanoparticles

Knyazev Yu.V.¹, Kuznetsov S.V.², Sedov V.S.², Martyanov A.K.², Tyazhelov I.A.²,
Nikolenko A.D.³, Platunov M.S.³, Semenov S.V.¹, Shestakov N.P.¹

1 – Kirensky Institute of Physics, Federal Research Center KSC SB RAS, Krasnoyarsk, Russia

2 – Prokhorov General Physics Institute of the Russian Academy of Sciences, Moscow, Russia

3 – Synchrotron radiation facility SKIF, Boreskov Institute of Catalysis SB RAS, Koltsovo, Russia
yuk@iph.krasn.ru

Design of the functional materials is permanently on the agenda. At last times, functional diamond-based materials attract a great interest due to their unique characteristics [1, 2]. Here, we present the synthesis and characterization of the functional magnetic material based on diamond thin films with embedded Fe-based nanoparticles. The synthesis consists of several stages. Diamond thin films were grown on silicon substrate by chemical vapour deposition (CVD) technique in vacuum in H_2/CH_4 plasma. Then, the Fe-based magnetic fluid was deposited on first diamond film. Then, the second CVD process was carried out with embedding Fe-based nanoparticles into diamond. Finally, a set of the composite diamond film were prepared.

The synthesized samples were characterized by SEM microscopy (see Fig. 1a), TEM microscopy, magnetization measurements, EXAFS and Mössbauer spectroscopy. Our results show that non-oxidized iron embedded between diamond layers (Samples 1 and 2), according to EXAFS (Fig.1b) and Mössbauer data in contrast to iron oxide on the sample's surface (Sample 3).

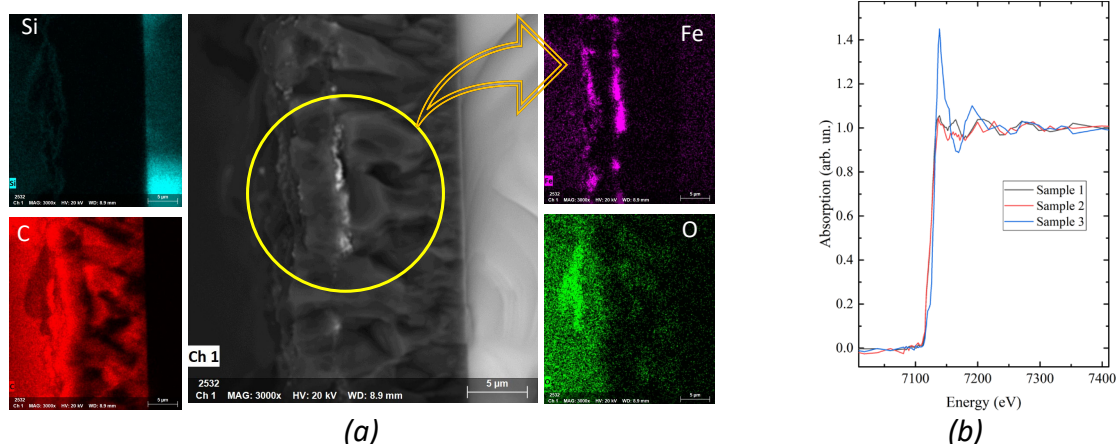


Fig. 1. SEM image and EDX mapping of the sample's end surface (a) and EXAFS spectra of three samples (b)

We believe that such iron embedding inside diamond may open the way to achieve high pressure in bulk samples like in diamond anvil cells.

Acknowledgement: This work was supported by the Russian Science Foundation, grant 22-13-00401. The research contribution of M. P. was funded by the Ministry of Science and Higher Education of the Russian Federation via the budget project of SRF SKIF, Boreskov Institute of Catalysis (project AAAA-A21-121011390011-4). The research contribution of Yu. K. was funded within the state assignment of Kirensky Institute of Physics.

References:

- [1] V. Sedov, S. Kuznetsov, A. Martyanov, V. Ralchenko. Functional Diamond (2022) 2:1 (2022) 53
[2] A. Yu., Neliubov et al., Phys. Rev. B(2023) 107, L081406

In situ XPS and NEXAFS Study of Halogenated Carbon for Accumulation of Alkali Metals

Fedoseeva Yu.V.¹, Vorfolomeeva A.A.¹, Shlyakhova E.V.¹, Sysoev V.I.¹, Makarova A.A.², Smirnov D.A.³, Bulusheva L.G.¹, Okotrub A.V.¹

1 – Nikolaev Institute of Inorganic Chemistry SB RAS, 3 Acad. Lavrentiev Ave., 630090 Novosibirsk, Russia

2 – Physical Chemistry, Institute of Chemistry and Biochemistry, Freie Universität Berlin, 14195 Berlin, Germany

3 – Institut für Festkörper- und Materialphysik, Technische Universität Dresden, 01062 Dresden, Germany
fedoseeva@niic.nsc.ru

Carbon materials are widely used as the active electrode materials for different electrochemical devices such as lithium-ion accumulators and supercapacitors by taking advantages of good electrical conductivity, high chemical stability, high surface area and pore structure. Defects inside carbon structure, functional groups and heteroatom-doping can improve the electrochemical performance. In this work, we study mesoporous N-doped carbon as anode material for sodium-ion accumulation. The anode materials were brominated and fluorinated in gas phase using Br₂ and BrF₃ as reactive agents. We found that the presence of defects and halogen atoms in the carbon materials resulted in the increase in their sodium-ion storage capacity. To gain insight into the effect of the interaction of sodium with halogenated carbon nanomaterials we used in situ X-ray photoelectron spectroscopy (XPS) and near-edge X-ray adsorption fine structure (NEXAFS) study. Sodiation and XPS and NEXAFS experiments were carried out on the Russian-German beamline (RGLB Dipole, BESSY II, Berlin, Germany) operated by Helmholtz-Zentrum Berlin für Materialien und Energie. In this model experiment, thermally evaporated sodium were deposited on the surface of carbon materials (graphite, porous carbon and N-doped porous carbon) and their brominated and fluorinated derivatives. Carbon nanotubes, graphite, porous carbon nanomaterials modified with nitrogen and bromine have been studied. The deposition of sodium was carried out in an ultra-high vacuum simultaneously on the surface of samples. After sodiation, the samples interacted with molecular oxygen or annealed in order to remove bonding between sodium with carbon. XPS and NEXAFS spectra were detected for initial samples and after sodiation and desodiation impact. The changes in the composition and electronic structure of carbon nanomaterials after their interaction with sodium were revealed. Quantum chemical calculation results were used for interpretation of the experimental data.

Acknowledgement: The work was financially supported by the Russian Science Foundation (grant 19-73-10068).

Current Status of the Development of a One-Coordinate X-Ray Counting Detector

Aulchenko V.M.¹, Glushak A.A.^{1,2,3,4,5,6}, Zhulanov V.V.^{1,2}, Titov V.M.¹, Shekhtman L.I.^{1,2,3,5}

1 – Budker Institute of Nuclear Physics SB RAS, Novosibirsk, Russian Federation

2 – Novosibirsk State University, Novosibirsk, Russian Federation

3 – Synchrotron Radiation Facility SKIF, Boreskov Institute of Catalysis SB RAS, Novosibirsk, Russian Federation

4 – Tomsk State University, Tomsk, Russian Federation

5 – Institute of Solid State Chemistry and Mechanochemistry, SB RAS, Novosibirsk, Russian Federation

6 – Novosibirsk State Technical University, Novosibirsk, Russian Federation

A.A.Glushak@inp.nsk.su

The one-coordinate X-ray detector for dynamic diffraction experiments for SRF SKIF is being developed at the Institute of Nuclear Physics of the Siberian Branch of the Russian Academy of Science. This detector can be used for studying structural-phase transformations in functional and structural materials by X-ray powder diffraction methods under the impact of high temperatures and reaction media.

In order to achieve a spatial resolution of better than 100 microns for photons with energy of 3-30 keV it is necessary to use a solid-state microstrip or pixel sensors in combination with specialized integrated circuits (ASIC). In the first version of prototype of the counting detector SciCODE the microstrip coordinate sensor based on gallium arsenide (GaAs) with strip pitch of 50 μm was used. In the new version of the prototype of SciCODE a silicon microstrip sensor also with a strip pitch of 50 μm is used. The detector operates in direct photon-counting mode, provides a spatial resolution of better than 100 microns and a counting rate of 1 MHz/channel. A specialized integrated circuit SciCODE8 has been developed for signal registration from the sensor strips in the detector. SciCODE8 has 8 electronic channels which can register individual photons and sort them according to their energy. Firmware and software were also developed for the detector prototype [1]. The main parameters of the detector electronics were measured. In addition, a 64-channel specialized integrated circuit SciCODE64 was developed and put into production, in which the necessary changes were made to the registration channel.

Acknowledgement: The work was partially supported by a grant under the Resolution of the Government of the Russian Federation 220 dated April 09, 2010. (Agreement 075-15-2022-1132 of 01.07.2022)

References:

[1] Aulchenko, V.; Glushak, A.; Shekhtman, L.; Titov, V.; Zhulanov, V. One-Dimensional Detector for Diffraction Experiments at a Synchrotron Radiation Beam. *Physics of Particles and Nuclei Letters*, Vol. 19, Is. 5, 2022.

Microfluidic Systems for the In Situ X-Ray Spectral Diagnostics and Screening of Synthesis Parameters

Guda A., Shapovalov V., Chapek S., Bulgakov A., Soldatov A.V.

The Smart Materials Research Institute, Southern Federal University, 344090, Rostov-on-Don, Russia
guda@sfedu.ru

In this work we demonstrated application of this approach to study of the relationships between Ag nanoparticle optical properties, size distribution and reaction parameters. Using in situ UV-Vis absorption spectroscopy and synchrotron based small angle X-ray scattering (SAXS) we were able to quickly screen the impact of synthesis conditions on surface plasmon resonance properties, growth time, size and polydispersity of Ag nanoparticles. ML models were further trained on the in situ UV-Vis data and demonstrated high prediction quality. The trained algorithm can be applied for the inverse problem to predict the experimental parameters required to obtain NPs with given spectral response. As an example, we were able to conclude that in our setup the most monodisperse NPs with the strongest plasmon resonance red-shifted peak should be obtained with nearly stoichiometric ascorbic acid and silver nitrate ratio with slight ascorbic acid excess, which was further validated by SAXS measurements. The approach, based on a 3d printed microfluidic devices optimized for conventional in situ spectroscopic characterization will increase the throughput of material diagnostics in laboratories and synchrotrons and accelerate the development of new functional nanomaterials.

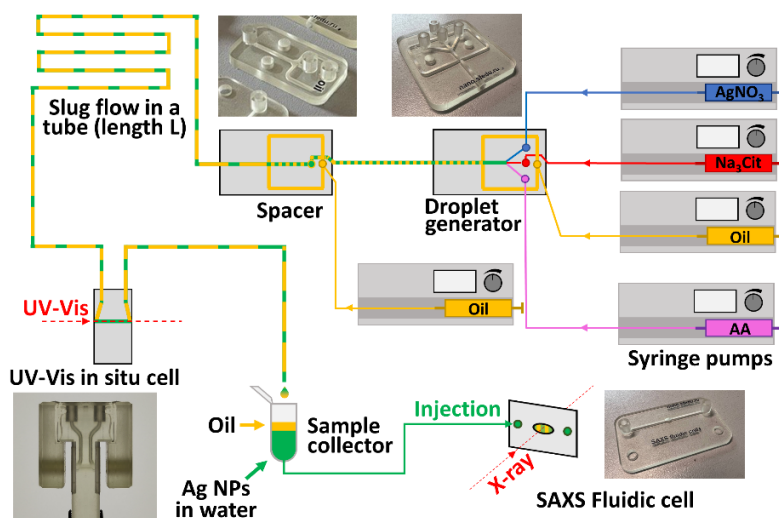


Figure 1. Scheme of the experimental setup

Efficient optimization of microfluidic synthesis requires in situ diagnostics and online data processing. In our work we demonstrate simple and versatile system based on 3d printed microfluidic components. DLP-SLA technology allows to easily manufacture microfluidic devices tailored to a specific need, such as mixing, water-in-oil slug generation and separation, in situ cells for UV-Vis spectroscopy and SAXS. Oil soaking of 3d-printed chips improves hydrophobicity of channel surface and use of the slug flow further prevents nanoparticle growth the channel walls and cuvette windows. Use of sufficiently long slugs and optimized optical path in the cuvette allows to obtain high-quality in situ optical spectroscopy data in a single shot from a

single slug, enabling the ability to test dozens of combinations of parameters per hour. For synchrotron studies it allows to obtain in situ data from slugs directly through a FEP tube in quasi-stationary regime, without need of microfocus beam and synchronization. The proposed system, combined with automated experiment control software, IHS-based sampling algorithm allows rapid and efficient screening of microfluidic reaction parameters

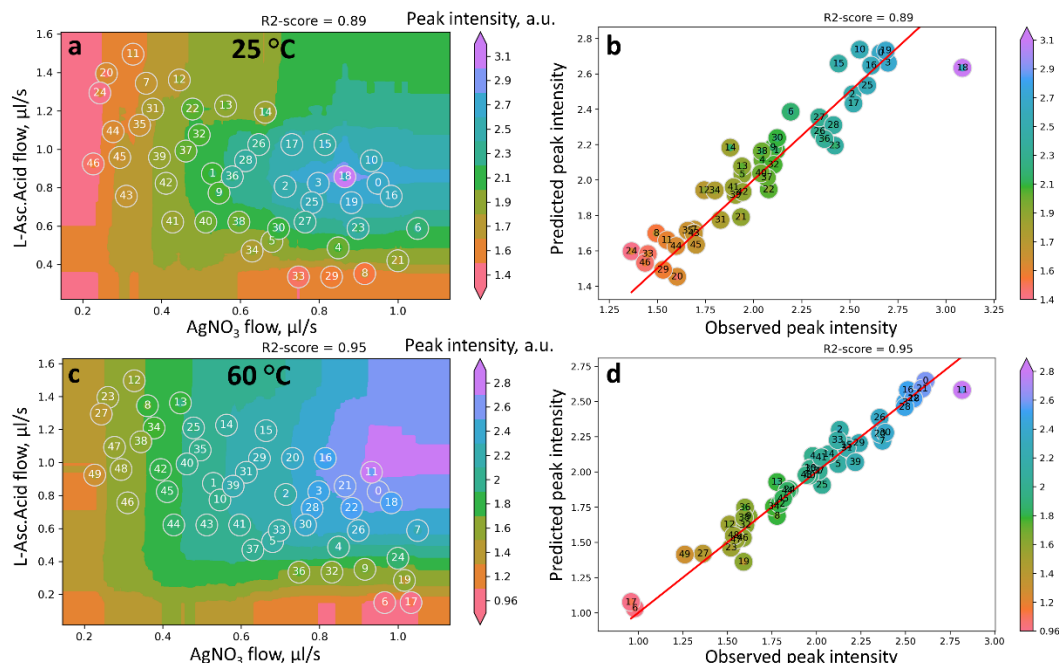


Figure 2. Model predicting the surface plasmon resonance peak intensity in the UV-Vis spectra of silver nanoparticles as a function of AgNO₃ and L-ascorbic acid flow rates for the synthesis at 25 °C (a) and 60 °C (c).

The set of descriptors of spectra was further analyzed using machine learning methods to obtain a model predicting the surface plasmon properties of Ag nanoparticles based on the synthesis conditions. The flow rates of the reactants were chosen as a set of variable parameters, while the position and intensity of the plasmon resonance peak were chosen as the main spectral descriptors for prediction. The background color in Figure 2 shows the results of the ML model training. The algorithm was trained on the basis of experimental points (white circles) and then it was applied to predict value of LSPR peak intensity and position at any point of the parameters space. The obtained models were cross-validated (using leave-one-out scheme) and checked for consistency with the experimental data and found to be highly reliable (minimal determination coefficient R²-score \geq 0.84). The higher value of the coefficient for the synthesis at 60 °C may indicate due to the narrower distribution of the characteristics of silver nanoparticles formed at this temperature, as elevated temperature might catalyze the reduction activity of trisodium citrate.

Acknowledgement: The authors acknowledge the Ministry of Science and Higher Education of the Russian Federation for the financial support (Agreement no. 075-15-2021-1363).

References:

Guda, A.A., et al., *The Journal of Physical Chemistry C* **127(2)**: p. 1097-1108 (2023)

Characterization of Altai Wapiti Chymosin Interaction with the Chymosin-Sensitive Region of Three Different κ -Caseins: Experimental and Modelling Studies

Borisevich S.S.¹, Ilyina M.G.¹, Khamitov E.M.², Diusenova S.E.^{1,3}, Belenkaya S.V.⁴, Shevtsov M.B.⁵, Borshchevskiy V.I.⁵, Kolosov P.V.⁶, Volosnikova E.A.⁴, Elchaninov V.V.⁷, Kolybalov D.S.^{1,3}, Arkhipov S.G.^{1,3}, Shcherbakov D.N.⁴

1 – Synchrotron Radiation Facility - Siberian Circular Photon Source "SKIF" Boreskov Institute of Catalysis of Siberian Branch of the Russian Academy of Sciences, Koltsovo, Russia

2 – Ufa Institute of Chemistry, Ufa Federal Research Center of the Russian Academy of Sciences, Ufa, Russian Federation

3 – Novosibirsk State University, Novosibirsk, Russia

4 – State Research Center of Virology and Biotechnology Vector, Koltsovo, Russia

5 – Research Center for Molecular Mechanisms of Aging and Age-Related Diseases, Moscow Institute of Physics and Technology, Moscow, Russia

6 – Altai State University, Barnaul, Russia

7 – Federal Altay Scientific Centre of Agrobiotechnologies, Siberian Institute of Cheese Making

sophiamonrel@gmail.com

Chymosin (Chym) is a milk-clotting enzyme (MCE) that belongs to the group of aspartate proteases. This enzyme is an essential component in the industrial production of cheese. The main biochemical characteristic of Chym as an MCE is a specific activity, which refers to its ability to hydrolyze (by Asp34 and Asp216 residues) the specific peptide bond located between 105 and 106 residues of κ -casein (κ C) and causes milk coagulation. Currently, there are only two molecular structures of Chym available: bovine (*Bos taurus*) (ChymB) and camel (*Camelus dromedarius*) (ChymC). Studies show that despite the enzymes structural folds and sequences similarity, ChymB is not able to coagulate camel milk, while ChymC can effectively do it with bovine milk [1]. The other type of Chym from an altai wapiti (*Cervus elaphus sibiricus*) (ChymW) showed similar to ChymB activity properties with three different κ C: altai wapiti (κ CW), bovine (κ CB) and camel (κ CC). According to chromatography-mass spectrometry, ChymW was found to hydrolyse the chymosin-sensitive part (96 - 119 residues) of κ CB and κ CW almost completely by 97 and 96% (pH 6.5), respectively, but it poorly hydrolyses the same part of κ CC by 19% (pH 6.5). Therefore, in order to understand the bonding process of κ Cs and ChymW, we studied the structural peculiar properties of three complexes: ChymW- κ CW, ChymW- κ CB and ChymW- κ CC using X-ray diffraction analysis and molecular dynamic methods.

The recombinant ChymW was obtained using the previously described methodology [2]. The protein was crystallized under the following conditions: 0.2 M CaCl₂, 0.1 M Tris (pH 8.0), 20% w/v PEG 6000. The obtained crystal form belongs to C2 space group with the cell parameters $a = 142.39(18)$, $b = 41.63(7)$, $c = 54.55(8)$ Å, $\beta = 98.311(8)^\circ$. The structure was

OP-27

solved by molecular replacement. The resulting structural model was refined at resolution 2.22 Å with the following validation parameters: $R_{work} = 19.81\%$ and $R_{free} = 24.23\%$.

The AlphaFold was used to predict the 3D structures of the chymosin-sensitive region for κ CB, κ CC and κ CW. To assess the affinity of the predicted κ Cs peptide fragments to ChymW, a protein-protein docking protocol was applied. Stable peptide-protein complexes obtained from the docking procedure were used for MD calculations, followed by selection of complex structures based on the RMSD of peptide segments across all MD frames (clustering) to find a statistically significant variant of peptide fragment positioning in the chymosin cavity. Using the theoretical approaches, the statistical probability of the κ Cs fragments positioning in the ChymW active site shows that the κ CB and κ CW fragments are closer to Asp34 and Asp216 inside the chymosin cleft compared to the κ CC fragment (fig.1).

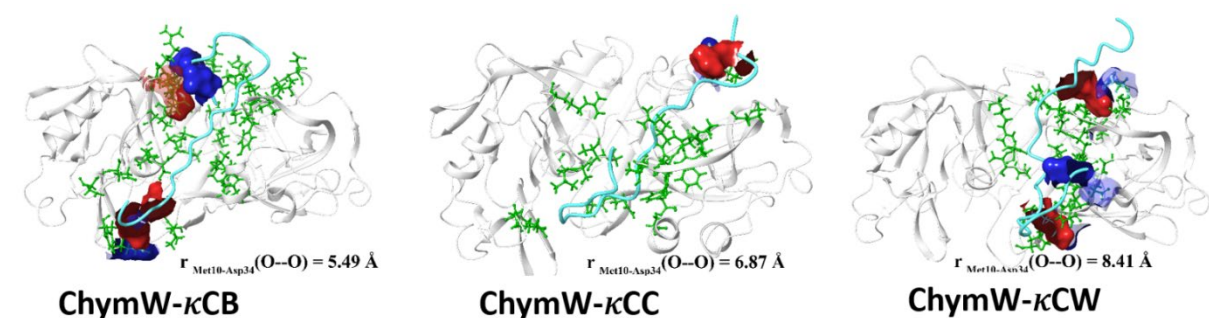


Fig. 1. The relative arrangement of key residues of the κ CB, κ CW and κ CC fragments with respect to the ChymW reactive center in pre-reaction complexes after the clustering procedure. The ChymW residues involved in interaction are highlighted in green.

References:

- [1] J. Langholm Jensen et al. J. Acta Crystallogr D Biol Crystallogr. 69 (5) (2013) 901.
- [2] S. V. Belenkaya, et al. J. Biotekhnologiya. 37 (2021) 20.

The Role of Small-Angle X-Ray Scattering and Molecular Simulations in Elucidation of Aptamers 3D Structure

Kichkailo A.S.^{1,2}, Zabluda V.N.^{1,3}, Moryachkov R.V.¹, Tomilin F.N.^{1,3}

1 – Federal Research Center “Krasnoyarsk Science Center SB RAS,” Krasnoyarsk, Russia

2 – Krasnoyarsk State Medical University, Krasnoyarsk, Russia

3 – Kirensky Institute of Physics, Krasnoyarsk, Russia

annazamay@yandex.ru

Small-angle X-ray scattering (SAXS) is a powerful synchrotron radiation technique for studying the overall shape and structural transitions of biomolecules in solution at nanometer resolution [1]. It is a well-established method for structural investigation of proteins, peptides, DNA, and RNA, and their complexes in solution quasi-physiological conditions [2]. SAXS has several advantages over the other methods of structural analysis: it does not require complicated sample preparation, and it features fast data collection and processing. This method is exceptionally useful for the elucidation of the spatial structures of the proteins and peptides, short DNAs, RNAs, and other small biological objects from 2 to 1000 nm and 5 kDa to 100 MDa in their native state in solution with the adjustable temperature, pH, and buffer composition [2,3].

SAXS can be used to the discovery of the binding sites and molecular interactions between different molecules. Using SAXS method we get the information about the maximum particle size, radius of gyration, molecular weight, volume, and spatial shape. The working concentration of the sample can vary from 0.5 to 10 mg/ml, volume 10 to 100 μ l [1-3].

Recent progress in molecular medicine has made ssDNA a useful tool with various applications. An important feature of DNA aptamers is mimicking antibodies. The molecular structure of this oligonucleotides determines their function. The promising approach to determine molecular shape in solution is a combination of SAXS together with molecular dynamic simulations. Computer modeling is used to sample possible conformations that molecules adopt in the solution, and ensembles of such structures can be re-weighted to fit into the SAXS experimental curves [2]. Initially in vitro selected 80-nucleotide aptamers have two constant 20-nucleotide primer regions on each side for PCR amplification [4]. There is a strong need to reduce the size of this aptamers for enhancing its binding properties and making it cheaper to synthesize. In this work, a much-truncated LC-18 (LC-18t) (Fig. 1A) is proposed. To obtain the molecular structure, a combination of theoretical methods, namely, DNA folding tools, quantum-chemical calculations, and MD simulations, were used (Fig. 1B). The simulated structures were compared with the experimental SAXS shape (Fig. 1C). The efficacy of the new truncated aptamer was verified experimentally for cancerous cells. It demonstrated the binding properties alike to those of its predecessor LC-18 [4].

For atomistic modelling of aptamer structures we suggest the following protocol: (1) use SAXS to determine the shape of the aptamer in an experiment, (2) do the initial design of

OP-28

molecular models by using OligoAnalyzer or MFold, (3) perform molecular modeling by using computational methods such as FMO or MD, and (4) compare atomic structure from simulations with the measured SAXS curve using CRY SOL or WAXSIS programs.

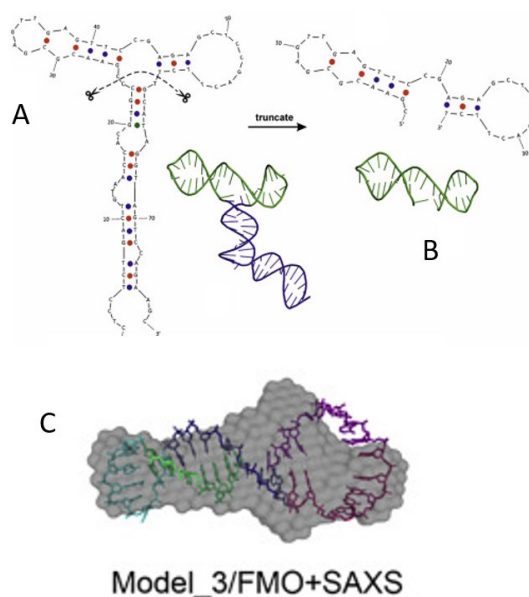


Fig. 1. Molecular modeling of the aptamer structure, its truncation and fitting to SAXS model.

The proposed procedure could also be employed for aptamer-target complexes. And by obtaining a reliable atomistic structure from simulations, one can rationalize the binding of an aptamer to a protein target. This can be very helpful in designing new, more efficient aptamers based on insight gained from molecular simulations.

Acknowledgement: This work was supported by the Russian Science Foundation grant no. 21-73-20240.

References:

- [1] Da Vela S., Svergun D. I. // Current research in structural biology. - 2020. - T. 2. - S. 164-170.
- [2] Tomilin F. N. et al. //Analytical and bioanalytical chemistry. - 2019. - T. 411. - No. 25. - S. 6723-6732.
- [3] Kikhney A. G., Svergun D. I. //FEBS letters. - 2015. - T. 589. - No. 19. - S. 2570-2577.
- [4] Morozov D. et al. //Molecular Therapy-Nucleic Acids. - 2021. - T. 25. - S. 316-327.

Microfluidic Synthesis of Vinyl Iodide

Bulgakov A.N., Krasnyakova I.O., Guda A.A., Soldatov A.V.

*The Smart Materials Research Institute at Southern Federal University, Rostov-on-Don,
Russia*

alexeybulgakov359@gmail.com

In catalysis, researchers always strive to maximize the catalyst performance and increase the product yield. Many researchers are trying to improve the catalyst itself when improvement of experimental conditions can have more impact. But selection of optimal reaction conditions to maximize the product yield during catalysis is a complicated task due to the influence of many factors affecting the process. Our main goal is to develop a universal method that allows us to establish the conditions under which the product yield on a particular catalyst will be maximum. In past recent years, microfluidic synthesis based on manipulates a small amount of fluids using small channels with sizes ten to hundreds micrometres have attracted a lot of attention and even largely formed new approaches to chemical engineering.[1] Here, the catalytic reaction is performed in some dynamically changed conditions using all benefits of microfluidic synthesis.

In this work, we performed optimization for synthesis of vinyl iodide taking place on the surface of commercial Pt nanocatalysts (K_2PtCl_6 , Sigma Aldrich) in presence of NaI and the addition of acetylene using the microfluidic system. First, we carried out several classic experiments in a flask at different temperatures (60 °C, 80 °C) analyzing reaction products by mass and Fourier-transformed infrared spectroscopies. Then, we have moved on to microfluidic synthesis to compare the effectiveness of this approach with the classical method. Finally, we optimized gas and liquid flows for more effective processes of catalytic reaction. For this aim, we have tried several flow relations in the range from 10 times larger gas flow in comparison to liquid flow to 100 times larger gas flow in comparison to liquid flow. Because of the unique chemical and physical features that occur in micron-sized fluids, this allows several advantages over traditional "macro" technologies. In addition, microfluidics devices are generally easy to use and produce, as well as cost-effective. Also, we have performed XAS spectra measurements under laboratory conditions, to determine the environment of iodine during the reaction.

As a result, we obtained improved solution for more effective way to synthesize vinyl iodide. Application of microfluidics approach demonstrated their supremacy over the classic synthesis.

This methodology opens a perspective for the optimization of relevant catalytic reactions using microfluidics by rational use of reactants and varying conditions. The demonstrated approach can be expanded for optimization of many other industrially relevant reactions and catalytic systems.

Acknowledgement: The research was supported by the Strategic Academic Leadership Program of the Southern Federal University ("Priority 2030").

References:

[1] Armstrong C.; Teixeira A., *React. Chem. Eng.*, (2020) 5 (1985) 2185–2203.

**Experimental Beamline “Serial Macromolecular Crystallography”
at 4th- Generation Synchrotron Radiation Source “SILA”**

Dorovatovskii P.V., Lazarenko V.A., Svetogorov R.D.
NRC “Kurchatov institute”, Moscow, Russia
Paulgemini@mail.ru

For the moment new facility "SILA" (synchrotron-laser), which will have no analogues in the world and will surpass in technical characteristics of the existing international sources of synchrotron radiation, is under development. Commissioning of the facility is planned for 2030.

12 experimental beamlines of the “first stage” will be implemented at the "SILA" synchrotron, with the possibility of expanding the list of stations to more than 40. One of the twelve beamlines will be dedicated to research in the field of macromolecular crystallography.

X-ray macromolecular crystallography, despite the strong development of electron microscopy techniques, are still remains the main method for obtaining the three-dimensional structure of macromolecules, whose capabilities were extended by the method of serial crystallography [1]-[2]. Future beamline “serial macromolecular crystallography” will be able to operate in several modes. Undulator source will cover all required energy range for macromolecular tasks. Due to three transfocator focusing scheme beamline will be able to operate in «pink beam mode», in «wide beam mode» and in «microfocus beam mode». In addition, due to the planned features of the diffractometer, it will be possible to quickly scan crystallization plates and “meshes”, as well as collect data of serial crystallography from few different crystals (only fixed target methods are planned to be implemented).

The high brightness of the source, the optical design of the beamline and the possibilities of the sample environment will make the beamline "serial macromolecular crystallography" flagship in the territory of the Russian Federation for the analysis of crystals of proteins, viruses and other macromolecular complexes.

References:

- [1] Ursby T. et al. MicroMAX—new opportunities in macromolecular crystallography //ACTA CRYSTALLOGRAPHICA A-FOUNDATION AND ADVANCES. – 2 ABBEY SQ, CHESTER, CH1 2HU, ENGLAND : INT UNION CRYSTALLOGRAPHY, 2021. – T. 77. – C. C817-C817.
- [2] Pearson A. R., Mehrabi P. Serial synchrotron crystallography for time-resolved structural biology //Current Opinion in Structural Biology. – 2020. – T. 65. – C. 168-174.

Poster Presentations

PP-1 ÷ PP-47

X-Ray Studies of Nanocluster Polyoxometalate Molybdenum Compounds

Akimov A.I.S.¹, Petrenko T.V.¹, Akimov A.S.^{1,2}

1 – Institute of Petroleum Chemistry SB of the RAS, Tomsk, Russia

2 – National Research Tomsk State University, Tomsk Russia

Akimov149@yandex.ru

To analyze the composition, structure, size, and shape of polyoxomolybdenum clusters, it is necessary to resort to various methods of analysis. Depending on the state of aggregation of the sample - liquid or solid phase (crystalline and amorphous), the range of methods also differs. Since the results of the XRF (powder diffraction) show that the solid phase product is almost completely X-ray amorphous. It follows from this that, like the XRD method, the method of X-ray diffraction analysis of a single crystal is also not applicable to similar samples. The main problem is the separation of molybdenum oxide clusters from the dispersion medium in crystalline form. To do this, it is required to destroy the layers of hydrate shells by using a significant amount of electrolytes [1].

Since in this work these compounds were initially obtained in the form of dispersions, we have to work with the sample in the liquid phase. In addition to IR spectroscopy, a complex of independent methods is required to characterize data due to the samples. For example, the simultaneous use of photon-correlation spectroscopy along with very high resolution microscopic methods (since the size of systems is on the order of 2-5 nm) [2], spectrophotometric analysis and Raman spectroscopy, an array of information (particle morphology, the presence / absence of nanocluster formations and a number of functional groups). Along with the above methods, one of the most promising methods for determining the structure and properties of molybdenum polyoxometalates is EXAFS spectroscopy.

Due to the fact that EXAFS- and XANES-spectroscopy methods allow obtaining unique information about the sample under study, which does not have long-range order. By analyzing the results obtained by EXAFS-spectroscopy after preliminary use of special methods of mathematical processing of experimental data, it is possible to identify distances, types, coordination numbers for various coordination spheres of the nearest environment of the studied atoms.

Acknowledgment: The work was carried out within the framework of the state task of the Institute of Chemical Sciences of the Siberian Branch of the Russian Academy of Sciences, funded by the Ministry of Science and Higher Education of the Russian Federation.

References:

- [1] A. Müller, S. Roy S, Coord Chem Rev. 245 (2003) 153-166.
- [2] T. Liu, E. Diemann, J Chem Educ. 84 (2007) 526-532.

Investigation of the Formation of a Ti-Al-Based Metal-Intermetallic Laminated (MIL) Composite during Heating Using Synchrotron Radiation

Aleksandrova N.S.

Novosibirsk State Technical University, Novosibirsk, Russia
aleksandrovanatalie99@gmail.com

The Ti-Al system is one of the metal systems predisposed to the chemical interaction of the initial metal components with the formation of intermetallics. It is noted that titanium aluminides have high hardness, heat resistance, corrosion resistance and low density [1]. In particular, MIL composites based on titanium and aluminum are considered promising materials for structural, aerospace and military applications due to the combination of high specific strength, relatively good impact toughness and low density [2, 3].

In this work, explosive welding was used to form the Ti-Al bimetal. Heat treatment was carried out to obtain a metal-intermetallic laminated composite. Diffraction patterns during heating were obtained using the VEPP-3 synchrotron radiation source at the Siberian Synchrotron and Terahertz Radiation Center. The experiments were carried out at the 6A beamline. The energy was 7.5 keV. The intensity map illustrating phase transformations and heating modes are shown in Figure 1, where the color change characterizes the intensity of reflections. Single diffraction patterns under various heat treatment modes and in the state after explosive welding are shown in Figure 2.

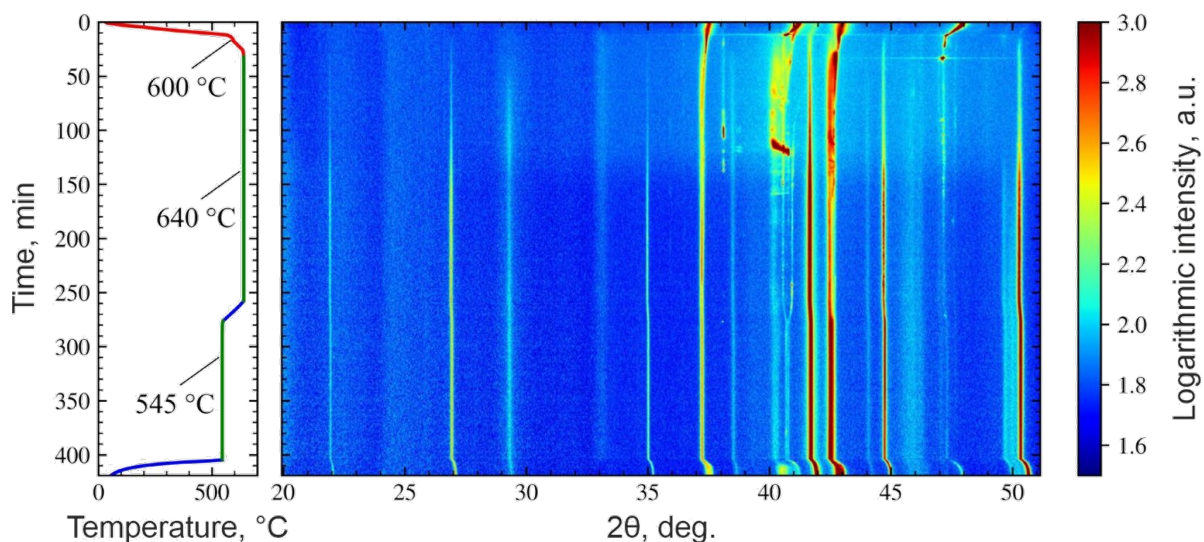


Fig. 1. The intensity map illustrating phase transformations and heating modes for Ti-Al-based MIL composite

The diffraction pattern before heating (Fig. 2a) shows that intermetallic TiAl_3 is formed after explosive welding. Moreover, subsequent annealing under various modes (Fig. 2b and 2c) doesn't lead to the formation of other intermetallics except for TiAl_3 . Also, during the experiments, the formation of titanium oxides is observed, which is related to the high activity of this metal.

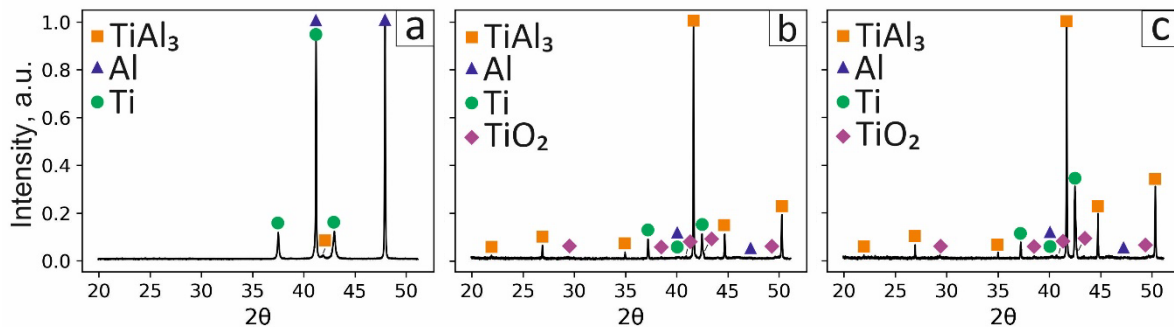


Fig. 2. Diffraction patterns of Ti-Al-based composite: a – before heating; b – 3 h at 640 °C; c – 1 h at 545 °C

To estimate the change in the growth rate of the TiAl_3 phase, the intensity of the reflection (200) versus time of the heating process graph was made (Fig. 3). The appearance of the reflection (200) occurs at the 19th minute of the heating process, which corresponds to a temperature of 597 °C. Up to 100 minutes of the experiment (~ 1 hour at 640 °C), there is a slight increase in the intensity of the reflection, indicating a low intermetallic growth rate. However, after that, there is an intensive growth of the intermetallic layer, that testifies to a rapid increase in intensity. Furthermore, at 312 minutes of the experiment, a decrease in the growth rate is observed due to a decrease in temperature to 545 °C.

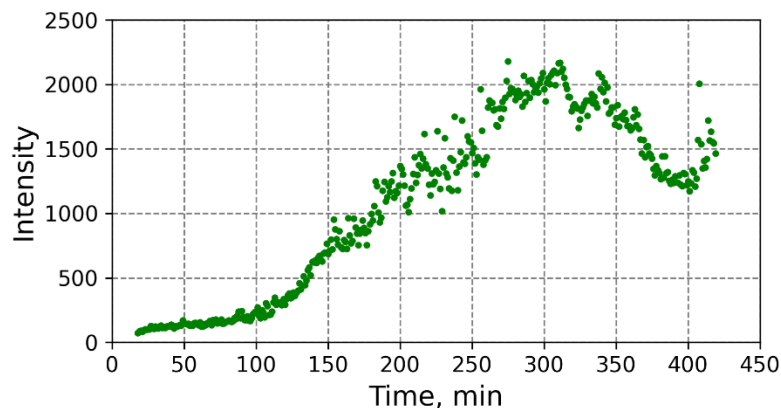


Fig. 3. Intensity of the reflection (200) versus time of the heating process graph

Thus, explosive welding and subsequent annealing leads to the formation of Ti-TiAl₃-Al composite. Moreover, various modes of heat treatment affect the growth rate of the TiAl₃ phase. It was established that an intensive increase in the growth rate of the TiAl₃ phase begins after ~ 1 hour at 640 °C.

References:

- [1] I.A. Bataev, A.A. Bataev, V.I. Mali, D.V. Pavliukova, Structural and mechanical properties of metallic-intermetallic laminate composites produced by explosive welding and annealing, Mater. Des. 35 (2012) 225-234.
- [2] D.V. Lazurenko, I.A. Bataev, Iu.N. Maliutina, V.S. Lozhkin, M.A. Esikov, A.M.J. Jorge, Explosively welded multilayer Ti-Al composites: Structure and transformation during heat treatment, Mater. Des. 102 (2016) 122-130.
- [3] N. Thiyaneshwaran, K. Sivaprasad, B. Ravisankar, Work hardening behavior of Ti/Al-based metal intermetallic laminates, Int. J. Adv. Manuf. Technol. 93 (2017) 361-374.

Resrtroration of the Density Distribution behind the Front of a Strong Shock Wave in a Porous Medium

Asylkaev A.M.^{1,2}

1 – Novosibirsk State University, Novosibirsk, Russia

2 – Lavrentiev Institute of Hydrodynamics SB RAS, Novosibirsk, Russia

a.asylkaev@g.nsu.ru

In the Siberian Branch of the Russian Academy of Sciences, a "Submicrosecond Diagnostics" station has been operating since 2005, where fast processes (including explosive ones) can be studied using powerful accelerators. X-ray pulses (synchrotron radiation, SR) allow measurements to be carried out in dynamic experiments with very small exposures (less than 1 ns), in which the results of interaction with matter are recorded at successive points in time (i.e., you can shoot a "movie").

The dynamics of density distribution in a porous substance under shock loading by explosion of cylindrical explosive charges based on triaminotrinitrobenzene (TATB) with a diameter of 40 mm was studied. The method for determining the parameters of compressed matter behind the shock wave front is based on measuring the intensity distribution of the passing SR from the VEPP-4 accelerator (electron energy – 4.5 GeV, wiggler with 9 poles). The registration of the transmitted radiation was carried out by the DIMEX X-ray detector, which was located parallel to the axis of the foam. The time between the images was determined by the number of bunches in the accelerator storage ring and was 203 ns (with 6 bunches). In such a fast mode, the detector can record 100 frames.

The density of matter along the SR beam varied greatly, which is why the absorption spectrum also changed. To calculate the density of the compressed substance, the absorption of the DIMEX detector was calibrated. To do this, a known mass of the same substance was placed in front of the detector. Using calibration, it is possible to restore the mass of the compressed substance along the SR (Fig. 1. shows the mass distribution during impact compression of the foam).

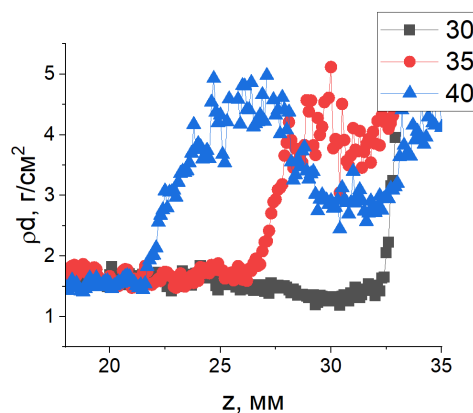


Fig. 1. The distribution of the foam mass along the SR beam; the time between frames C30, C35, C40 is equal to 1 microsecond

Acknowledgement: This work was carried out with the financial support of the Priority 2030 program

Features of X-ray Photoelectron Spectra of Cobalt and Cobalt Oxides

Aydakov E.E., Saraev A.A.

Boreskov Institute of Catalysis, Novosibirsk, Russia

e.ajdakov@g.nsu.ru

The determination of cobalt oxidation state and chemical environment is of paramount importance in the investigation of cobalt-based systems. X-ray photoelectron spectroscopy is one method that allows for the exploration of surface properties, such as cationic distribution and relative concentrations in the analysis zone. Cobalt photoelectron spectra exhibit a complex structure, particularly the Co 2p spectrum, which manifests as a doublet due to spin-orbit splitting. The magnitude of spin-orbit splitting and the binding energy position of the Co 2p peak depend on the cobalt's charge state. Furthermore, the presence and intensity of corresponding X-ray satellites to the main peak depend on the local chemical environment of cobalt cations. Such intricate structure sometimes leads to ambiguous interpretation of experimental data, particularly in the presence of multiple cobalt-containing compounds, such as cobalt oxide mixtures. One approach to addressing this issue is the investigation of reference cobalt compounds, with control over all stages of cobalt compound synthesis.

The synthesis of cobalt oxides was carried out at various temperatures ranging from 50°C to 500°C in an oxidizing atmosphere, followed by characterization using X-ray diffraction with synchrotron radiation and investigation using X-ray photoelectron spectroscopy. The study focused on the investigation of cobalt oxides CoO and Co₃O₄, which were synthesized in a specially designed chamber connected to a spectrometer by oxidizing metallic cobalt foil. Additionally, the process of cobalt oxides reduction by hydrogen and carbon monoxide at pressures of 50 mbar was examined. X-ray photoelectron spectra of cobalt (Co 2p, Co 3s, Co 3p) were obtained in all experiments. The phase composition of the obtained reference cobalt compounds was determined using X-ray diffraction on the "Precision Diffractometry" station at BINP SB RAS in Novosibirsk, Russia. The conducted research allowed for the refinement of spectral characteristics of the reference cobalt compounds, as well as the determination of their chemical states and behavior during reduction reactions. It is worth noting that it was not possible to synthesize and obtain X-ray photoelectron spectra of Co₂O₃ oxide, which, according to the literature, is an unstable cobalt compound. Commercially available Co₂O₃ oxides are susceptible to oxidation to Co₃O₄ upon exposure to oxygen in the air [1].

As a result, the synthesis conditions and temperature ranges for the existence of cobalt oxides CoO and Co₃O₄ were established depending on external conditions, such as oxidizing and reducing atmospheres. The spectral characteristics (binding energy of 2p, 3p, and 3s levels, spin-orbit splitting parameters, presence/absence and position of plasmon loss peaks and X-ray satellites) of the reference cobalt compounds, including metallic cobalt and cobalt oxides CoO and Co₃O₄, were determined. Using X-ray photoelectron spectroscopy and X-ray

PP-04

phase analysis, it has been determined that the reduction of Co_3O_4 oxide to the metallic state occurs through the formation of an intermediate phase of cobalt oxide, CoO .

Acknowledgement: This work was supported by the Russian Science Foundation, grant 14-13-12345.

References:

[1] Chuang T.J., Brundle C.R., Rice D.W. Interpretation of the x-ray photoemission spectra of cobalt oxides and cobalt oxide surfaces // *Surface Science*. 1976. Vol. 59, № 2. P. 413–429.

Effect of Hydrostatic Compression on the Structural Changes of δ -Chlorpropamide

Bogdanov N.E.^{1,2}, Zakharov B.A.^{1,2}, Boldyreva E.V.^{1,2}

1 – Boreskov Institute of Catalysis SB RAS, Novosibirsk, Russia

2 – Novosibirsk State University, Novosibirsk, Russia
nebo1329@gmail.com

The study of the polymorphism of drugs under different conditions is important to control their properties at different stages of preparation of dosage forms. An antidiabetic drug – chlorpropamide – is one of the most famous model objects. It is highly prone to polymorphism. Therefore, it is an excellent system to study structural response to temperature and pressure variations. This work is devoted to the study of the effect of high pressures on structural changes in the crystals of its δ -polymorph.

For a detailed study of structural transformations, 3 series of experiments were carried out using different X-ray sources: a laboratory X-ray tube (Rigaku Synergy S) and a synchrotron source (BM-01 and ID27, ESRF, France). The use of high-intensity SR beams made it possible for the first time to reveal and confirm the phase transition with the formation of an incommensurately modulated phase characterized by modulation vector $q=0.27b$ at pressures above 2.3 GPa. At pressure above 4 GPa, in various experiments, the formation of a superstructure was observed - a high-pressure phase with a tripled, relative to the initial, parameter b . A series of experiments on a laboratory radiation source confirmed the formation of a superstructure, but showed the possibility of its formation at much lower pressures taking into account longer exposure times, which indicates the influence of kinetic factors on the structural rearrangement with a consequent increase of pressure.

This work was supported by the Ministry of Science and Higher Education of the Russian Federation jointly by the Boreskov Institute of Catalysis of Siberian Branch, Russian Academy of Sciences (project AAAA-A21-121011390011-4) and Novosibirsk State University (Program "Priority-2030"). Laboratory experiments were performed at the solid state chemistry department and the MDEST laboratory and in the demonstration center Rigaku RESE (Frankfurt, Germany). Synchrotron experiments were performed at the European Synchrotron Radiation Facility (ESRF, Grenoble, France) at beamlines BM-01 and ID27.

Synchrotron Spectroscopy Study of the Effect of Carbon Support on the Transformation of Molybdenum Sulfides under Annealing

Bulusheva L.G., Fedoseeva Yu.V., Kotsun A.A., Okotrub A.V.
Nikolaev Institute of Inorganic Chemistry, Novosibirsk, Russia
bul@niic.nsc.ru

Molybdenum disulfide (MoS_2) is the second two-dimensional material after graphene that has received a lot of attention from the research community. In contrast to graphene, MoS_2 is a semiconductor with a varied band gap depending on the number of adjacent layers, which makes it a candidate for use in electronic and optoelectronic circuits, memory elements, etc. A large surface area needed for the adsorption of electrolyte ions and redox reactions occurring with the participation of MoS_2 cause the study of MoS_2 -based materials for energy conversion and storage. The relentless attention to MoS_2 is also due to the availability of reagents for synthesis and the possibility of creating various architectures and combinations with other compounds, including carbon structures. One of the convenient precursors for obtaining MoS_2 films and nanostructures is ammonium tetrathiomolybdate $(\text{NH}_4)_2\text{MoS}_4$, containing both molybdenum and sulfur. The study of the thermal transformation of $(\text{NH}_4)_2\text{MoS}_4$ by in-situ X-ray photoelectron spectroscopy (XPS) showed the formation of amorphous MoS_x at 150 °C and crystalline MoS_2 after 400 °C [1]. Measurements of the products obtained after annealing at 560 and 650 °C did not revealed any further changes in their composition.

In this work, we studied the effect of a carbon component on the conversion of MoS_x , obtained by treating thin $(\text{NH}_4)_2\text{MoS}_4$ deposits in an argon flow at 120 °C. XPS and NEXAFS measurements were carried out using the synchrotron radiation of the Russian-Germany beamline at the BESSY II center (Berlin, Germany). The initial MoS_x were prepared on a silicon substrate and substrates coated with CVD-synthesized few-layered graphene or single-walled carbon nanotubes (SWCNTs). The samples were annealed in a spectrometer chamber under ultrahigh vacuum conditions at 600 °C, 800 °C and 1000 °C and the spectra of constituent elements were recorded after each annealing step. The formation of Mo in the metallic state at 1000 °C was found in the samples located on silicon and graphene substrates and the fraction of this state was larger in the former case. In the case of the SWCNT substrate, no conversion was observed and, moreover, the edge sulfur states were preserved, which indicates the slow kinetics of sulfur removal. The data obtained can be useful in the development of composites and hybrids from carbon and molybdenum sulfides.

Acknowledgement: This work was supported by the Russian Science Foundation, grant 23-73-00048.

References:

[1] L. Sygellou, *Appl. Surf. Sci.* 476 (2019) 1079.

The XAS Magic to Prove Solvent-Specific Reduction of Pt^{IV} into Pt^{II} with NaI in Acetone Solution

Krasniakova I.O.¹, Nikitenko D.V.², Krasnyakova T.V.², Guda A.A.¹, Mitchenko S.A.²

1 – The Smart Materials Research Institute at the Southern Federal University,
Rostov-on-Don, Russia

2 – Institute of Physical Organic and Coal Chemistry, Donetsk, Russia
adjirina@yandex.ru

One of the trends in organic synthesis is cross-electrophile coupling - a direct coupling of two electrophiles. The stepwise mechanism of such reactions assumes a reduction step, for example, of the product of the oxidative addition of the first electrophile to the metal complex.

It is known [1] that Pt^{II} complexes readily undergo oxidative addition reactions with organic iodides RI to form RPt^{IV}. The latter are capable to equilibrium reduction by I⁻ into the corresponding RPt^{II} derivatives. This equilibrium is usually shifted towards RPt^{IV}, but in an acetone solution of NaI it can be shifted in the opposite side by binding the released iodine into a polymeric insoluble complex [Na(C₃H₆O)₃]_n(I₂)_n. In the ¹⁹⁵Pt-NMR spectrum of aqueous solutions of Pt iodo complexes, the Pt^{II} signal was found at -5478 ppm while the Pt^{IV} signal was at -6234 ppm [2]. When Pt^{II} or Pt^{IV} is dissolved in acetone containing NaI, the same signal is registered in the ¹⁹⁵Pt-NMR spectrum at -5035 ppm regardless of the oxidation state of the starting Pt complex. This indirectly indicates the reduction of Pt^{IV} to Pt^{II} by I⁻ upon dissolution. A direct method to prove the change in the oxidation state of Pt^{IV} in an acetone solution of NaI might be the XAS, which is selective to the local structure of an element.

Indeed, the Pt-L₃ XAS spectra of the Pt^{II} and Pt^{IV} iodo complexes in aqueous solutions differ significantly. In the XANES spectrum, the maximum of the white line of the Pt^{IV} sample is blue-shifted, and its height is markedly higher compared to these parameters for Pt^{II}. The Pt-I coordination numbers estimated from the FT-EXAFS data are also different and equal to 4 (Pt^{II}) and 6 (Pt^{IV}). A completely different outcome is observed for the acetone solution of the Pt iodo complexes and NaI: the XAS spectra in both XANES and EXAFS regions are identical and match to Pt^{II} regardless of the oxidation state of the initial platinum. The Pt-I coordination numbers are also the same and equal to 4 matching the square-planar Pt^{II} complexes. Hence, Pt^{IV} iodo complexes are reduced to Pt^{II} ones with I⁻ in acetone solutions.

Acknowledgement: The authors acknowledge the Ministry of Science and Higher Education of the Russian Federation for financial support (Agreement № 075-15-2021-1363).

References:

- [1] V.V. Zamashchikov, S.L. Litvinenko, S.A. Mitchenko, O.N. Pryadko, *Metalloorganicheskaya khimiya*. 6 (1992) 1272.
[2] O.V. Khazipov, T.V. Krasnyakova, D.V. Nikitenko, M.A. Merzlikina, E.V. Khomutova, S.A. Mitchenko, *Journal of Organometallic Chemistry*. 867 (2018) 333.

Detection of Low-Z Elements by SR-XRF Method on the VEPP-4M Storage Ring

Goldenberg B.G.^{1,2,3}, Gusev I.S.², Krupovich E.S.^{1,4}, Legkodymov A.A.^{1,2}, Kolmogorov Yu.P.⁵

1 – SRF SKIF, Boreskov Institute of Catalysis, Novosibirsk, Russia

2 – Budker Institute of Nuclear Physics, Novosibirsk, Russia

3 – Novosibirsk State University, Novosibirsk, Russia

4 – Nikolaev Institute of Inorganic Chemistry, Novosibirsk, Russia

5 – Sobolev Institute of Geology and Mineralogy, Novosibirsk, Russia

b.g.goldenberg@srf-skif.ru

Synchrotron radiation X-ray fluorescence (SR-XRF) is a well-established highly sensitive method of panoramic study of elemental composition. This method is in development for many years in Budker Institute of Nuclear Physics. Despite its versatility, SR-XRF can't capture all the elements using single a common setting, thus the equipment has to be optimized for a specific excitation spectrum and specific detection conditions. At the station "Local and scanning X-ray fluorescent elemental analysis" on the storage ring VEPP-3 [1], routine methods for studying the concentration of chemical elements from K to U were worked out, using SR with energy of photons 12-25 keV as an exciting radiation. At the station "Rigid X-ray" on the storage ring VEPP-4 [2] photons with energy of more than 100 keV are used to excite the fluorescence of rare-earth and heavy elements. Attempts to measure the content of low-Z elements Al, Si, P, S, Cl (relevant for the study of plant samples, such as grass, leaves, shoots [3]) were not successful. This is a consequence of the fact that, under typical experimental conditions at this station, low-energy characteristic fluorescence from low-Z elements (for example, Si Ka - 1.74 keV) is significantly absorbed in atmospheric air and the background radiation suppresses the useful signal.

The aim of the work was to expand the possibilities of using SR-XRF in the area of detection of low-Z elements.

The "technological station" on the SR beamline from the VEPP-4M storage ring is intended for a training demonstration of the basics of working with synchrotron research equipment. The station is equipped with X-ray Channel-Cut Si (111) Crystal monochromators, x-ray slits, vacuum chambers for monochromators and vacuum chambers for sample and detector Amptek XR100CR. To study the content of light elements in plant samples, the VEPP-4M storage mode was selected at an electron energy of 3.5 GeV. And the line of 3.53 keV (below the K-edge of potassium – 3.589 keV) was selected from the spectrum by a monochromator. Due to the fact that channel-cut Si (111) crystal monochromators also passes the third harmonic (for 3.53 keV is 10.63 keV), it was not possible to completely exclude the excitation of elements heavier than K, however, the background level of scattered radiation decreased compared to the case of excitation at high energy (for example, 7.3 keV).

Figure 1 shows the fluorescence spectra of the standard sample of the grass mixture "Tr1" at an excitation energy of 3.53 keV and 7.3 keV. In the first case, the lower limit of detection for silicon is 450 ppm, in the second case, it is impossible to reliably determine silicon.

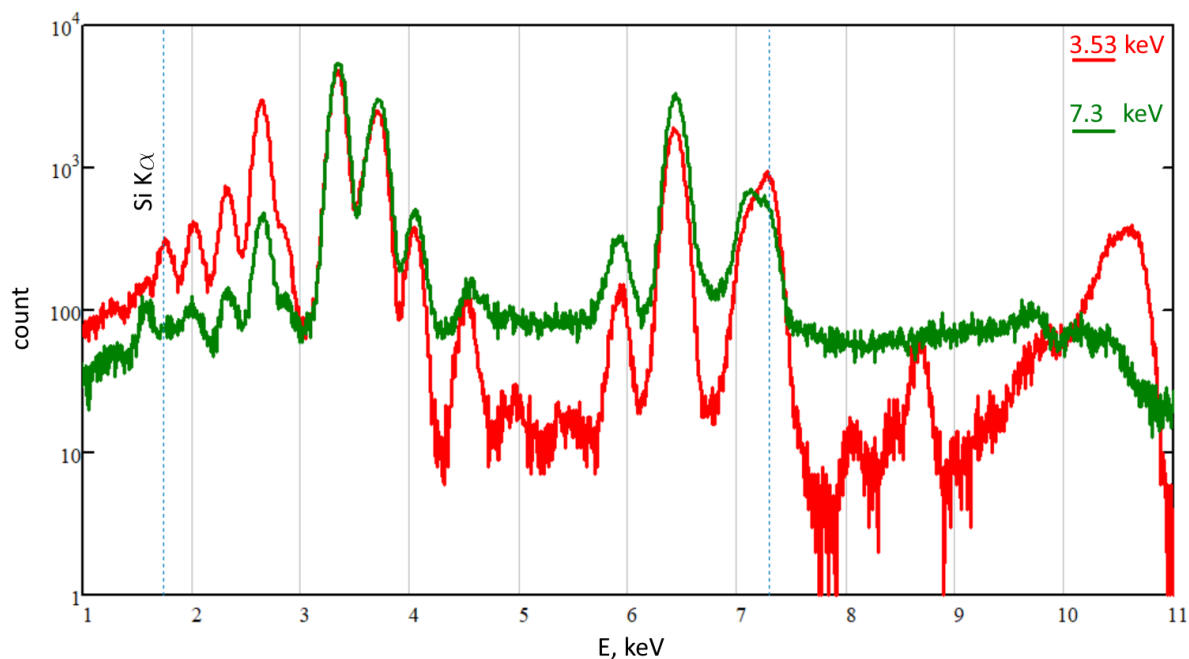


Fig. 1. Fluorescence of standard sample of the grass mixture "Tr1 " at an excitation energy of 3.53 keV and 7.3 keV.

The features of the SR-XRF research of low-Z elements and plans for the development of the station will be presented in the article.

Acknowledgement: The work was done at the shared research center SSTRC on the basis of the VEPP-4 - VEPP-2000 complex at BINP SB RAS.

References:

- [1] Trunova V.A., Zvereva V.V. J. of Structural Chemistry. 2016. V. 57. № 7. p. 1327-1333.
- [2] Legkodymov A.A., Kuper K.E., Baranov G.N., Kolmogorov Y.P. Bulletin of the Russian Academy of Sciences: Physics. 2019. V. 83. № 2. p. 112-115.
- [3] Амброс Е.В., Крупович Е.С., Колмогоров Ю.П. и др. Тезисы докладов VI Всероссийской научной конференции с международным участием "УСТОЙЧИВОСТЬ РАСТЕНИЙ И МИКРООРГАНИЗМОВ К НЕБЛАГОПРИЯТНЫМ ФАКТОРАМ СРЕДЫ" (Иркутск, Большое Голоустное 3–7 июля 2023 г.), СИФИБР СО РАН, ФГБОУ ВО ИГУ, 2023, стр. 154

Method for Estimating the Content of Planar Defects in Structures of the A_2BO_4 Type from Diffraction Data

Gorkusha A.S.^{1,2}, Cherepanova S.V.², Shmakov A.N.^{1,2,3}, Tsybulya S.V.^{1,2}

1 – Novosibirsk State University, Novosibirsk, Russia

2 – Boreskov Institute of Catalysis, Novosibirsk, Russia

3 – Siberian Circular Photon Source "SKIF" Boreskov Institute of Catalysis, Koltsovo, Russia

a.gorkusha@g.nsu.ru

Recently, layered perovskite-like oxides of the Ruddlesden-Popper (R-P) series $A_{n+1}B_nO_{3n+1}$ are considered as potential materials for various electrochemical devices, selective oxygen-conducting membranes, catalysts for oxidative reactions, etc. For example, Sr_2TiO_4 is actively studied as a material for a catalyst for the oxidative coupling of methane (OCM). Our previous studies of these systems have shown that Sr_2TiO_4 obtained using the solid-phase synthesis method is often characterized by the presence of multiple planar defects in the particle volume, which violate the order in the alternation of layers in the [001] direction (Fig. 1) [1, 2]:

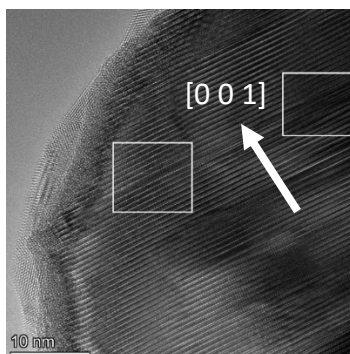


Fig. 1. TEM image of the Sr_2TiO_4 structure

The existence of such a defect is explained by the crystal-chemical features of the R-P structures. These phases consist of n layers with a perovskite (ABO_3) type structure enclosed between layers with a rock salt (AO) type structure, and, accordingly, their general formula can be written in a more visual form as $AO(ABO_3)_n$. The presence of such similar structural elements means that fragments with either one or two alternating perovskite-like layers can be quite easily formed in the sample volume, which leads to disturbances in the alternation of structure layers.

Simulation of diffraction patterns in the presence of such defects showed that, as the concentration of defects increases, diffraction maxima with nonzero indices l shift relative to their positions in a defect-free system [1]. Based on this effect, we proposed a method for estimating the content of planar defects in A_2BO_4 structures: using the following relation

$$\Delta = [2/(d_{103})^2 - 1/(d_{110})^2]/[1/(d_{004})^2]$$

together with the values of interplanar distances obtained directly from the experiment, it is possible to use the calibration plot in Fig. 2 to determine the parameter δ characterizing the concentration of planar defects in the structure.

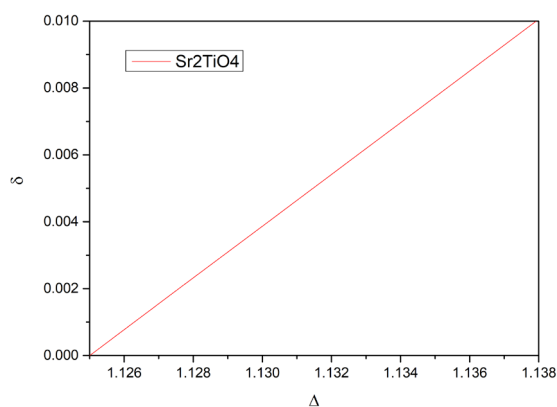


Fig. 2. Calibration plot for determining the content of planar defects in A_2BO_4 structures

The technique was tested on Sr₂TiO₄ samples, the diffraction patterns of which were obtained using synchrotron radiation. The use of SR provides the necessary accuracy in determining the positions of the peaks required for this technique.

Using this technique, it is possible to estimate the content of planar defects not only in Sr₂TiO₄, but also in all other tetragonal systems with the A₂BO₄ structure, since the shift of diffraction maxima does not depend on the chemical composition or unit cell parameters of a specific object under study.

Acknowledgement: The work was supported by the PRIORITY 2030 program (NSU).

References:

- [1] A. Gorkusha, S. Tsybulya, S. Cherepanova, E. Gerasimov, S. Pavlova, *Materials* 2022, **15**, 7642.
- [2] S. Pavlova, Y. Ivanova, S. Tsybulya, S. Chesalov, A. Nartova, E. Suprun, L. Isupova, *Catalysts* 2022, **12**, 929.

A New Method for Studying Inter-Atomic Interactions Based on the Non-Linear Dispersion of the Resonances in Resonant Inelastic X-Ray Scattering Map

Ignatova N.Y.¹, Polyutov S.P.¹, Kimberg V.V.^{1,2}, Krasnov P.O.¹, Gel'mukhanov F. Kh.^{1,2}

*1 – International Research Center of Spectroscopy and Quantum Chemistry,
Siberian Federal University, Krasnoyarsk, Russia*

*2 – Royal Institute of Technology, Stockholm, Sweden
nyignatova@sfu-kras.ru*

Novel high-power and frequency-tunable X-rays light sources, such as synchrotrons and X-ray free electron lasers (XFELs), are widely used in studies of the atomic structure of matter and the dynamics of fast processes by such spectroscopy methods as resonant inelastic X-ray (RIXS) and Auger (RAS) scattering [1]. One of the important applications of RIXS and RAS spectroscopy is the study of the interatomic interaction of matter in various aggregate states [2]. A distinctive feature of resonant scattering namely as the Raman dispersion is often broken near the absorption resonance. We have found a simple relationship between deviation from linear Raman dispersion and interatomic potentials. Our results are illustrated by spectra calculations conducted using the wave packet technique and the corresponding analysis of the experimental RAS spectra of the sulfur hexafluoride (SF₆) molecule.

Acknowledgement: This work was supported by the Russian Science Foundation, grant 21-12-00193.

References:

- [1] F. Gel'mukhanov, M. Odelius, S.P. Polyutov, A. Föhlisch, and V. Kimberg, Rev. Mod. Phys. 93 (2021), 035001.
- [2] V. Vaz da Cruz, N. Ignatova, et al., J. Chem. Phys. 150 (2019), 234301.

Ionizing Detectors Based on Perovskite Absorbers

Ishteev A.¹, Konstantinova K.^{1,2}, Saranin D.¹

1 – *The Laboratory of Advanced Solar Energy (LASE), NUST MISIS, 4, Leninskiy avenue, 119049, Moscow, Russia*

2 – *Research and Practical Clinical Center for Diagnostics and Telemedicine Technologies of the Moscow Health Care Department, 24 Petrovka st., bld. 1, 127051, Moscow, Russia*
arturishteev@misis.ru

Lead-halide perovskites showcase significant promise for both photovoltaic and sensing purposes, attributed to their superior absorption capabilities, extensive mobility-lifetime products, resilience to structural defects, and the versatility of high Z atom-infused chemical compositions. They are rapidly gaining attention in the domain of ionizing radiation sensing, with proven robustness against intense radiation. The advancements in halide perovskite (HP) research hint at a transformative leap in ionizing radiation detection, encompassing enhanced detection metrics, enduring stability, facile low-temperature processing, and the advantage of adaptable, lightweight integration owing to potential flexibility.

Contrasting conventional ionizing radiation detection materials, the energy gap of HP offers adaptability, spanning between 1.2 to 2.8 eV, and can be modulated via both cationic and anionic substitutions. A paramount technological edge of the halide perovskite methodology lies in its 100°C solution processing, endorsing diverse printing techniques – from ink-jet and slot-die to spray, all harmonized with malleable substrates, inclusive of both plastics and glass.

Our research delves into the morphological and photonic alterations in perovskite crystals post e-beam exposure at heightened flux (10^{15} electrons per cm^2 with a 5 MeV energy) and an extraordinarily elevated dose of 25 MRAD. Insights from ellipsometry highlighted an amplified presence of Urbach tails, indicative of radiation-provoked defects. Radiation-exposed MAPbBr₃ monocrystals, upon Kelvin probe microscopy assessment, unveiled a trap-initiated Fermi level anchoring at +0.56 eV, juxtaposed against their untouched counterparts. Yet, evaluations via X-ray diffraction coupled with dual-photon excited photoluminescence microscopy for optical depth confirmed that, irrespective of the substantial irradiation, both structural and optical facets remain unaffected[1].

Acknowledgement: Authors gratefully acknowledge the financial support from the Russian Science Foundation (No. 21-19-00853).

References:

[1] A. Ishteev, K. Konstantinova, D. Saranin, and A. Di Carlo, "Investigation of structural and optical properties of MAPbBr₃ monocrystals under fast electrons irradiation," *J. Mater. Chem. C*, vol. accepted, 2022.

Effect of Temperature, Hydrostatic Pressure and Irradiation on Photosensitive Complexes $[\text{Co}(\text{NH}_3)_5\text{NO}_2]\text{XNO}_3$, $\text{X} = \text{Br, I}$ and $[\text{Co}(\text{NH}_3)_5\text{NO}_2]_2\text{I}_3\text{Cl}$

Kalinina P.P.^{1,2}, Zakharov B.A.^{1,2}

1 – Boreskov Institute of Catalysis, Novosibirsk, Russia

2 – Novosibirsk State University, Novosibirsk, Russia

p.kalinina@g.nsu.ru

Crystalline substances with macroscopic mechanical response occurring under external forces due to a chemical reaction or a phase transition, are of great interest to research. Understanding the nature of such phenomena is important for development of molecular machines, switches and devices that make it possible to convert radiation energy to mechanical work.

Cobalt (III) complexes with the general formula $[\text{Co}(\text{NH}_3)_5\text{NO}_2]\text{XY}$ are one of the most studied compounds in which macroscopic mechanical response occurs under irradiation due to a photoisomerisation reaction $[\text{Co}(\text{NH}_3)_5\text{NO}_2]\text{XY} \rightarrow [\text{Co}(\text{NH}_3)_5\text{ONO}]\text{XY}$. In the present work we have studied previously unknown complexes $[\text{Co}(\text{NH}_3)_5\text{NO}_2]\text{XNO}_3$, $\text{X} = \text{Br, I}$ and $[\text{Co}(\text{NH}_3)_5\text{NO}_2]_2\text{I}_3\text{Cl}$. The aim of this work is to establish correlations between the photoisomerisation reaction, anion, crystal structure and anisotropy of its deformation on external influences (temperature, pressure and irradiation) for crystals of complexes $[\text{Co}(\text{NH}_3)_5\text{NO}_2]\text{XNO}_3$, $\text{X} = \text{Br, I}$ and $[\text{Co}(\text{NH}_3)_5\text{NO}_2]_2\text{I}_3\text{Cl}$. Structural changes of crystals of complexes $[\text{Co}(\text{NH}_3)_5\text{NO}_2]\text{XNO}_3$, $\text{X} = \text{Br, I}$ and $[\text{Co}(\text{NH}_3)_5\text{NO}_2]_2\text{I}_3\text{Cl}$ upon cooling, increasing pressure and irradiation with visible light were studied by single-crystal X-ray diffraction under laboratory conditions. IR-spectroscopy, PXRD and DSC were used as additional methods. Series of experiments under irradiation showed different behavior of all three crystals during the photoisomerisation reaction. This is caused by differences in crystal structures and differences in surroundings of nitrogroups. Series of experiments upon cooling showed that all three crystals shrink anisotropically, and anomalies not related to phase transitions are observed in changes of the unit cell parameters with temperature. The hydrostatic pressure series for $[\text{Co}(\text{NH}_3)_5\text{NO}_2]\text{BrNO}_3$ crystal showed that the substance undergoes a phase transition in the pressure range between 2.9 GPa and 3.6 GPa. The hydrostatic pressure series for $[\text{Co}(\text{NH}_3)_5\text{NO}_2]\text{INO}_3$ crystal showed that no phase transitions are observed in the structure at pressures up to 6.0 GPa. Interrelations between structural changes observed during irradiation, cooling and hydrostatic compression are revealed.

Acknowledgement: This work was supported by the Ministry of science and higher education of Russian Federation. That work was performed in Boreskov institute of Catalysis SB RAS (project AAAA-A21-121011390011-4) and in Novosibirsk State University (strategic academic leadership program “Priority 2030”). The equipment of MDEST laboratory at NSU was used.

DFT-Modeling of Structural Evolution in Crystals of Organic Piezoelectrics on the Example of γ -Glycine

Khainovsky M.A.^{1,2}

1 – Novosibirsk State University, Novosibirsk, Russia

2 – Borekov Institute of Catalysis of the Siberian Branch of Russian Academy of Sciences,
Novosibirsk, Russia
ma.khainovskiy@gmail.com

For crystalline materials, quantum chemical modeling of macro- and micro-changes under extreme conditions of high pressure or temperature is widely used. It allows one to predict, among other things, the mechanical properties of solids: fragility (or rigidity), elasticity (or plasticity), and (if present) piezoelectricity. For molecular crystals, changes in these properties are directly related to changes in various intermolecular interactions, with special attention paid to hydrogen bonds, the diversity of which largely determines the mechanical properties of organic crystals.

Theoretical (density functional theory) and experimental methods (x-ray diffraction) complement each other and collectively provide the most complete information about the relationship between structure and properties, the role of intermolecular interactions in the formation of the spatial structure of crystals, as well as its response to external influences (deformation of the structure, phase transitions). The use of synchrotron radiation sources allows obtaining structural data, which is the best starting point for periodic DFT calculations

Earlier, we took the first steps in establishing the relationship between changes in macroscopic descriptors of elastic and piezoelectric properties and the behavior of the electronic medium at the critical points of H-bonds using the example of β -glycine. Now we have extended the obtained approach to another polymorphic modification - γ -glycine - and compared the behavior of a structure built from layers with the behavior of a structure formed by triple helices.

The descriptors of internal pressure and binding, as well as the stress tensors necessary to clarify the microscopic mechanism of the occurrence of electrical moments in atomic and molecular fragments of organic piezoelectric crystals, are calculated. The relationship between macroscopic elastic characteristics and microscopic characteristics of electron density for different types of structures has been established (using the example of two polymorphic modifications of glycine).

Acknowledgement: The research was also carried out (in part) with funds from the Priority 2030 strategic academic leadership program at Novosibirsk State University
This work was carried out with the financial support of the Ministry of Science and Higher Education of the Russian Federation (Institute of Catalysis SB RAS; program of the Network Center for Advanced Research "Green Chemistry for Sustainable Development: from fundamental principles to new materials", D.I. Mendeleev Russian Chemical Technical University)
Scientific Supervisors: D.Sc. (Chemistry) E.V. Boldyreva, D.Sc. (Physics and Mathematics) V.G. Tsirelson

EXAFS Spectroscopy for Establishing the Structure of Eu(III) Complexes in Solution: Advantages, Limitations, Supporting Methods

Konopkina E.A.¹, Novichkov D.A.¹, Trigub A.L.², Matveev P.I.¹, Borisova N.E.¹

1 – Department of Chemistry, Lomonosov Moscow State University, Moscow, Russian Federation

2 – National Research Center “Kurchatov Institute”, Moscow, Russian Federation
Konopkina.kate@gmail.com

The efficient and safe operation of nuclear power plants is closely connected to management of high-level waste (HLW). It is a complex multicomponent system that requires separation into fractions depending on the chemical and nuclear-physical properties of its constituents. This approach ensures the safest and most efficient way to prepare components for disposal and further recycling.

One of the components that require separation from these systems are lanthanides. They are neutron poisons, and make it hard to process the rest of the components in high-level radioactive waste. For these purposes, the most technologically promising method is solvent extraction. To date, numerous groups of extractants have been investigated [1], which vary in their efficiency and selectivity in binding f-elements. Nevertheless, the search for the "ideal" extractant continues. To best show how the structure of the extractant affects the binding of the cation, it is necessary to study in detail and comprehensively the structure of the resulting complex.

Despite the fact that SC-X-ray diffraction can unambiguously determine the structure of a crystal, a comparison of the properties and structures in a single crystal and a solution is debatable.

The EXAFS method makes it possible to obtain information about the coordination environment of the central atom of a complex compound in both the solid and liquid phases. This is especially important for the solvent extraction method, where complex formation is the determining process in the redistribution of components between phases.

In our work, we studied the structure of the Eu(III) complex with a new extractant, pyridine diphosphonate, in solution [2,3]. We have described the coordination environment of the central atom: we have obtained distances, coordination numbers, values of the Debye-Waller factor (Figure 1).

It is shown that the distances between europium and the nearest oxygen atoms (attributed to either –P=O group or nitrates, Eu-O_{P=O}, NO₃) for Py-PO-iPr·Eu(NO₃)₃ complexes are equal to 2.43-2.44 Å. The distances between europium and the nearest nitrogen atoms (attributed to either pyridine core or nitrates, Eu-N_{Py}, NO₃) are different and equal to 2.62 Å and 2.55 Å respectively.

We also used a number of auxiliary methods, such as: UV-vis titration and NMR titration to confirm the data obtained by the EXAFS method, as well as to obtain additional information

on the effect of the cation radius on the binding efficiency. We consistently established and confirmed the stoichiometry of the complexes by the NMR and UV-vis titration, proving that both ML and ML2 complexes are present in the system.

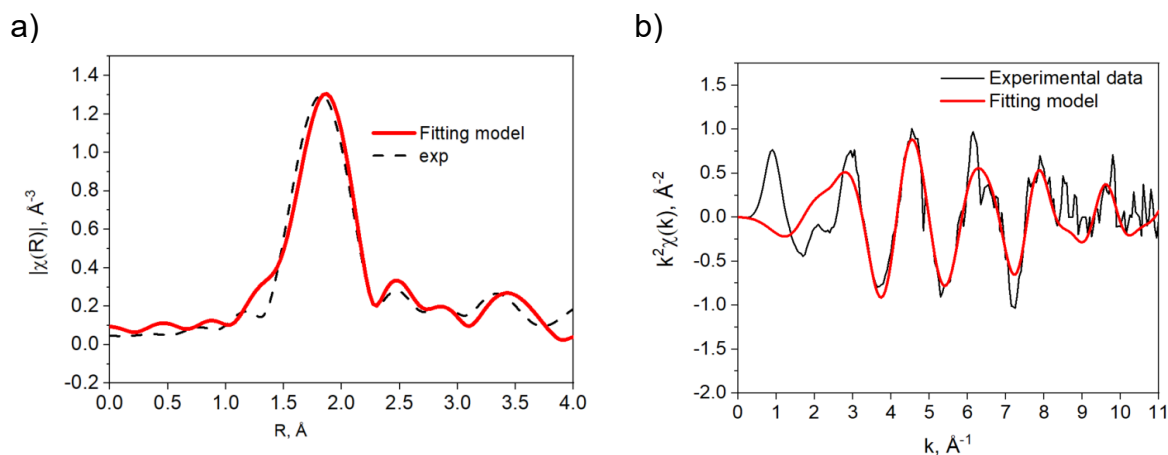


Figure 1 Fourier transform magnitude (a) and k -space (b) of experimental EXAFS spectra at europium L3 edge (dash line ---) and best fit results (solid line —) for complexes Py-PO-*i*Pr·Eu(NO₃)₃. k -range of 3–11 Å⁻¹, R -range 1–3.8 Å, $s_0^2 = 1$.

Acknowledgement: This work was supported by the Russian Science Foundation, grant 23-73-30006.

References:

- [1] Evsiunina M. V. et al. Solvent Extraction Systems for Separation of An(III) and Ln(III): Overview of Static and Dynamic Tests // Moscow Univ. Chem. Bull. 2021. Vol. 76, № 5. P. 287–315.
- [2] Konopkina E.A. et al. Pyridine-di-phosphonates as chelators for trivalent f-elements: kinetics, thermodynamic and interfacial study of Am(III)/Eu(III) solvent extraction // Dalton Trans. Royal Society of Chemistry, 2022. Vol. 51. P. 11180–11192.
- [3] Konopkina E.A. et al. Solvent Extraction and Complexation Studies of Pyridine-di-Phosphonates with Lanthanides(III) in Solutions // Solvent Extr. Ion Exch. Taylor & Francis, 2023. Vol. 0, № 0. P. 1–27.

In Situ XRD Synchrotron Investigation of Cr/Ta-Coated Zr-1Nb Alloy under High-Temperature Oxidation

Korneev S.P., Syrtanov M.S.
Tomsk Polytechnic University, Tomsk, Russia
spk6@tpu.ru

Most reactors use zirconium alloy as fuel rod cladding material because of its corrosion resistance and low neutron absorption cross section. However, one of the main drawbacks of zirconium alloys is that they oxidize when overheated and cause an uncontrolled exothermic reaction with water (steam), which leads to the formation of hydrogen: $Zr + 2H_2O \rightarrow ZrO_2 + H_2$ [1]. It was this type of reaction that led to hydrogen explosions during the Fukushima nuclear disaster.

A coating can be applied to the zirconium cladding to slow down the oxidation process. However, such a coating must remain stable under standard reactor conditions and must not lose its properties during the entire lifetime of the fuel element.

The most proven coating material is chromium. The Cr_2O_3 film formed by chromium oxidation acts as a diffusion barrier for oxygen [2]. In addition, chromium has a good adhesion property, its modulus of elasticity is twice that of zirconium, which helps to improve the strength of the cladding [3]. However, due to the interdiffusion of chromium and zirconium at high temperatures, a Laves Cr_2Zr phase is formed at the "coating-substrate" interface, resulting in increased diffusion into the zirconium alloy [2].

To prevent interdiffusion of chromium and zirconium, many scientific groups suggest using an intermediate barrier layer. It is important that the barrier layer material does not affect reactor economy and does not form eutectic and other compounds with chromium and zirconium at high temperatures. In a number of papers [4,5], the use of tantalum as a diffusion barrier was considered promising because of its low diffusion coefficient and solubility limit in β -Zr. However, until now, the oxidation behavior of the Cr/Ta-coated Zr-1Nb alloy has not been sufficiently investigated.

Thus, the purpose of this work is to conduct in situ XRD synchrotron investigation of Cr/Ta-coated Zr-1Nb alloy under high-temperature oxidation.

The Cr/Ta-coated Zr-1Nb alloy samples were tested for corrosion resistance at 1100 °C. The use of the Ta intermediate layer reduces the weight gain ($\sim 24.6 \text{ mg/cm}^2$) compared to the uncoated Zr-1Nb sample ($\sim 93.3 \text{ mg/cm}^2$). According to SEM data, the thickness of the residual chromium layer in the case of the Cr/Ta coated sample is greater ($\sim 5.4 \text{ }\mu\text{m}$) than in the case of single-layer Cr coating ($\sim 4 \text{ }\mu\text{m}$ [6]). The formation of the Cr_2Ta phase at the interface between the chromium coating and the tantalum sublayer was detected by XRD.

PP-15

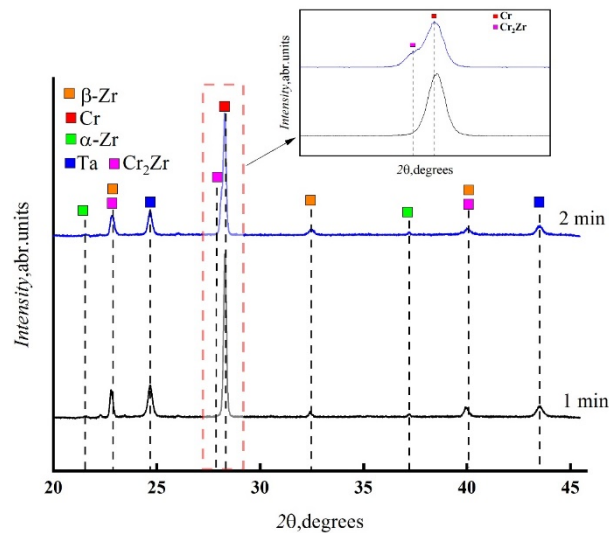


Fig.1. Phase transformations in Cr/Ta coated zirconium alloy during aging at 1250 °C

In situ diffraction studies of phase transformations in the Cr/Ta/Zr system during linear heating in vacuum to a temperature of 1250 °C followed by irradiation were performed to reveal the mechanisms of Cr, Ta and Zr interdiffusion. Oxidation of the test sample at 1250 °C for 2 minutes leads to an asymmetry of the α -Cr phase in the (110) direction, indicating the formation of the Cr₂Zr eutectic phase (Fig. 1). Further exposure leads to partial melting of the sample of Zr-1Nb alloy coated with Cr/Ta.

Acknowledgement: The research was funded by Russian Science Foundation (grant No. 21-79-00175)

References:

- [1] Terrani K. A. Accident tolerant fuel cladding development: Promise, status, and challenges // Journal of Nuclear Materials. – 2018. – Vol. 501. – P. 13-30.
- [2] Krejčí, J., Ševeček, M., Kabátová, J., Manoch, F., Kočí, J., Cvrček et al., 2018. Experimental behavior of chromium-based coatings. Proc. TopFuel.
- [3] Yang, J., Steinbrück, M., Grosse, M., Liu, J., Zhang, J., Yun, D., & Wang, S. (2022). Review on chromium coated zirconium alloy accident tolerant fuel cladding. Journal of Alloys and Compounds, 895, 162450. <https://doi.org/10.1016/j.jallcom.2021.162450>.
- [4] Rafael Isayev, Pavel Dzhumaev Interaction of a diffusion barrier from the refractory metals with a zirconium alloy and a chrome coating of an accident tolerant fuel // Nuclear Engineering and Design. - 2023. - №407.
- [5] Kashkarov, E., Afornu, B. K., Sidelev, D. V., Krinitcyn, M. G., Gouws, V., & Lider, A. M. (2021). Recent Advances in Protective Coatings for Accident Tolerant Zr-Based Fuel Claddings. *Coatings*, 11(5), 557. <https://doi.org/10.3390/coatings11050557>.
- [6] H.-G. Kim, I.-H. Kim, Y.-I. Jung, D.-J. Park, J.-Y. Park, Y.-H. Koo, Adhesion property and high-temperature oxidation behavior of Cr-coated Zircaloy-4 cladding tube prepared by 3D laser coating, J. Nucl. Mater. 465 (2015) 531–539.

The Lanthanide Doped Chromium Disulfides $\text{CuCr}_{0.99}\text{Ln}_{0.01}\text{S}_2$ (Ln=La...Lu): XANES Investigation

Korotaev E.V.¹, Syrokvashin M.M.¹, Nikolenko A.D.^{2,3}

1 – Nikolaev Institute of Inorganic Chemistry, Novosibirsk, Russia

2 – Budker Institute of Nuclear Physics, Novosibirsk, Russia

3 – SRF SKIF, Boreskov Institute of Catalysis, Novosibirsk, Russia

korotaev@niic.nsc.ru

The CuCrS_2 - based solid solution are considered as the promising functional materials for modern electronics applications due to the potential properties for practical usage: ionic conductivity [1], thermoelectric properties [2], helimagnetic arrangement [3], photoconductive properties [4], colossal magnetoresistance and phase metal-insulator transition [5].

The cationic substitution of chromium atoms with transition metal atoms ($\text{CuCr}_{1-x}\text{M}_x\text{S}_2$, M = V, Fe, Mn), the co-intercalation of the Van der Waals gap with two atom types ($\text{Cu}_{1-x}\text{Ag}_x\text{CrS}_2$) and the chalcogen substitution ($\text{CuCrS}_{2-x}\text{X}_x$, X = S, Se, Te) allow one to control the electric and magnetic properties of CuCrS_2 -based compounds. It was shown that the low dopant solid solutions $\text{CuCr}_{1-x}\text{Ln}_x\text{S}_2$ exhibit promising thermoelectric properties [2]. One of the key aspects to control the electrophysical properties of thermoelectric materials is the understanding of the spatial structure features especially the substituted atoms localization behavior. In this regard, the data concerning the atoms local environment could be obtained using X-ray absorption edges near edge structure (XANES).

This study involves a detailed study of the lanthanide doped solid solutions $\text{CuCr}_{0.99}\text{Ln}_{0.01}\text{S}_2$ (Ln=La...Lu) XANES spectra fine structure. A comprehensive experimental and theoretical study of the X-ray absorption edges of the matrix elements and the lanthanide atoms in the cation-substituted disulfides $\text{CuCr}_{0.99}\text{Ln}_{0.01}\text{S}_2$ was carried out. Based on the theoretical model XANES spectra fine structure the local environment of the matrix elements and lanthanides was studied using the finite-difference methods (FDMNES software package).

Acknowledgement: This study was funded by the Russian Science Foundation (project No. 19-73-10073, <https://rscf.ru/project/19-73-10073/> (accessed on 16 June 2023)).

References:

- [1] G.R. Akmanova, A.D. Davleshina, *Lett.Mater.* 3 (2013) 76.
- [2] E.V. Korotaev, M.M. Syrokvashin, I.Yu. Filatova et al., *Materials* 16 (2023) 2431.
- [3] A. Karmakar, K. Dey, S. Chatterjee et al., *Appl. Phys. Lett.* 104 (2014) 052906.
- [4] J.J. Sanchez Rodriguez, A.N. Nunez Leon, J. Abbasi et al., *Nanomaterials* 12 (2022) 4164
- [5] G.M. Abramova, G.A. Petrakovskii, *Low Temp. Phys.* 32 (2006) 954.

Pump-Probe Spectroscopy of Vibrational Wave Packet Revival for Mapping Molecular Potentials

Blinov S.N.¹, Kimberg V.V.¹, Krasnov P.O.¹, Gelmukhanov F.Kh.^{1,2}, Polyutov S.P.¹

1 – Siberian Federal University, Krasnoyarsk, Russia

2 – KTH Royal Institute of Technology, Stockholm, Sweden

kpo1980@gmail.com

Ultrafast pump-probe spectroscopy is an extremely useful tool for studying dynamics when the first (pump) pulse is used to start an electronic or nuclear process, and the second (probe) pulse, arriving with a time delay, tests the system response in terms of absorption or photoemission spectroscopy, allowing to track the evolution of the system in real-time.

Due to recent advances in the field of X-ray free electron lasers (XFEL) [1] and high-order harmonic generation sources (HHG) [2,3], modern X-ray spectroscopy [4,5] gives new possibilities for ultrafast pump-probe methods. The main advantage of using X-rays is their high selectivity for chemical elements because of the high localization of the core orbitals, which makes it possible to address the atomic center of interest in complex molecular systems.

Recently, considerable attention has been paid to time-resolved X-ray spectroscopy for studying photo-excited molecular processes [5,6]. Prior to the XFEL era, these experiments were limited to a time resolution of 100 ps, restricting time-resolved research to the study of metastable states and preventing direct understanding of the fundamental dynamics occurring in the femtosecond time scale, for example, near conical intersections. With the advent of the XFEL and HHG facilities, the availability of wavelength-tunable ultrashort X-ray pulses as part of various pump-probe techniques makes it possible to directly map non-adiabatic nuclear dynamics. The limited spectral resolution of stationary X-ray spectroscopy can be overcome by using high temporal resolution in real-time X-ray measurements of vibrational and rotational dynamics. This makes modern X-ray spectroscopy an important additional tool for mapping intra- and intermolecular potential energy surfaces [7-9] along with traditional and nonlinear vibrational spectroscopy (VUV, IR, THz, IR-Raman, etc) [10]. A technique combining IR-pump with X-ray-probe processes was theoretically developed almost two decades ago [11,12], where its high phase sensitivity was shown.

Further development of the theoretical framework for simulations of the ionization-induced vibrational dynamics probed with short-time-delayed X-ray pulses is presented here. The NO molecule was considered a study case since it was carefully addressed in recent experimental [13] and theoretical [11,14] studies. In the beginning, the molecular ensemble is irradiated by a short pump pulse ionizing the valence electron from the highest-occupied molecular orbital. At this, various mechanisms of ionization such as the one-photon process triggered by an ultraviolet pulse, infrared multiphoton ionization, and tunneling ionization in the case of strong infrared radiation were examined by us. All considered ionization regimes

lead to the electronic ground state of the cation NO⁺. Since the equilibrium internuclear distance of the cation differs sufficiently from the neutral molecule, the ionization triggers vibrational wave packet (VWP) dynamics in the cation, which is studied by time-resolved X-ray absorption spectroscopy (TRXAS) using short time-delayed X-ray pulses. The present pump-probe scheme explored here is theoretically based on a fully quantum-mechanical description of the VWP and correspondent TRXAS profile, utilizing the concept of forward and backward propagation time [11,12]. The effect of the shape and duration of the X-ray probe pulse on the TRXAS profile was also investigated. As a result, it was definitely shown that the VWP trajectory is accurately reflected in TRXAS, which makes this technique a very useful tool for extracting parameters of molecular potential-energy curves with reasonable accuracy [15].

Acknowledgement: This work was supported by the Russian Science Foundation, grant 21-12-00193.

References:

- [1] J. Duris, et al., *Nat. Photonics* 14 (2020) 30.
- [2] A. Johnson, et al., *Sci. Adv.* 4 (2018) eaar3761.
- [3] E. Lindroth, et al., *Nat. Rev. Phys.* 1 (2019) 107.
- [4] M. Kowalewski, et al., *Chem. Rev.* 117 (2017) 12165.
- [5] F. Gel'mukhanov, et al., *Rev. Mod. Phys.* 93 (2021) 035001.
- [6] L. Varvarezos, et al., *J. Phys. Chem. Lett.* 14 (2023) 24.
- [7] S. Mukamel, *Annu. Rev. Phys. Chem.* 51 (2000) 691.
- [8] C. Miron, et al., *Nat. Phys.* 8 (2012) 135.
- [9] V. Kimberg, C. Miron, *J. Electron Spectrosc. Relat. Phenom.* 195 (2014) 301.
- [10] C. Baiz, et al., *Chem. Rev.* 120 (2020) 7152.
- [11] F. Guimarães, et al., *Phys. Rev. A* 72 (2005) 012714.
- [12] V. Felicissimo, et al., *J. Chem. Phys.* 122 (2005) 094319.
- [13] N. Saito, et al., *Optica* 6 (2019) 1542.
- [14] F. Guimarães, et al., *Chem. Phys. Lett.* 405 (2005) 398.
- [15] S. Blinov, et al., *Phys. Rev. A* (2023). In press.

XAS Investigation of U Local Structure in Nuclear Legacy Sites

Krot A.D.¹, Trigub A.L.², Yapaskurt V.O.¹, Tolpeshta I.I.¹, Vlasova I.E.¹

1 – Lomonosov Moscow State University, Moscow, Russia

2 – National Research Center “Kurchatov Institute”, Moscow, Russia

Anna.d.krot@gmail.com

As a result of past activities in nuclear industry, a lot of radioactive waste and objects called “nuclear legacy sites” were created. Operation with such objects requires a vast scientific basis from nano- to macroscale. A special attention should be paid to Uranium, as the most strongly involved element in the nuclear sector. Complexity of contaminated nuclear legacy sites and low concentration of U in samples limit a set of instrumental techniques available for identification of U speciation. One of the available methods is identification of U phases by analyzing U local surrounding, determined from the analysis of the Extended X-ray Absorption Fine Structure (EXAFS) Spectra. To accurately identify U speciation in nuclear legacy sites, a huge base of model compounds is required. Aim of our work was to create the base of model systems and identify U speciation in radioactively contaminated soil from Sublimate Enterprise of FSUE “AECC”.

Model systems were used to (i) determine characteristic EXAFS parameters, which could be used to identify U phases in different surroundings; (ii) to study patterns of U behaviour under various conditions and in presence of several sorbents. Model systems include: U(VI) intrinsic phases; binary systems of U sorbed on a set of clay minerals and organic sorbents under various pH and [U] conditions; ternary systems of U sorbed on Fe³⁺-organic nanoaggregates; multicomponent systems of U sorbed on soil of different composition. Finally, relying on interpretation of EXAFS parameters, and model systems, U speciation was determined in two fractions of radioactively contaminated soil from Sublimate Enterprise of FSUE “AECC”: fraction with particle size less than 100 µm and coal fragments from “light” fraction.

Investigation of model systems show that EXAFS parameters of U sorbed on clay minerals of smectite group and organic sorbents are slightly sensitive to pH and U concentration in studied ranges. In ternary systems with Fe³⁺-organic matter nanoaggregates U is predominantly associated with organic matter. In systems with soil (in the presence of Fe oxides, organic matter and clay minerals) U is mainly associated with clay minerals, Fe oxides and organic matter play minor role. In radioactively contaminated soil with particle size <100 µm U is present as uranyl intrinsic phases: oxyhydroxides and carbonates. In coal fragments from “light” fraction U forms uranyl complexes with natural organic matter.

Acknowledgement: Authors acknowledge Prof. Dr. K. Kvashnina and PhD E. Bazarkina for their help in XAS data collection at Rossendorf Beamline of ESRF. This work was supported by the Russian Science Foundation, grant 19-73-20051 and Interdisciplinary Scientific and Educational School of Moscow University «Future Planet and Global Environmental Change».

Study of CA(TCA)/SWCNTs Hybrid Sensor Materials by XES, NEXAFS, XPS, and Quantum Chemistry Methods

Lavrukhina S.A., Fedorenko A.D., Sysoev V.I., Semushkina G.I., Okotrub A.V.
Nikolaev Institute of Inorganic Chemistry, Novosibirsk, Russia
x-rayspectroscopy@mail.ru

Nitrogen dioxide (NO_2) is one of the main air pollutants released into the atmosphere during the combustion of various types of fuel. Since even trace amounts of NO_2 can cause serious health effects, its accurate and rapid detection is an important issue. For these purposes, gas sensors based on metal oxides are currently widely used. However, they operate at elevated temperatures and have low selectivity [1]. The search for new sensor materials with high sensitivity and operating at room temperature is topical. Currently, various gas sensors based on carbon nanotubes (CNTs) are being widely studied to detect toxic gases with high selectivity, such as NO_2 [2], NH_3 [2, 3], H_2S [4], organic vapor, etc., allowing to obtain a response at room temperature, due to the fast response, large absorption capacity and resistance to the environment [5].

At the same time, chemical functionalization, the introduction of vacancy defects, the deposition of metal or semiconductor particles, or the formation of heterojunctions with other materials improve the sensor properties of CNTs.

The sensory properties of CNTs can also be improved using the principles of molecular recognition and molecular receptor. Calixarenes (CAs) and thiacalixarenes (TCAs) are molecular receptors that have hydrophobic and hydrophilic cavities capable of encapsulating gas molecules, as well as the ease of functionalization of their upper or lower rims, which makes it possible to create a receptor with desired properties for a particular analyte [6]. However, the low electrical conductivity of the CA or TCA is the main obstacle to the creation of a chemical resistive sensor based on it alone. In this regard, it is promising to use a hybrid material based on SWCNTs and CA\TCA to create a highly efficient sensor operating at room temperature.

Sensor response parameters are largely determined by the nature of the interaction of the analyzed gas with the sensitive layer of the sensor. The formation of hybrid structures based on thin films (graphene, carbon nanotubes) acting as a carrier and CA or TCA deposited on their surface can be associated with a significant change in the electronic structure of both the film itself and CA/TCA, which in turn can lead to changes in receptor and selective properties. Thus, the necessary information for the development of new sensors is the discovery of the relationship between the geometric and electronic structure of the sensitive layer and the parameters of the sensory response to predict the receptor and selective properties of CA molecules. XPS, RES, RAS and quantum chemistry methods are powerful tools for studying the electronic structure of molecules.

In this work, we studied the electronic structure of CA\TCA and hybrid sensor materials CA(TCA)/SWCNTs by highly characteristic and efficient methods of X-ray photoelectron (XPS), X-ray emission (XES) and X-ray absorption spectroscopy (XANES) in combination with quantum chemistry methods. The features of the electronic structure of CA and TCA molecules, as well as the influence of the conformation of molecules on the electronic structure of TCA of the cone and 1,3-alternate conformation and its acyclic analogue (Fig. 1), were studied using X-ray emission $OK\alpha_{1,2}$ -spectra and K-edges absorption of carbon. XPS was used to study the change in the electronic structure upon interaction with SWCNTs. In the Orca 4.2.1 program, the interaction of a CA molecule with SWCNTs was calculated, as well as the interaction of the studied molecules of CA, TCA with an acceptor (NO_2) and donor (NH_3) gas, and the adsorption energy was calculated. Based on the obtained experimental and theoretical data, composition and energy position of HOMO and LUMO of molecules; possible donor and acceptor centers were determined. The receptor, selective, and sensor properties were compared with the electronic structure of the studied compounds. A technique for synthesizing a hybrid material based on single-walled carbon nanotubes (SWCNTs) and CA\TCA was developed and optimized. The sensory responses of hybrid materials with respect to electron-donor and acceptor molecules have been experimentally studied.

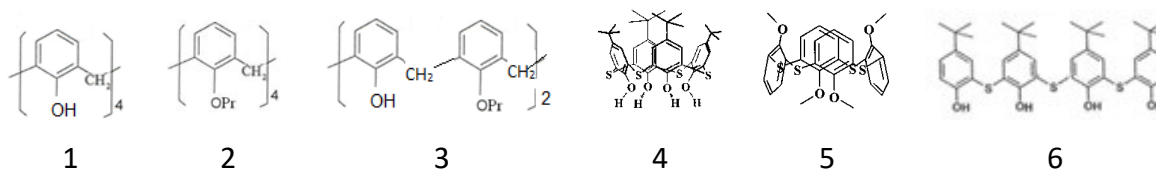


Fig. 1. CA (1-3) and TCA (4-6) used in the work

References:

- [1] Yang, S.; Lei, G.; Xu, H.; Lan, Z.; Wang, Z.; Gu, H. Metal Oxide Based Heterojunctions for Gas Sensors: A Review. *Nanomaterials* 2021, 11, 1026. <https://doi.org/10.3390/nano11041026>
- [2] G.P. Evans, D.J. Buckley, N.T. Skipper, I.P. Parkin, Single-walled carbonnanotube composite inks for printed gas sensors: enhanced detection of NO_2 , NH_3 , EtOH and acetone, *RSC Adv.* 4 (2014) 51395–51403.
- [3] F. Rigoni, S. Tognolini, P. Borghetti, G. Drera, S. Pagliara, A. Goldoni, L. Sangaletti, Enhancing the sensitivity of chemiresistor gas sensors based on pristine carbon nanotubes to detect low-ppb ammonia concentrations in the environment, *Analyst* 138 (2013) 7392–7399.
- [4] Zhao, Y., Zhang, J., Wang, Y. et al. A Highly Sensitive and Room Temperature CNTs/SnO₂/CuO Sensor for H₂S Gas Sensing Applications. *Nanoscale Res Lett* 15, 40 (2020). <https://doi.org/10.1186/s11671-020-3265-7>
- [5] J. Chaste, A. Eichler, J. Moser, G. Ceballos, R. Rurali, A. Bachtold, Ananomechanical mass sensor with yoctogram resolution, *Nat. Nanotechnol.* 7(2012) 301–304.
- [6] Sarkar, T., Srinives, S., Rodriquez, A., & Mulchandani, A. (2018). Single-Walled Carbon Nanotube-Calixarene Based Chemiresistor for Volatile Organic Compounds. *Electroanalysis*. doi:10.1002/elan.201800199

Mechanistic Study of Methanol Oxidation over Monolayer V₂O₅/CeO₂ and V₂O₅/TiO₂ Catalysts

Litvintseva K.A.^{1,2}, Chesalov Yu.A.¹, Selivanova A.V.¹, Saraev A.A.^{1,2}, Kaichev V.V.^{1,2}

1 – Boreskov Institute of Catalysis, Novosibirsk, Russia

2 – Novosibirsk State University, Novosibirsk, Russia

k.litvintseva@g.nsu.ru

The oxidation of methanol over V₂O₅/CeO₂ and V₂O₅/TiO₂ catalysts was studied by X-ray photoelectron spectroscopy (XPS) and Fourier-transform infrared spectroscopy (FTIRS) at temperatures between 100 and 300°C. XPS was used to analyze the catalyst state after treatments in pure methanol or in methanol/oxygen mixtures; FTIRS was used for *operando* studies reaction intermediates adsorbed on the catalyst surfaces and gaseous products.

According to *operando* FTIRS measurements, in both cases, at low temperatures methanol is oxidized to methyl formate (HCOOCH₃), formaldehyde (HCHO) and dimethoxymethane (H₂C(OCH₃)₂) mainly. CO and CO₂ were detected among the gaseous products at high temperatures. Methoxy groups, formates, and dioxymethylene species were detected on the catalyst surface under reaction conditions. It was found that the V₂O₅/CeO₂ catalyst is less active than the V₂O₅/TiO₂ catalyst and the products of selective oxidation appear on it at higher temperatures; the V₂O₅/CeO₂ catalyst is more active in the total oxidation of methanol to CO₂.

For both catalysts XPS data confirmed the partial reduction of V⁵⁺ cations to the V⁴⁺ and V³⁺ states in the absence of oxygen in the reaction mixture, as well as the partial reduction of V⁵⁺ cations to the V⁴⁺ state in the presence of oxygen in the gas phase over the catalyst. It is also confirmed that CeO₂ support is reducible (Ce⁴⁺ is reduced to Ce³⁺), while TiO₂ support is nonreducible (the cations are in the Ti⁴⁺ state). This means that in both cases the reaction proceeds according to the redox mechanism of Mars–Van Krevelen. A detailed mechanism for the selective oxidation of methanol over vanadium oxide-based catalysts is discussed.

Acknowledgement: This work was supported by the program «Priority 2030».

Investigation of Polymorphic Transition in Carbamazepine Induced by Mechanical Treatment

Losev E.A.^{1,2,3}, Zheltikova D.Ya.¹, Boldyreva E.V.^{1,2}

1 – Novosibirsk State University, Novosibirsk, Russia

2 – Boreskov Institute of Catalysis, Novosibirsk, Russia

3 – Voevodsky Institute of Chemical Kinetics and Combustion SB RAS, Novosibirsk, Russia

losev.88@mail.ru

An application of synchrotron radiation facilities to study of mechanochemical reactions makes it possible to investigate the kinetics and mechanisms of solid-phase transformations, as well as to avoid an interruption of mechanochemical processing when studying the process in *in-situ* mode. In the absence of access to the synchrotron radiation sources, mechanochemical transformations can be investigated *ex-situ*, using laboratory X-ray sources.

The purpose of this work was to study the effect of parameters of mechanical treatment on polymorphic transitions in carbamazepine. Carbamazepine is a biologically active compound that is active component of antiepileptic and anticonvulsant drugs, such as Tegretol®, Zeptol®, Finlepsin®, etc. Carbamazepine is able to crystallize in various polymorphic modifications (5 forms), differing in the packing of molecules in the crystal structure. In the current study an influence of time processing scheme, a type of vibrating ball mill and ball-to-powder mass ratio on the polymorphic transition from III to IV form of carbamazepine were investigated. In addition, the importance of controlling the purity of a mechanochemical experiment is demonstrated. The fact of radical acceleration of the transition III→IV was found when contamination was introduced from the fingers of the experimenter. When trying to identify the key component of contamination responsible for the observed effect, the possibility of obtaining the most metastable form of carbamazepine (polymorph II) mechanochemically with the introduction of minor additives (5 molar %) of saturated fatty acids into the system was shown for the first time. The observed effects are explained based on the crystal structure of carbamazepine polymorphs, the structure of the additives introduced and the processes occurring under mechanical treatment. The obtained data emphasize the importance of detailed planning and implementation of mechanochemical treatment, as well as the selection of experimental parameters to control over obtaining the required polymorphic modifications.

Acknowledgement: This research was supported by the Russian Foundation of Basic Research (project 19-29-12026-mk); Ministry of Science and Higher Education of Russia; project AAAA-A21 121011390011-4 at Boreskov Institute of Catalysis SB RAS and project “Priority 2030” at Novosibirsk State University. The equipment of the laboratory MDEST of the REC INChT, Novosibirsk State University was used.

X-Ray and Computational Studies of Platinum Acetate Polymorphs and Solvatomorphs

Maximova A.D., Yakushev I.A.

Kurnakov Institute of General and Inorganic Chemistry of the Russian Academy of Sciences,
Moscow, Russia
mr.albatroz@yandex.ru

Crystalline platinum(II) acetate $[\text{Pt}_4(\mu\text{-OCOMe})_8]$ stands out from the most of platinum group metal carboxylates. Despite numerous attempts to obtain it as starting material for research and practical purposes, until recent times [1] only modest information was available about this substance. Some single-crystal XRD studies of specimens revealed the tetragonal crystals (space group $P4_32_12$) formed by the tetranuclear molecules $[\text{Pt}_4(\text{OCOMe})_8]$ with short Pt–Pt distances; further studies also found the prismatic crystals of monoclinic polymorph with space group $P2_1/c$ formed by almost the same tetranuclear molecules $[\text{Pt}_4(\text{OCOMe})_8]$ [2] (Fig. 1a). In this work using synchrotron radiation single crystal X-ray diffraction (“Belok” beamline, Kurchatov synchrotron radiation source) we have revealed the existence of the one new polymorph (space group $C2/c$) and one new solvatomorph of platinum(II) acetate and attempted to clarify the origin of this unexpected polymorphism [3] by Hirschfeld surface analysis method (Fig. 1b).

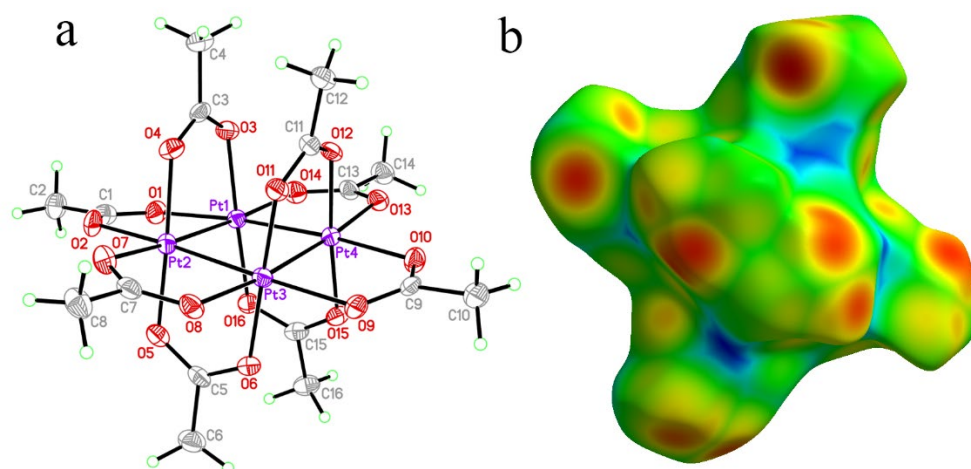


Fig. 1a. Crystal structure of tetranuclear $[\text{Pt}_4(\text{OCOMe})_8]$ and its Hirshfeld surface.

Acknowledgement: The work was carried out in terms of State assignment of the Kurnakov Institute of General and Inorganic Chemistry (Russian Academy of Sciences) in the field of fundamental research.

References:

- [1] Markov, A. A., Yakushev, I. A., Churakov, A. V., Khrustalev, V. N., Cherkashina, N. V., Stolarov, I. P., Vargaftik, M. N. et al. Mendeleev Communications (2019) V. 29(5) p. 489.
- [2] Carrondo, M.A.A.F. de C.T.; Skapski, A.C. X-ray crystal structure of the monoclinic form of cyclo-tetrakis[di- μ -acetato-platinum(II)]: a square-cluster platinum complex. Acta Crystallogr. Sect. B 1978, 34, 3576–3581.
- [3] E.A. Sosunov, A.D. Maksimova, I.A. Yakushev, N.K. Ogarkova, M.N. Vargaftik, A.S. Popova. Russian Journal of Coordination Chemistry (2023), submitted for publication.

Unusual Lattice Parameters Behavior for $\text{La}_{1.9}\text{Ca}_{0.1}\text{NiO}_{4+\delta}$ at the Temperatures below Oxygen Loss

Mishchenko D.D., Vinokurov Z.S., Shmakov A.N.
 SRF SKIF BIC SB RAS, Koltsovo, Russia
 q14999@yandex.ru

Materials structurally related to 1st order Ruddlesden-Popper phases are promising candidates for intermediate temperature solid oxide fuel cells (IT-SOFC) cathodes. Lanthanide nickelates in particular ($\text{Ln}_2\text{NiO}_{4+\delta}$, Ln = La, Pr, Nd) are often considered as such. These compounds possess high levels of mixed ionic-electronic conductivities due to its ability to accumulate large amounts of highly mobile interstitial oxygen (δ) in the structure [1].

Undoped $\text{La}_2\text{NiO}_{4+\delta}$ has insufficient electrical conductivity for using it as an IT-SOFC cathode. Doping by aliovalent alkaline earth elements, for example Ca^{2+} , substantially increases electrical conductivity owned to electronic holes concentration increase. Despite this Ca doping should be approached with care since it decreases the amount of interstitial oxygen in the structure which in turn deteriorate oxygen mobility [2]. Although there are some works showing that low doping (5 mol. %) level actually positively influence both electrical and oxygen mobility [3].

Studying structure of $\text{La}_{2-x}\text{Ca}_x\text{NiO}_{4+\delta}$ ($x = 0, 0.1, 0.2, 0.3, 0.4$) series by *in situ* XRD diffraction [4,5] we observed unusual lattice parameters behavior for $x = 0-0.2$ samples. This behavior consisted of strong opposite change of a and c lattice parameter at 200-450 °C upon heating of the as-synthesized samples in an inert atmosphere. The most prominent this effect was observed for $\text{La}_{1.9}\text{Ca}_{0.1}\text{NiO}_{4+\delta}$ sample (Fig. 1).

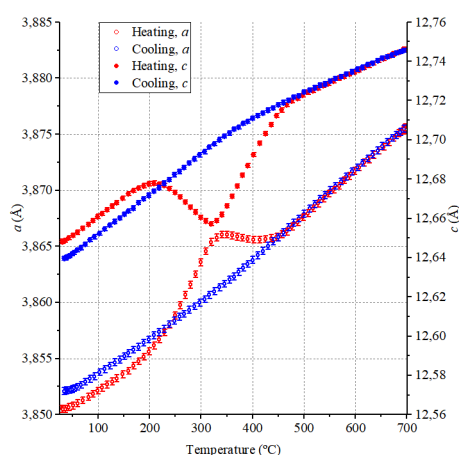


Fig. 1. Unusual lattice parameters change for LCNO01 sample

Unusual lattice parameter change can be divided into two different regions separated by a deflection point at around 325 °C where direction of lattice parameters change goes to the opposite. We managed to reproduce such a behavior by quenching the sample from 1100 °C to RT in air. Therefore, we suggested that unusual lattice parameter change connected to the relaxation of metastable state of the sample after synthesis.

Isotope exchange data combined with TGA data suggested that the process before the deflection point constituted of the interstitial oxygen rearrangement inside the structure, and after the deflection point the process can include oxygen content change. XRD showed that the relaxation before the deflection point leads to the broadening of the reflections with strong / Miller indexes which we managed to describe using Stephens anisotropic microstrain model [6] realized in GSAS-II program package [7]. The model showed significantly bigger microstrains in [001] direction. Williamson-Hall plot also showed the decrease in coherent scattering region for sample in this state. This implies the formation of defects upon metastable state relaxation.

To study the configuration of these defects we used HR-TEM. We prepared the sample in three states: quenched from 1100 °C to RT in air (metastable); annealed at 250 °C after quenching in an inert atmosphere (low-temperature relaxed); annealed at 500 °C after quenching in an air (high-temperature relaxed). Turned out that the quenched sample had low-defect structure. Low-temperature relaxed one had a lot of disorientated planar defects as well as amorphization of the surface and the presence of nanoparticles on the surface. High-temperature relaxed one also had planar defects but orientated at the particular directions – such defect configuration did not affect its diffraction profile.

Acknowledgement: The reported study was funded within the framework of budgeted project for Synchrotron radiation facility SKIF, Boreskov institute of catalysis.

References:

- [1] Tarutin, A.P.; Lyagaeva, J.G.; Medvedev, D.A.; Bi, L.; Yaremchenko, A.A. *J. Mater. Chem. A* 2021, 9, 154–195.
- [2] Tropin, E.S.; Ananyev, M.V.; Farlenkov, A.S.; Khodimchuk, A.V.; Berenov, A.V.; Fetisov, A.V.; Eremin, V.A.; Kolchugin, A.A. *Journal of Solid State Chemistry* 2018, 262, 199–213.
- [3] Shen, Y.; Zhao, H.; Liu, X.; Xu, N. *Phys. Chem. Chem. Phys.* 2010, 12, 15124.
- [4] Pikalova, E.; Sadykov, V.; Sadovskaya, E.; Yermeev, N.; Kolchugin, A.; Shmakov, A.; Vinokurov, Z.; Mishchenko, D.; Filonova, E.; Belyaev, V. *Crystals* 2021, 11, 297.
- [5] Mishchenko, D.; Vinokurov, Z.; Gerasimov, E.; Filonova, E.; Shmakov, A.; Pikalova, E. *Crystals* 2022, 12, 344.
- [6] Stephens, P.W. *J Appl Crystallogr.* 1999, 32, 281–289.
- [7] Toby, B.H.; Von Dreele, R.B. *J Appl Crystallogr* 2013, 46, 544–549.

Determination of Active Sites of Ru- and Ir-Catalysts during Hydrogenation of Bio-Oils and Aromatics

Naranov E.¹, Sadovnikov A.¹, Arapova O.¹, Guda A.²

1 – Topchiev Institute of Petrochemical Synthesis, Russian Academy of Sciences, Leninsky prospekt, bld. 29, 119991, Moscow, Russia

2 – The Smart Materials Research Institute, Southern Federal University, Sladkova Street 178/24, Rostov-on-Don 344090, Russia
naranov@ips.ac.ru

There are many studies reporting hydrogenation processes in water using different heterogeneous and homogeneous catalysts, e.g. Ru, Re, Rh, Pd, and Pt [1–14]. These catalysts exhibit high activity in HDO process. Among these noble metals, ruthenium is oxophilic, highly active in hydrogenation in the aqueous and organic phase and least expensive [15–20]. These facts initiated further studies where the different form of ruthenium was compared to the common reduced Ru catalysts. It was found that the hydrous form was more active compared to conventionally used ones, since the water molecules near the Ru species adsorb the substrate on their surface through hydrogen bonding followed by HDO [19,21,22]. However, there is a lack of information regarding the nature of Ru active sites in aqueous solutions. The structure of ruthenium hydrous oxides is still unknown as well as the reason of its high activity. More physico-chemical data about the nature of such acid sites are of paramount importance for the development of effective HDO catalysts. In this work, the in situ formation of ruthenium hydrous oxide supported on MFI nanosheets is reported. The evolution of the phase transformation ruthenium oxide (IV) → ruthenium hydrous oxide in aqueous solution during HDO process was thoroughly investigated [23–25]. For the first time, in situ X-ray absorption near edge structure (XANES) data under high pressure and temperature was collected during HDO process (Fig. 1).

Hydrogenation of petroleum fractions is one of the most large-scale processes in oil refining. This process allows you to clean hydrocarbons from sulfur and nitrogen compounds, as well as from resinous components. Selective ring opening of cyclic naphthenes is an alternative technology to reduce the level of naphthenes in hydrogenated fractions by breaking the internal C–C bonds to produce paraffins with the same number of carbon atoms, and consequently increasing the cetane number of the resulting diesel fuels [26–28]. The Ir-containing samples on porous materials were synthesized as the catalysts of ring-opening of naphthenes. The phase transformation Iridium oxide (IV) → Iridium (0) was thoroughly investigated using X-ray absorption near edge structure (XANES) data.

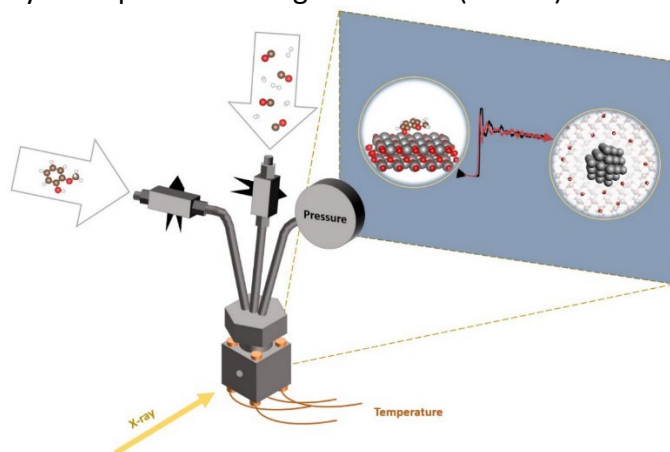


Fig. 1. The scheme of an in situ experiment for Ru-catalysts nature determination by XAS during hydrogenation

Acknowledgement: This work was supported by the Russian Science Foundation, grant № 22-79-10294

References:

- [1] E.R. Naranov, A.S. Badeeva, A.A. Sadovnikov, S. V. Kardashev, A.L. Maksimov, S. V. Lysenko, V.A. Vinokurov, E.A. Karakhanov, *Pet. Chem.* 56 (2016) 599–606.
- [2] D.A. Shavaleev, M.L. Pavlov, R.A. Basimova, E.R. Naranov, *Pet. Chem.* 60 (2020) 1164–1169.
- [3] C.E.J.J. Vriamont, T. Chen, C. Romain, P. Corbett, P. Manageracharath, J. Peet, C.M. Conifer, J.P. Hallett, G.J.P. Britovsek, *ACS Catal.* 9 (2019) 2345–2354.
- [4] A. Stanislaus, B. Cooper, *Catal. Rev.* 36 (1994) 75–123.
- [5] S. Salakhum, T. Yutthalekha, M. Chareonpanich, J. Limtrakul, C. Wattanakit, *Microporous Mesoporous Mater.* 258 (2018) 141–150.
- [6] R.A. Ortega-Domínguez, H. Vargas-Villagrán, C. Peñalosa-Orta, K. Saavedra-Rubio, X. Bokhimi, T.E. Klimova, *Fuel* 198 (2017) 110–122.
- [7] E.R. Naranov, A.A. Sadovnikov, A.L. Bugaev, D.A. Shavaleev, A.L. Maximov, *Catal. Today* 378 (2021) 149–157.
- [8] E.R. Naranov, O. V. Golubev, A.I. Guseva, P.A. Nikulshin, A.L. Maksimov, E.A. Karakhanov, *Pet. Chem. Neft.* 57 (2017) 965–5441.
- [9] E.V. Rakhmanov, S.V. Baranova, Z. Wang, A.V. Tarakanova, S.V. Kardashev, A.V. Akopyan, E.R. Naranov, M.S. Oshchepkov, A.V. Anisimov, *Pet. Chem.* 54 (2014).
- [10] D. Fairuzov, I. Gerzeliev, A. Maximov, E. Naranov, *Catalysts* 11 (2021).
- [11] E.R. Naranov, A.L. Maximov, *Catal. Today* 329 (2019) 94–101.
- [12] E.R. Naranov, K.I. Dement'ev, I.M. Gerzeliev, N.V. Kolesnichenko, E.A. Roldugina, A.L. Maksimov, *Pet. Chem.* 59 (2019).
- [13] E.R. Naranov, A.S. Badeeva, A.A. Sadovnikov, S. V. Kardashev, A.L. Maksimov, S. V. Lysenko, V.A. Vinokurov, E.A. Karakhanov, *Pet. Chem.* 56 (2016) 599–606.
- [14] S.G.A. Ferraz, B.M. Santos, F.M.Z. Zotin, L.R.R. Araujo, J.L. Zotin, *Ind. Eng. Chem. Res.* 54 (2015) 2646–2656.
- [15] J. October, S.F. Mapolie, *J. Organomet. Chem.* 840 (2017) 1–10.
- [16] Q. Tan, G. Wang, L. Nie, A. Dinse, C. Buda, J. Shabaker, D.E. Resasco, *ACS Catal.* 5 (2015) 6271–6283.
- [17] J. Shangguan, A.J.R. Hensley, M. V. Gradiski, N. Pfriem, J.S. McEwen, R.H. Morris, Y.H.C. Chin, *ACS Catal.* 10 (2020) 12310–12332.
- [18] A. Aho, S. Roggan, O.A. Simakova, T. Salmi, D.Y. Murzin, *Catal. Today* 241 (2015) 195–199.
- [19] A. Kumar, B. Thallada, *Sustain. Energy Fuels* 5 (2021) 3802–3817.
- [20] J. Liu, P. Bai, X.S. Zhao, *Phys. Chem. Chem. Phys.* 13 (2011) 3758–3763.
- [21] S. Gundekari, K. Srinivasan, *Appl. Catal. A Gen.* 569 (2019) 117–125.
- [22] S.H. Lee, P. Liu, H.M. Cheong, C. Edwin Treacy, S.K. Deb, in: *Solid State Ionics*, Elsevier, 2003, pp. 217–221.
- [23] E.R. Naranov, A.A. Sadovnikov, O. V. Arapova, A.L. Bugaev, O.A. Usoltsev, D.N. Gorbunov, V. Russo, D.Y. Murzin, A.L. Maximov, *Catal. Sci. Technol.* 13 (2023) 1571–1583.
- [24] P. V. Shvets, P.A. Prokopovich, A.I. Dolgoborodov, O.A. Usoltsev, A.A. Skorynina, E.G. Kozyr, V. V. Shapovalov, A.A. Guda, A.L. Bugaev, E.R. Naranov, D.N. Gorbunov, K. Janssens, D.E. De Vos, A.L. Trigub, E. Fonda, M.B. Leshchinsky, V.R. Zagackij, A. V. Soldatov, A.Y. Goikhman, *Catalysts* 12 (2022) 1264.
- [25] E. Naranov, A. Sadovnikov, O. Arapova, T. Kuchinskaya, O. Usoltsev, A. Bugaev, K. Janssens, D. De Vos, A. Maximov, *Appl. Catal. B Environ.* 334 (2023) 122861.
- [26] D. Kubička, N. Kumar, P. Mäki-Arvela, M. Tiitta, V. Niemi, T. Salmi, D.Y. Murzin, *J. Catal.* 222 (2004) 65–79.
- [27] D. Kubička, N. Kumar, P. Mäki-Arvela, M. Tiitta, V. Niemi, T. Salmi, D.Y. Murzin, *J. Catal.* 222 (2004) 65–79.
- [28] D. Jampaiah, D.Y. Murzin, A.F. Lee, D. Schaller, S.K. Bhargava, B. Tabulo, K. Wilson, *Energy Environ. Sci.* 15 (2022) 1760–1804.

Evolution of the Structure of a Metal Wire under Tension, Observed by Synchrotron X-Ray Diffraction

Nasennik I.E.^{1,2}

1 – Novosibirsk State Technical University, Novosibirsk, Russia

*2 – Lavrentyev Institute of Hydrodynamics SB RAS, Novosibirsk, Russia
goga.mer@mail.ru*

One of the most powerful in-situ techniques to study the structure of metals under tension is synchrotron X-ray diffraction. This method can be used to measure the lattice parameters as well as to characterize the microstructure of the sample by peak profile analysis.

In this study, we investigated a copper wire annealed at 850°C for 2 hours. The diameter of the wire was 1.5 mm. The experiments were carried out at “Rigid rentgenoscopy” beamline of VEPP-4 source. The tensile test was carried out at a rate of 0.05 mm/s. The final strain of the wire was $\varepsilon = 16\%$. The X-ray diffraction (XRD) patterns were obtained in transmission mode. The photon energy was 54,06 keV (which corresponds to the wavelength of 0.229 Å). The XRD patterns were recorded using Mar345 imaging-plate area detector (the working area was a circle with a diameter of 345 mm). The sample-to-detector distance was 0,508 m.

Several peak profile analysis models were used to determine the size of coherent scattering regions (CSRs) and the lattice microstrains. Namely we used Scherrer formula as well as classical and modified Williamson-Hall methods [1,2]. We show that the most noticeable changes in the microstructure occurred at the beginning of the experiment.

References:

- [1] Williamson, G. K., and W. H. Hall. "X-ray line broadening from filed aluminium and wolfram." *Acta metallurgica* 1.1 (1953): 22-31.
- [2] Ungár, T., and A. Borbély. "The effect of dislocation contrast on x-ray line broadening: a new approach to line profile analysis." *Applied Physics Letters* 69.21 (1996): 3173-3175.

Synthesis and Structural Investigation of Carboxylic Platinum-Based Complexes for Catalytical and Biological Application

Nesterenko M.Yu., Panina M.V., Yakushev I.A.

*Kurnakov Institute of General and Inorganic Chemistry of the Russian Academy of Sciences,
Moscow, Russia
alena.gaverment@gmail.com*

Water-soluble carboxylic square-planar platinum(II) complexes reveal antiproliferative activity [1]. Nowadays a lot of complexes with aromatic N-donors and bidentate carboxylates are known. Despite this, few crystal structures with monodentate carboxylates were presented [2], and a facile production method for this species was not discovered yet. In our previous work [3] we investigated that cationic complex $[PtPy_4](OOCMe)_2$ rapidly reacts with other carboxylic acids and gives corresponding salts according to scheme below. Further, thermal-driven transformations lead to crystalline mononuclear complexes with high yields (Fig. 1).

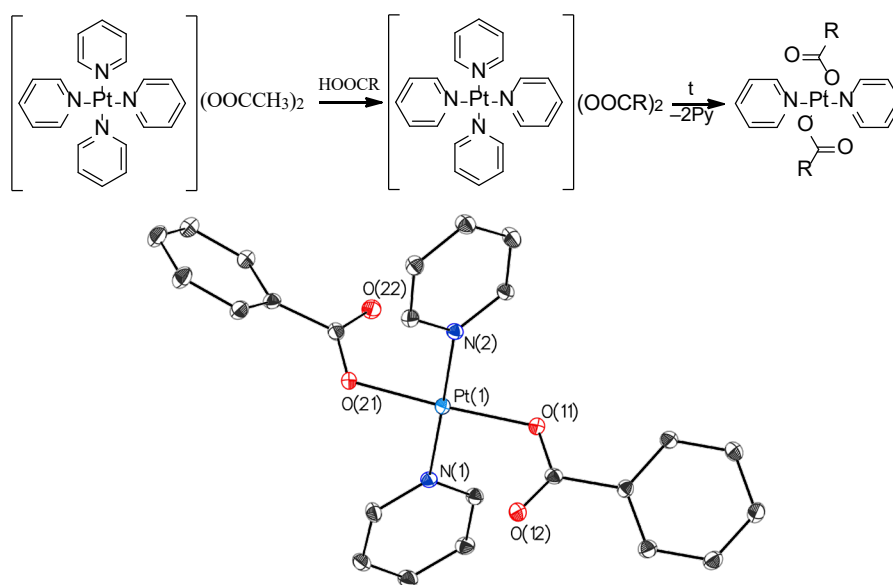


Fig. 1. Crystal structure of $[PtPy_2(OOCPh)_2]$

In this work, we prepared a number of novel cationic complexes $[PtPy_4](OOCR)_2$ with various carboxylate anions and have developed two synthetic methods for producing mononuclear Pt(II) complexes of general formula $[PtPy_2(OOCR)_2]$, which is not known before. The crystal structures of both cationic and molecular complexes were established by synchrotron radiation single crystal X-ray diffraction technique, and spectroscopic methods confirmed the composition of the prepared samples.

Acknowledgement: The work was carried out in terms of State assignment of the Kurnakov Institute of General and Inorganic Chemistry (Russian Academy of Sciences) in the field of fundamental research.

References:

- [1] Milica N. Dimitrijević Stojanović; Andjela A. Franich; Milena M. Jurišević et al. *Journal of Inorganic Biochemistry* (2022) p. 111773
- [2] Yakushev I.A., Ogarkova N.K., Khramov E.V., Smirnova N.S., Nesterenko M.Yu., Cherkashina N.V., et al. *Mendeleev Communications* (2023) V. 33. No. 4. p. 487.
- [3] I.A. Yakushev, M.Yu. Nesterenko, P.V. Dorovatovskii, et al. *Russian Journal of Coordination Chemistry* (2022) V. 48, No. 12, p. 935.

Phase Composition of Biomineral Objects by Hard X-Ray Diffracton Data

Nizovskii A.I.¹, Shmakov A.N.², Ligkodymov A.A.², Bukhtiyarov V.I.¹

1 – Boreskov Institute of Catalysis, Novosibirsk, Russia

2 – SRF SKIF, Novosibirsk, Russia

alexniz@inbox.ru

Currently there are a lot of publications about the actuality of kidney stones analysis and rise of nephrolithiasis morbidity. Till now the exact diagnostics of kidney stone disease is based on indirect signs such as radiograph and urinalisis. These data do not provide information on the mineral composition of the patient's kidney stones. The importance of such an analysis is related to the choice of the most effective method of treating patients and at the same time minimizing the risks of further complications. The application of hard X-ray diffraction In Vivo may be a possible solution of the problem. The report represents the results of model X-ray diffraction experiments using radiation of 69.5 keV.

The experiment was executed at synchrotron radiation beamline No.8 of VEPP-4M storage ring at Siberian Synchrotron and Terahertz Radiation Centre, Budker Institute of Nuclear Physics, Novosibirsk, Russia. The kidney stones inserted to phantom objects modeling patient's body were investigated by means of X-ray diffraction using high energy radiation of 69.5 keV. In contrast to previous experiments [1] using radiation of 33.7 keV the penetration ability of radiation increases essentially, the absorption decreases that reduces the radiation load on patient. The factor of patient weight becomes less critical.

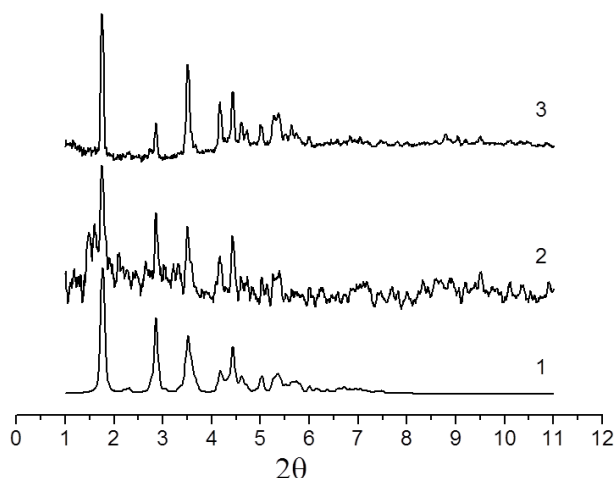


Fig. 1.

- 1 – Calculated XRD pattern of whewellite ($\text{CaC}_2\text{O}_4 \cdot \text{H}_2\text{O}$), ICDD PDF-2, No.20-231;
 2 – XRD pattern of the stone inserted into phantom object with background subtracted;
 3 – XRD pattern of loose stone.

Acknowledgement: This work was supported by the Ministry of Science and Higher Education of the Russian Federation within the governmental order for Boreskov Institute of Catalysis.

References:

[1] Ancharov A.I., Potapov S.S., Moiseenko T.N., Feofilov I.V., Nizovskii A.I.. Model Experiment of in vivo Synchrotron X-Ray Diffraction of Human Kidney Stones. Nuclear Instruments and Methods in Physics Research Section A. 2007. V. 575. N 1-2. P. 221-224.

In-Situ X-Ray Synchrotron Diffraction Study of Solid–Liquid Transitions in the Structure of Al-Co-Cr-Fe-Ni High-Entropy Alloys during Heating

Ogneva T.S.¹, Emurlaev K.S.¹, Malyutina Yu.N.¹, Kuper K.E.²

1 – Novosibirsk State Technical University, Novosibirsk, Russia

2 – Budker Institute of Nuclear Physics, Novosibirsk, Russia

ogneva@corp.nstu.ru

Al-Co-Cr-Fe-Ni high-entropy alloys have high wear resistance, strength, hardness, and oxidation resistance at elevated temperatures. For this reason, one potential application of these alloys is the formation of coatings on widely used constructional materials. In this work, high -entropy Al–Co– Cr–Fe– Ni coatings were formed on low-carbon steel substrates by non-vacuum electron beam cladding. Powder mixtures containing Co, Cr, Al, and Ni were used, and the molar fraction of Al in the powder mixtures varied from 0.5 to 1.5. Fe was passed into the coating composition from the substrate material.

EDX analysis showed that the Al content significantly affects the Fe content, which is transferred into the composition of the coating from the steel substrate. The decrease of the Al molar fraction in the powder mixtures from 1.5 to 0.5 led to an increase in the Fe concentration in the coatings from 9.9 to 48.1 at. %. Samples obtained by cladding powder mixtures with 0.5, 1, and 1.5 molar fractions of Al correspond to the compositions $Al_{0.5}CoCrFe_{3.2}Ni$, $AlCoCrFe_{0.6}Ni$, and $Al_{1.5}CoCrFe_{0.5}Ni$, respectively. The first sample consisted of the fcc phase, the second sample consisted of the bcc + fcc phase, and the third sample consisted predominantly of the bcc phase. In addition, the bcc phase includes ordered A2 and disordered B2 structures. Differences in Fe content may be explained by differences in the solidification temperatures of the coatings with different Al contents. To investigate this effect, the samples were heated up to melting temperatures and analyzed using in-situ synchrotron X-ray diffraction during heating.

The obtained samples were investigated via transmission mode with the wavelength was 0.2479 Å, the beam size was $250 \times 250 \mu m^2$, the distance from the samples to the detector was 286.6 mm. Samples for heating with an area 5×5 mm and a thickness of 0.5 mm were cut from the coating. Heating was performed using an ytterbium fiber laser. Diffraction patterns were taken in the temperature range from 700 °C until the temperature at which a halo appeared on the diffraction patterns. A halo indicated the presence of the liquid phase. The diffraction patterns were recorded with a Mar345 detector (resolution 3500×3500 pixels, pixel size $100 \times 100 \mu m^2$), and the exposure time was 2 minutes.

In the sample $Al_{0.5}CoCrFe_{3.2}Ni$, the process of melting begins at $\sim 1125^\circ C$, at this temperature, almost all reflections of the fcc phase disappear from the diffraction patterns. According to the phase diagram of $AlCoCrNi-Fe_x$ by Zhang et al. [1], alloys with Fe concentration of $x=2...3$ begin to melt at $\sim 1290^\circ C$. Probably because the $Al_{0.5}CoCrFe_{3.2}Ni$ sample contained two times less Al with respect to Cr, Co, and Ni, the solidus temperature of

the sample $\text{Al}_{0.5}\text{CoCrFe}_{3.2}\text{Ni}$ is slightly lower than the values calculated in [1] for alloys with almost similar concentrations of Fe.

The $\text{Al}_{1.5}\text{CoCrFe}_{0.5}\text{Ni}$ sample begins to melt in the temperature range 1400–1425 °C. Its solidus temperature is 30–100 °C lower than the melting temperature of the alloy $\text{Al}_{1.5}\text{CoCrFeNi}$ studied in [3–5]. This could be related to a significant lack of Fe in this sample. In addition, according to [3–5], the $\text{Al}_{1.5}\text{CrCoFeNi}$ alloy completely passes into the liquid state in the temperature range 1460–1500 °C. However, the liquidus temperature of the sample when heated up to 1500 °C has not yet been reached. At this temperature, only the B2 phase remains in the crystalline state because of its high melting point. It was shown in [3–5] that the lack of Fe and excess of Al in Al-Co-Cr-Fe-Ni alloys increases the proportion of the B2 phase. Therefore, the $\text{Al}_{1.5}\text{CoCrFe}_{0.5}\text{Ni}$ sample has a quite high melting point exceeding 1500 °C.

The conclusion can be made that the coating Al-Co-Cr-Fe-Ni formed with 0.5 molar fraction of Al has a solidus temperature of approximately 1125 °C; thus, 48.1 at. % of Fe dissolved in the coating up to the moment of crystallization. When cladding of the coating with 1.5 molar fraction of Al, the alloy has a relatively high solidus temperature ~1400 °C and a liquidus temperature of over 1500 °C; therefore, the period of crystallization in this case was shorter, and only 9.9 at. % dissolved in the coating during crystallization.

Acknowledgement: This research was supported by a grant from the Russian Science Foundation, No. 22-23-20192, <https://rscf.ru/project/22-23-20192/>, and grant No. p-31 from the Government of the Novosibirsk Region

References:

- [1] G.J. Zhang, Q.W. Tian, K.X. Yin, S.Q. Niu, M.H. Wu, W.W. Wang, Y.N. Wang, J.C. Huang, *Intermetallics*. 119 (2020). <https://doi.org/10.1016/j.intermet.2020.106722>.
- [2] Y. Zhang, X. Yang, P.K. Liaw, *JOM*. 64 (2012) 830–838. <https://doi.org/10.1007/s11837-012-0366-5>.
- [3] K. Kuwabara, H. Shiratori, T. Fujieda, K. Yamanaka, Y. Koizumi, A. Chiba, *Addit. Manuf.* 23 (2018) 264–271. <https://doi.org/10.1016/j.addma.2018.06.006>.
- [4] O. Stryzhyboroda, V.T. Witusiewicz, S. Gein, D. Röhrens, U. Hecht, *Front. Mater.* 7 (2020). <https://www.frontiersin.org/articles/10.3389/fmats.2020.00270>.
- [5] M. Ostrowska, P. Riani, B. Bocklund, Z.-K. Liu, G. Cacciamani, *J. Alloys Compd.* 897 (2022) 162722.

In Situ XRD Study of TiC Coating for HfH_x Neutron Control Rods

Pirozhkov A.V., Sidelev D.V.

National Research Tomsk Polytechnic University, Tomsk, Russia

pirog@tpu.ru

Hafnium hydride (HfH₂) is considered as one of the alternatives to B₄C for the manufacture of neutron control rods [1]. The use of hafnium as a substitute is justified by its large fast neutron capture cross section. And the presence of hydrogen makes it possible to slow down fast neutrons to thermal ones. Another significant advantage of Hf is that the interaction of its isotopes with neutrons occurs without the formation of He, which has a positive effect on reliability and increases service life. There is a positive experience of using hafnium as control/emergency rods in research reactors in Japan, the USA and Russia.

However, studies of HfH₂ at high temperatures (1400°C) have shown decreases in the fast neutron capture cross section compared to B₄C and HfB₂ compounds. Such a decrease is associated with the processes of hydrogen desorption at high temperatures. To prevent oxidation processes, it is proposed to use TiC coatings obtained by magnetron sputtering [2].

In this work, we studied samples with uncoated and coated. TiC coatings were deposited on hafnium hydride pellets 10 mm in diameter and 1 mm thick by magnetron sputtering. After the coatings were applied, In situ XRD studies were carried out using synchrotron radiation at the Precision Diffractometry II station of the Siberian Center for Synchrotron and Terahertz Radiation of the Institute of Nuclear Physics. Budker SB RAS (Novosibirsk, Russia). The samples were first heated from 30 to 900°C at a rate of 20°C/min, kept at the maximum temperature for 10 minutes, and cooled from 900 to 30°C at a rate of 20°C/min. A quadrupole mass spectrometer SRS UGA100 was used to study hydrogen desorption from the sample.

An analysis of the change in the phase composition of the uncoated sample demonstrates a sharp drop in the HfH₂ content and an increase in HfO₂, which indicates active desorption processes upon reaching a temperature of 900°C. Studies carried out for samples coated with TiC show that when the maximum temperature of 900°C is reached and the holding starts, there is a sharp increase in TiO₂. After a short holding time, the content of TiO₂ drops sharply, while the content in HfO₂ begins to increase. It can be assumed that this is due to the destruction of the TiC coating. This is confirmed by the mass spectrometry data, which show that at the moment of coating destruction, the maximum release of hydrogen from the sample occurs.

According to the results of the data obtained, it can be said that TiC coatings are not able to prevent desorption from the sample HfH₂ at high temperatures due to the destruction of the coatings themselves. It is assumed that the destruction is associated with a large difference in the coefficients of thermal expansion of the substrate and coating material.

Acknowledgement: The study was supported by the State Assignment within the framework of the scientific project No. FSWW-2021-0017.

References:

- [1] K. Konashi, T. Iwasaki, T. Terai, M. Yamawaki, K. Kurosaki, K. Itoh. in: Proc. 2006 Int. Congress on Advances in Nuclear Power Plants, Embedded Top. (2006)2213–2217.
- [2] D.V. Sidelev, E.B. Kashkarov, M.S. Syrtanov, V.P. Krivobokov. Nickel-chromium (Ni–Cr) coatings deposited by magnetron sputtering for accident tolerant nuclear fuel claddings // Surface and Coatings Technology. 369 (2019) 69-78.

Structure Investigation of Carbon Materials by Synchrotron Radiation

Popova A.N., Sozinov S.A.

*Federal Research Center of Coal and Coal Chemistry SB RAS, Kemerovo, Russia
h991@yandex.ru*

Research on carbon materials using synchrotron radiation has been a significant area of study in recent years. Synchrotron radiation is a powerful tool for investigating the structure, properties, and behavior of carbon-based materials at the molecular level. It allows scientists to gain valuable insights into the atomic and electronic structure of these materials, as well as their chemical composition and functional properties.

One of the key advantages of synchrotron radiation is its ability to provide highly intense and tunable X-ray beams. These X-rays can be used to probe the structure and dynamics of carbon materials with exceptional precision. By analyzing the scattering and absorption of X-rays, researchers can determine the arrangement of atoms, molecular bonding, and crystallographic properties of carbon materials.

Synchrotron-based techniques such as X-ray diffraction, X-ray absorption spectroscopy, and X-ray photoelectron spectroscopy have been widely used to study various carbon materials, including graphene, carbon nanotubes, carbon fibers, and amorphous carbon. These techniques allow researchers to investigate the structural defects, surface chemistry, and electronic properties of carbon materials, providing valuable information for their optimization and application in fields such as energy storage, catalysis, electronics, and environmental remediation.

X-ray diffraction (XRD) is the main method for phase analysis of carbon materials using SR. By directing a beam of X-rays onto the sample, researchers can analyze the resulting diffraction pattern to determine the arrangement of carbon atoms and the crystal structure of the material. This information helps identify the different phases present, such as graphite, amorphous carbon, or other carbon allotropes. Additionally, XRD can reveal details about the stacking order and orientation of carbon layers in materials like graphene.

The research conducted using synchrotron radiation has significantly contributed to our understanding of carbon materials and has paved the way for the development of advanced carbon-based technologies. It has enabled scientists to explore the fundamental properties of these materials and uncover new possibilities for their application in various industries.

This knowledge is essential for optimizing their properties and tailoring them for various applications, including energy storage, electronics, catalysis, and materials science in general.

Acknowledgement: This work was supported by the Russian Science Foundation, grant 22-23-20153.

High Pressure Synchrotron Study of Double Manganite NdBaMn₂O₆

Pryanichnikov S.V.¹, Likhacheva A.Yu.², Sterkhov E.V.¹, Sidorov V.A.³, Titova S.G.¹

1 – Institute of Metallurgy UB RAS, Ekaterinburg, Russia

2 – G.I.Budker Institute of Nuclear Physics SB RAS, Novosibirsk, Russia

3 – Institute of High Pressure Physics RAS, Moscow, Russia

stepian@yandex.ru

Double manganites of rare earth elements have the layered structure consisting of alternating sequence of $RMnO_3$ and $BaMnO_3$ unit cells, R – rare earth element. In comparison with disordered $(R,Ba)MnO_3$ manganites they have significantly higher temperatures of magnetic and electric phase transitions, that makes double manganites more attractive for application.

For the first time we investigated the phase state, crystal structure and physical properties (electrical resistivity, ac magnetic susceptibility, ac heat capacity) for $NdBaMn_2O_6$. The measurements of physical properties were performed in temperature range 100 – 300 K and pressure range 0 – 6 GPa. Crystal structure was studied by powder diffraction using synchrotron radiation in temperature range 300 – 523 K and pressure range 0 – 1.5 GPa. The diffraction experiments were performed at the 4th beamline of the VEPP-3 storage ring using the resistively heated diamond anvils cell and wolfram gaskets, MAR345 IP detector, $\lambda = 0.3685 \text{ \AA}$, gold internal standard.

(T, P) diagram of electric and magnetic states of $NdBaMn_2O_6$ is constructed. It is established that external pressure leads to increase of Neel temperature and decrease of the metal-insulator transition.

Coefficients of compression at different temperatures, coefficients of thermal expansion at external pressure 0.5 and 1.5 GPa are determined. Mn-O bond lengths and their change at metal-insulator phase transition are calculated using Rietveld method.

Acknowledgement: The work was done at the shared research center SSTRC on the basis of the VEPP-4 - VEPP-2000 complex at BINP SB RAS.

Transition Metal Nanocomposites as a Catalyst for Hydrogen Production: Structure and Evolution Synchrotron Study

Roldugin V.A., Medvedev P.V., Gritsai M.A., Soldatov M.A.

*The Smart Materials Research Institute, Southern Federal University, Rostov-on-Don, Russia
roldugin.victor@gmail.com*

The depletion of fossil fuel resources and climate changes associated with global warming exacerbate the need of transition to renewable energy sources. Among other alternatives, hydrogen is environmentally friendly and allows to directly convert the chemical energy of the fuel into electrical energy. The performance of hydrogen production by electrolysis is driven by the development of stable and efficient, but at the same time abundant and inexpensive catalysts, for example, based on transition metals. The key factor on the way to obtain such materials is a detailed understanding of local atomic and electronic structure dynamics and the mechanisms of processes taking place in electrochemical reactions.

In this contribution nanostructured Ir-Co and Ru-Co electrocatalysts deposited on the nitrogen-doped carbon cloth have been investigated by X-ray absorption spectroscopy (XAS) at the structural material science beamline of the Kurchatov specialized source of synchrotron radiation "KISI-Kurchatov" [1]. Experiment was held in the fluorescence mode using photo-electrochemical cell designed for *in situ/operando* measurements as well as laboratory electrochemistry routine (Fig. 1). As a result, the Ru and Co K-edge, Ir L₃-edge spectra were obtained and the dynamics of the catalysts in contact with the 1M potassium hydroxide solution electrolyte have been studied.

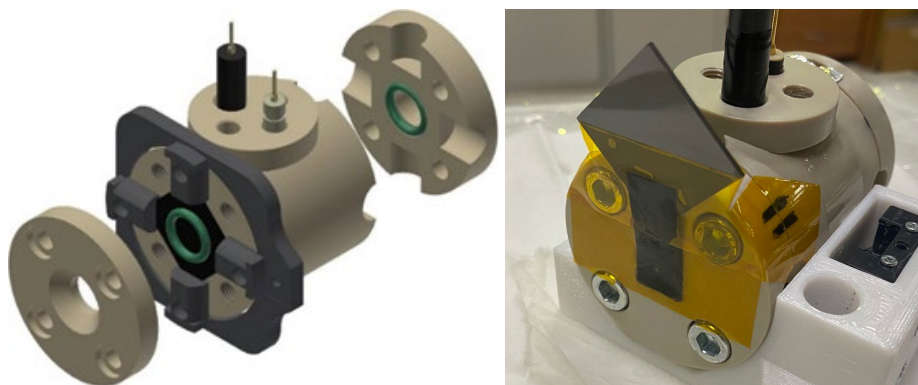


Fig. 1. *In situ/operando* photo-electrochemical cell.

Linear combination fit (LCF) of the Co K-edge spectra reveals the coexistence of Co in different oxidation states for both Ru-Co and Ir-Co samples (Table 1). According to the LCF analysis of the S2 sample before and after immersing in the 1M KOH electrolyte solution fraction of the Co²⁺ decreases from about 19 % to 9 %, while amount of Co³⁺ increases from 5 % up to 15 %. Moreover, high concentration (~75 %) of metal Co, that was not affected by the KOH solution, implies core-shell structure of Co nanoparticles, where metal Co correspond to unaffected core and Co²⁺ phase corresponds to shell, that was then oxidized to Co³⁺.

Table 1. Results of linear combination fit at the Co K-edge.

Sample	Composition	Co foil	Co(acac) ₂	Co(OH) ₃
S1	Ru-Co	59.6 %	40.4 %	not used
S2	Ir-Co	66.6 %	33.4 %	not used
S3	Ru-Co	70.9 %	29.1 %	not used
S4	Ru-Co	33.1 %	29.6 %	37.2 %
S5	Ru-Co	32.9 %	39.6 %	27.5 %
S6	Ir-Co	22.5 %	27.7 %	49.8 %

The Ir L₃-edge spectra of the S6 sample shows the negative edge position shift and the increase of white line peak width in comparison with IrO₂, indicating the presence of Ir³⁺ and co-existence of Ir³⁺ and Ir⁴⁺ oxidation states. Latter was confirmed by the white line position calibration curve made from the literature data [2]. Fourier transformed (FT) extended X-ray absorption fine structure (EXAFS) data show similarities of the first coordination shell ($R = 1.6 \text{ \AA}$, no phase correction) to those of IrO₂, implying octahedral coordination and $\sim 1.98 \text{ \AA}$ Ir-O distance. Evolution of the S2 sample in the 1M potassium hydroxide reveals partial oxidation process of Ir³⁺ to Ir⁴⁺.

Theoretical analysis of the X-ray absorption near edge structure (XANES) for the Ru K-edge spectrum of the S1 sample as well as attempts to fit corresponding FT-EXAFS signal result in suggestion that ruthenium is presented in the form of both Ru-N single sites and small atomic clusters. That means the S1 catalyst contains in some ratio single Ru atoms incorporated in N-doped carbon support and small ruthenium clusters, both acting as catalytic sites.

Thus, synchrotron X-ray absorption spectroscopy together with *in situ/operando* photo-electrochemical cell are powerful and effective technique for the investigation of catalytic processes. It was revealed that nanostructured Ru-Co material consists of core-shell cobalt nanoparticles with significantly oxidized shell and ruthenium composition in the form of single atoms and small atomic clusters simultaneously.

Acknowledgement: The authors acknowledge the Ministry of Science and Higher Education of the Russian Federation for financial support (Agreement № 075-15-2021-1363) and Uday Narayan Maiti from the Indian Institute of Technology Guwahati for provided catalyst samples and scientific discussion.

References:

- [1] Chernyshov, A.A., A.A. Veligzhanin, and Y.V. Zubavichus, Structural Materials Science end-station at the Kurchatov Synchrotron Radiation Source: Recent instrumentation upgrades and experimental results. Nuclear Instruments and Methods in Physics Research Section A: Accelerators, Spectrometers, Detectors and Associated Equipment, 2009. 603(1): p. 95-98;
- [2] Sardar, K., et al., Water-Splitting Electrocatalysis in Acid Conditions Using Ruthenate-Iridate Pyrochlores. Angewandte Chemie International Edition, 2014. 53(41): p. 10960-10964.

Local Electric Field Enhancement Around Ag Nanoparticles and their Agglomerates in Silicate and Zinc-Phosphate Glasses

Rubanik D.S.¹, Srabionyan V.V.¹, Vetchinnikov M.V.², Durymanov V.A.¹, Viklenko I.A.¹,
Avakyan L.A.¹, Shakhgildyan G.Yu.², Sigaev V.N.², Bugaev L.A.¹

1 – Southern Federal University, Rostov-on-Don, Russia

2 – Mendeleev University of Chemical Technology, Moscow, Russia

missdare.dr@gmail.com

Modifications of glasses by various kinds of metallic nanoparticles (NPs) are extensively studied with the aim to obtain improved optical characteristics. Silver NPs are of especial interest because of the presence of a well-defined localized surface plasmon resonance (LSPR) [1] in the visible region of optical extinction spectra, which enables the localization and retention of the energy of incident light in space on the nanometer scale and in time on the femtosecond scale. One of the most significant and rapidly developing directions here is the use of LSPR in Ag particles for generation of laser media with the improved luminescence characteristics and in particular, their use as the effective sensitizers for amplification of laser transitions in rare earth (RE) ions embedded in glasses. Different studies of the mechanisms of the effects of noble-metals NPs on the luminescence characteristics of RE ions revealed the predominant effect of local electric field (LEF) enhancement, caused by their LSPR, if the RE ions are located in the vicinity of NPs [2]

In this work we have studied atomic structure of Ag color centers in glass using Ag K-edge XAFS spectra and obtained distribution of LEF in the vicinity of monometallic Ag NPs synthesized in glass matrix [3], depending on the particles sizes (D), concentration, and degree of their agglomeration. Using simulations for given concentrations and the obtaining average sizes of plasmonic nanoparticles in glass, the dependences of the radial distribution of RE ions relative to the surface of average NP at various ion concentrations were determined. These dependences allow to suggest the most suitable synthesis conditions (loaded concentrations of plasmonic metals and RE ions, kinds of the glass treatment by temperature or laser irradiation for NPs creation) which can provide the high probability of localization of RE ions in the places around NPs, where the LEF enhancement is strong enough, i.e. is not weakened significantly with distance from the particle's surface.

Acknowledgement: This work was supported by the Russian Science Foundation, grant 23-12-00102.

References:

- [1] V. V. Srabionyan, L.A. Avakyan, V.A. Durymanov, D.S. Rubanik, I.A. Viklenko, A.V. Skunova, L.A. Bugaev, *J.Ph.&Chem.Sol.* 179 (2023)
- [2] W. Zhang, J. Lin, M. Cheng, S. Zhang, Y. Jia , J. Zhao *J Quant Spectrosc Radiat Transf* 159 (2015)
- [3] M. Heinz, V.V. Srabionyan, A.L. Bugaev, V.V. Pryadchenko, E.V. Ishenko, L.A. Avakyan, Y.V. Zubavichus, J. Ihlemann, J. Meinertz, E. Pippel, et al., *J. Alloys Compd.* 681 (2016) 307–315

Beamline for Studying Fast-Flowing Processes at the Synchrotron Radiation Facility SKIF

Rubtsov I.A.¹, Bukhtiyarov A.V.¹, Zubavichus Y.V.¹, Kazantsev S.R.¹, Kashkarov A.O.², Kuper K.E.¹, Prueel E.R.², Studennikov A.A.¹, Ten K.A.², Tolochko B.P.³, Halemenchuk V.P.², Shekhtman L.I.⁴

1 – SRF SKIF, Boreskov Institute of Catalysis, Novosibirsk, Russia

2 – Lavrentiev Institute of Hydrodynamics, Novosibirsk, Russia

3 – Institute of Solid State Chemistry and Mechanochemistry, Novosibirsk, Russia

4 – Budker Institute of Nuclear Physics, Novosibirsk, Russia

i.a.rubtsov@srf-skif.ru

“Fast Processes” is one out of 1st priority beamlines of SRF SKIF (Synchrotron Radiation Facility - Siberian Circular Photon Source "SKIF") synchrotron which will be created under a state contract with LIH SB RAS at the end of 2024.

The beamline would include two independent instruments installed at a wiggler source, i.e., Dynamic processes and Plasma. The beamline is designed to meet a wide range of research and technological challenges related to processes occurring in nano- and microsecond timescales. The current conceptual design of the beamline aims at a complex approach to structural studies of various objects relying on high-brightness synchrotron radiation beams.

The beamline would implement X-ray diffraction, small-angle scattering, and radiography techniques with a high temporal resolution, with a typical delay between frames down to 2.8 ns and exposures of about 50 ps.

Acknowledgement: This work (authors from SRF "SKIF") was partially supported by the Ministry of Science and Higher Education of the Russian Federation within the governmental order for SRF "SKIF" Boreskov Institute of Catalysis (project 122070400119-7)

The *In-Situ* XAS and *Ex-Situ* XPS Studies of the Oxidation State on a RuO₂-Based Catalyst after Hydrogenation of Oxygen Containing Substances

Sadovnikov A.¹, Naranov E.¹, Guda A.²

1 – Topchiev Institute of Petrochemical Synthesis, Russian Academy of Sciences, Leninsky prospekt, bld. 29, 119991, Moscow, Russia

2 – The Smart Materials Research Institute, Southern Federal University, Sladkova Street 178/24, Rostov-on-Don 344090, Russia
sadovnikov@ips.ac.ru

The catalytic systems based on Ru are often used for the HDO process [1-3]. Additional energy costs due to the pre-reduction of these catalysts limit their potential for industrial applications. There are some studies demonstrating the prevailing catalytic activity of partially oxidized Ru catalysts compared to reduced ones [4-7], but there are also opposite results [8]. Investigation of the oxidation state of Ru after HDO of oxygenates such as guaiacol and diphenyl ether without prior reduction of the catalyst should attempt to resolve the researchers' shortcomings. Ruthenium was selected as the catalytic metal being deposited on different porous support [9,10]. The results of X-ray absorption spectroscopy (XAS) and X-ray photoelectron spectroscopy (XPS) made it possible to determine the phase evolution of ruthenium catalysts.

Figures 1 and 2 show the XPS and *in-situ* XAS spectra of the HRO/S1-S4 samples after the hydrogenation reaction of guaiacol in water. Table 1 shows the results of linear combination fitting (LCF) and fitting of the Ru 3p_{3/2} spectra.

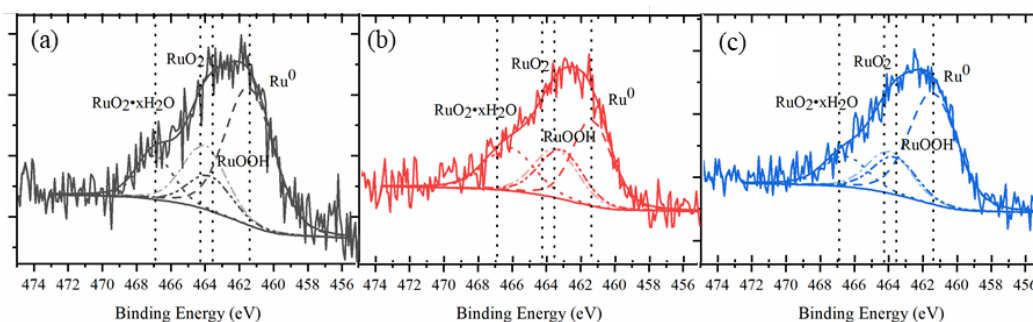


Fig. 1. XPS spectra of Ru 3p_{3/2} for HRO/S1 (a), S2 (b), S4 (c)

Table 1. Fractions of RuO₂, Ru⁰ and RuOOH phases determined by LCF|XPS.

Sample	RuO ₂ (RuO ₂ ·xH ₂ O)	Ru ⁰	RuOOH
RuO ₂ /S1	0.45 0.35	0.34 0.53	0.21 0.12
RuO ₂ /S2	0.41 0.43	0.35 0.35	0.24 0.22
RuO ₂ /S4	0.40 0.31	0.29 0.53	0.31 0.16
RuO ₂ /S4, no substrate	0.33	0.55	0.12

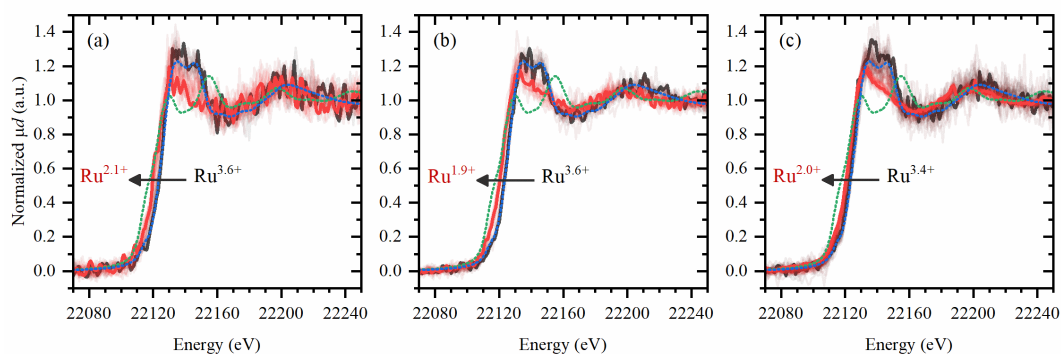


Fig. 2. In-situ XANES data (from black to red) during guaiacol hydrogenation over $\text{RuO}_2/\text{S1}$ (a), $\text{RuO}_2/\text{S2}$ (b) and $\text{RuO}_2/\text{S4}$ (c) compared to RuO_2 (dashed blue line) and Ru foil references (dashed green line).

The analysis of RuO_2 -based catalysts in the hydrogenation of guaiacol by XPS and *in-situ* XAS analysis showed that both ruthenium metal and ruthenium hydrous oxide were simultaneously formed in the reaction course.

Acknowledgement: The work was financially supported by the Russian Science Foundation (project № 22-79-10294).

References:

- [1] E.A. Roldugina, E.R. Naranov, A.L. Maximov, E.A. Karakhanov, *Appl. Catal. A Gen.* 553 (2018) 24–35.
- [2] E.R. Naranov, A.L. Maximov, *Catal. Today* 329 (2019) 94–101.
- [3] D. Tsaplin, A. Sadovnikov, D. Ramazanov, D. Gorbunov, V. Ryleeva, A. Maximov, K. Wang, E. Naranov, *Micro* 3(2023) 610-619.
- [4] S. Gundekari, K. Srinivasan, *Appl. Catal. A Gen.* 569 (2019) 117–125.
- [5] A. Kumar, B. Thallada, *Sustain. Energy Fuels* 5 (2021) 3802–3817.
- [6] R. Insyani, A.F. Barus, R. Gunawan, J. Park, G.T. Jaya, H.S. Cahyadi, M.G. Sibi, S.K. Kwak, D. Verma, J. Kim, *Appl. Catal. B Environ.* 291 (2021).
- [7] E.R. Naranov, A.A. Sadovnikov, O.V. Arapova, A.L. Bugaev, O.A. Usoltsev, D.N. Gorbunov, V. Russo, D.Yu. Murzin, A.L. Maximov, *Catal. Sci. Technol.* 13 (2023) 1571-1583
- [8] G. Jiang, Y. Hu, G. Xu, X. Mu, H. Liu, *ACS Sustain. Chem. Eng.* 6 (2018) 5772–5783.
- [9] A.A. Sadovnikov, O.V. Arapova, V. Russo, A.L. Maximov, D.Yu. Murzin, E.R. Naranov, *Ind. Eng. Chem. Res.* 61 (2022) 1994–2009
- [10] E.R. Naranov, A.A. Sadovnikov, A.L. Bugaev, D.A. Shavaleev, A.L. Maximov, *Catal. Today* 378 (2021) 149–157.

Photochemical Degradation of Fluorinated Graphite with Embedded Nitrogen Oxides under White-Beam Synchrotron Radiation

Semushkina G.I.¹, Fedoseeva Y.V.¹, Makarova A.A.², Pinakov D.V.¹, Chekhova G.N.¹,
Okotrub A.V.¹, Bulusheva L.G.¹

1 – Nikolaev Institute of Inorganic Chemistry SB RAS, Novosibirsk, Russia

2 – Physikalische Chemie, Institut für Chemie und Biochemie, Freie Universität Berlin,
Berlin, Germany

semushkina.g@niic.nsc.ru

Fluorinated graphite (FG) is a three-dimensional material consisting of alternating layers of fluorinated graphene weakly interacting with each other through van der Waals forces. The layered structure of FG has several interesting properties, such as a high surface area, mechanical strength, electrical conductivity, and thermal stability. The presence of fluorine atoms in FG also increases its resistance to chemical reactions, which makes it useful for a variety of applications. In addition to being a container for storage of various substances, FG can also be used in the production of batteries and energy storage devices, as a catalyst support, and as a sorbent for air and water purification from pollutants. Nitrogen oxides (NO_x) are the most common and dangerous pollutants, so finding ways to safely store them is crucial. FG's ability to store nitrogen oxides in its large interlayer space and resist reactions with them is a promising solution. The study of the stability of FG intercalated with nitrogen oxides to external environmental influences, such as heating and photon action, is an urgent task in materials science.

The aim of this work is a comparative study of the evolution of the composition and structure of NO_x@FG and empty FG in ultra-high vacuum under the action of a polychromatic photon beam from a synchrotron radiation (SR) source BESSY II using *in situ* XPS and NEXAFS. Density functional theory calculations of a fluorinated graphene fragment are used to interpret experimental data.

Layered fluorinated graphite material can become an efficient nanoreactor for photochemical reactions. In this work, we compared the photochemical behavior of partially fluorinated graphite and FG containing nitrogen oxides molecules in the interlayer space (NO_x@FG) under the action of a high-intense polychromatic photon beam from a source of synchrotron radiation BESSY II. It was found that nitrogen oxides promote the photo-induced degradation of the FG matrix, namely, its partial defluorination, the formation of vacancies and doping with nitrogen, while the empty FG has a high photoresistance to synchrotron radiation. The results obtained can be used in the development of new approaches to the modification of graphene layers and in the creation of photostable materials for optical elements.

Structural Changes in Rochelle Salt on Cooling Across the Ferroelectric Phase Transition Points

Sharaya S.S.^{1,2}, Zakharov B.A.^{2,1}, Boldyreva E.V.^{2,1}

1 – Novosibirsk State University, Novosibirsk, Russia

2 – Boreskov Institute of Catalysis, Novosibirsk, Russia

s.sharaya@g.nsu.ru

Rochelle salt was the first compound for which ferroelectric properties were detected. Since this time a number of diffraction investigations were performed to link together ferroelectric properties with the crystal structure. However, the problems with determining the structural changes responsible for its phase transitions are still not unambiguously solved, e.g. the weak difference between the polar and nonpolar phases and the presence of disorder in the nonpolar phase are still disputable [1, 2]. In this work for the first time, diffraction data were collected at multiple temperature points on cooling from 308 to 100 K (this interval includes both Curie temperatures – 255 K and 297 K).

The diffraction data confirmed the presence of significant ADPs anisotropy for the K1 atom and the oxygens of crystallization water molecules in its coordination sphere. We compared the results of refining the displacement parameters of the K1 atom which are considered to be responsible for polarization effect, using three different models: a harmonic model with and without disorder, and an anharmonic model. The analysis of the thermal dependence of the anisotropic displacement parameters of K1 and O8 allowed us to estimate the contributions of static and dynamic disorder of atoms to the electron density distribution in the crystal structure. Temperature changes in the geometry of hydrogen bonds and coordination polyhedra were also refined and analyzed.

Acknowledgement: The work was supported by the Ministry of Science and Higher Education of the Russian Federation jointly by the Boreskov Institute of Catalysis (project AAAA-A21-121011390011-4) and under the “Priority 2030” program in cooperation with Novosibirsk State University.

References:

- [1] T. Mitsui, Physical Review 111, (1958) 1259-1267.
- [2] F. Mo, R. H. Mathiesen, J. A. Beukes, K. M. Vu, IUCrJ 2, (2015), 19-28

Synchrotron and X-Ray Techniques for Hyaluronic Acid-Based Nanomaterials

Snetkov P.P., Morozkina S.N., Romanov A.E.

ITMO University, Saint Petersburg, Russia

ppsnetkov@itmo.ru

Hyaluronic acid being as a natural linear non-sulfated polysaccharide forms the basis of the extracellular, pericellular, and intracellular cell matrixes. Moreover, it plays critical role in several essential biological processes, such as metabolism, tissue regeneration, cell proliferation and migration, inflammation, immune answers, etc. Note that the effect of exogenous hyaluronic acid directly depends on the molecular weight of the polymer [1].

Due to its unique biological properties, hyaluronic acid could be used for various biomedical applications: drug delivery systems, viscosupplementation treatment, ocular surgery, wound healing, etc. One of the most important issues is targeted delivery systems, which, on the one hand, allows to increase the solubility and efficacy of the encapsulated hydrophobic drugs, and, on the other hand, to provide targeted delivery driven by the specific cell receptors (CD44, CD168, HARE, LYVE1, TLRs) [2].

In spite of the comprehensive analysis of physico-chemical, chemical, morphological, pharmaceutical, and other performance characteristics of such hyaluronic acid-based nanostructures and materials, its structure and the hyaluronic acid conformation are unknown. At the same time the understanding of the structure formed represent the fundamental scientific issue and allow to understand and to predict the properties of the biopolymer composites.

The analytical techniques based on synchrotron and X-ray radiation have the great potential for above mentioned purposes. For example, it allows to study the changes of hyaluronic acid conformations into solutions influenced by various factors [3], to determine the layer-by-layer structure of dexamethasone-filled nanoparticles based on HA [4], and to understand the mechanism of interactions between the cell receptors and HA-conjugates [5].

In this study the brief summary of the application of synchrotron and X-ray applications for biopolymer-based materials will be demonstrated, and the recent results of such analysing the curcumin-loaded hyaluronic acid matrixes [6] will be discussed in details.

Acknowledgement: This work was supported by the Ministry of Science and Higher Education of the Russian Federation (agreement No. 075-15-2021-1349).

References:

- [1] N.G. Kotla et al. *J. Control. Release.* 336 (2021) 598-620.
- [2] A.M. Carvalho, R.L. Reis, I. Pashkuleva. *Adv. Healthcare Mater.* 12 (2023) 2202118.
- [3] F. Horkay et al. *J. Chem. Phys.* 131(18) (2009) 184902.
- [4] C.I. Camara et al. *Int. J. Mol. Sci.* 22 (2021) 10480.
- [5] J. Škerlová et al. *J. Struct. Biol.* 191(2) (2015) 214–223.
- [6] P. Snetkov et al. *Pharmaceutics.* 14(6) (2022) 1186.

ARPES Study of the Bismuth Thin Films Electronic Structure on the InAs(111)A-(2x2) Surface

Solovova N.Yu.¹, Golyashov V.A.^{1,2,3}, Tereshenko O.E.^{1,2,3}

1 – Novosibirsk State University, Novosibirsk, Russia

2 – Rzhanov Institute Semiconductor Physics, Novosibirsk, Russia

3 – SRF "SKIF", Koltsovo, Russia

n.solovova@g.nsu.ru

The aim of this work is to study the growth conditions, crystal and electronic structure of bismuth thin films grown on the InAs(111)A-(2x2) surface using X-ray photoelectron spectroscopy (XPS) and angle-resolved photoelectron spectroscopy (ARPES), the main modern experimental techniques for studying the electronic structure and chemical state of atoms on solid surfaces and interfaces. XPS and ARPES are going to be implemented at Siberian Circular Photon Source (SKIF) station 1-6-2 "Electronic Structure" in Novosibirsk.

The exploration of new materials with unique properties is an important task to improve the characteristics of semiconductor devices. Bismuth films are of particular interest due to high carrier mobility and the strong spin - orbital interaction (SOI). The latter made it possible to obtain a graphene-like structure of bismuth atoms with a more than 0.8 eV wide gap in the Dirac spectrum and topologically non-trivial edge states inside the gap [1]. It is worth noting that the choice of substrate material has a significant impact on the properties of thin films. In this work, n-InAs(111)A-(2x2) was chosen as a substrate because of two-dimensional electron gas (2DEG) formation on its surfaces and possible coupling of SOI in Bi to InAs surface 2DEG. It could be interesting for creating transistors based on the spin degree of freedom [2].

Thin (0.5-40 Å) bismuth layers were deposited from a Knudsen cell on a surface of a InAs(111)A substrate with (2x2) reconstruction at various temperatures. ARPES and XPS measurements were carried out in the Rzhanov Institute of Semiconductor Physics SB RAS (Novosibirsk, Russia) on the SPECS ProvenX-ARPES facility at $h\nu = 21.22$ eV for ARPES and $h\nu = 1486.7$ eV for XPS. Spin-resolved ARPES measurements were made at Hiroshima Synchrotron Radiation Center BL-9B ESPRESSO end station.

It was shown that pseudomorphic epitaxial growth of bismuth layers with Bi(111) structure takes place during the initial stages of bismuth deposition on InAs surface at room temperature. The critical thickness of Bi epitaxial films on InAs was estimated to be less than 25 Å. The electronic structure has a semi-metallic character with the Fermi surface crossed by electron and hole bands usually observed on Bi(111) thin films. The properties of the films grown at room temperature are in general agreement with the data described in the literature [3].

The deposition of bismuth on the InAs surface at high ($\sim 250^\circ\text{C}$) temperatures was studied for the first time. It was shown that under these conditions the growth of the film is self-limited by a thickness of 3.5 Å. The limitation is probably due to the desorption of bismuth

atoms from the surface of the film during growth. There are no chemical shifts corresponding to Bi-As and Bi-In bonds detected in the X-ray photoelectron spectra, indicating the formation of a quasi-free two-dimensional structure. Low energy electron diffraction measurements showed the formation of a superstructure of Bi atoms on the surface with a reconstruction ($2\sqrt{3}\times 3$) and a rectangular unit cell with dimensions $\sim 13 \text{ \AA} \times 15 \text{ \AA}$. The estimated concentration of bismuth atoms in such film is $\sim 10^{15} \text{ cm}^{-2}$. ARPES measurements revealed that 2DEG states near the InAs surface are preserved in the electronic structure. Additionally, parabolic electronic and hole bismuth states with strong anisotropy appear in the InAs band gap at the Γ -point of the Brillouin zone of the superstructure ($2\sqrt{3}\times 3$) ($m_e^* \sim 0.2m_0 - 0.6m_0$ and $m_h^* \sim 0.2m_0 - 0.4m_0$, m_0 – free electron mass). The electronic structure of the ($2\sqrt{3}\times 3$)-Bi/InAs system has a semiconductor character with a band gap $\sim 150 \text{ meV}$. ARPES measurements are shown in the figure 1. Spin-resolved ARPES measurement revealed that in the vicinity of the superstructure ($2\sqrt{3}\times 3$) Γ point parabolic electronic and hole bismuth states are strongly spin polarized.

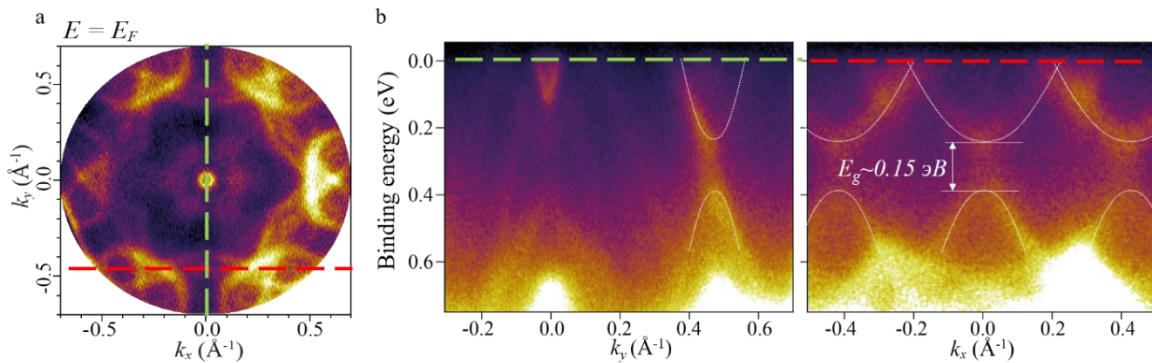


Fig. 1. a) Fermi surface map b) Dispersion of electron states in the directions shown in a) measured on the ($2\sqrt{3}\times 3$)-Bi/InAs(111) surface at a film thickness of $\sim 3.5 \text{ \AA}$.

Acknowledgement: This work was financially supported by the Priority 2030 program.

References:

- [1] Reis F. et al. Bismuthene on a SiC substrate: A candidate for a high-temperature quantum spin Hall material //Science. – 2017. – T. 357. – №. 6348. – C. 287-290.
- [2] Datta S., Das B. Electronic analog of the electro-optic modulator //Applied Physics Letters. – 1990. – T. 56. – №. 7. – C. 665-667.
- [3] Nicolai L. et al. Bi monocrystal formation on InAs (111) A and B substrates //arXiv preprint arXiv:1807.00306. – 2018.

XAFS Study of the Local Atomic Structure of Copper Centers in Cu-MOR

Sukharina G.B., Ermakova A.M., Ponosova E.E., Gladchenko-Jevelekis J. N.,
Shemetova E.I., Pryadchenko V.V., Srabionyan V.V., Avakyan L.A., Bugaev L.A.
Southern Federal University, Rostov-on-Don, Russia
gbsukharina@sfedu.ru

Copper-containing zeolites of the Cu-MOR type are promising materials for solution of the topical problem of conversion methane to methanol. The catalytic activity of such materials is largely determined by the local atomic structure of the copper centers. Therefore, to obtain effective catalysts, it is extremely important to establish the features of the synthesis–structure–catalytic activity dependence [1,2].

In this work two methods of synthesis of copper-containing zeolites are compared: liquid-phase ion exchanged using copper (II) acetate and solid-phase ion exchanged copper (II) chloride. Each of synthesis techniques are characterized by different yield of methanol [3]. Thus, to understand the dependence of the methanol yield on the catalytic cycle number, it is necessary to study the structure of copper centers at each step of first and at several subsequent cycles.

The active centers of Cu-MOR zeolites were studied using X-ray absorption spectroscopy and computer modeling. Analysis of the experimental and theoretical Cu *K*-XANES spectra calculated for possible structural models of copper centers in Cu-MOR was carried out. The spectra were calculated using the FDMNES software package [4].

Based on the obtained data, the most probable local atomic environments of copper formed using solid-phase and liquid-phase ion exchanged synthesis at each step of the first cycle and several subsequent cycles were determined. Using this structural information and analysis of the available data, the correlation between the structural features of the formed copper centers in Cu-MOR and the methanol yield at first cycle depending on the synthesis method was established.

Acknowledgement: This work was supported by the Russian Science Foundation, grant No.23-22-00438. We would like to thank Prof. J.A van Bokhoven for participation in this work.

References:

- [1] V.V. Pryadchenko, G.B. Sukharina et al., *Tech. Phys.* 66.9 (2021) 1018-1024
- [2] V.V. Srabionyan, G.B. Sukharina et al., *J. Phys. Chem. C* 125.46 (2021) 25867-25878.
- [3] S.E. Bozbag, E.M.C. Alayon et al., *Catal. Sci. Technol.* 6.13 (2016) 5011-5022.
- [4] Y. Joly, *Phys. Rev. B* 63 (2001) 125120

Molecular Simulations and Restoration of the Atomic Structure of DNA-Aptamers from SAXS Data

Tomilin F.N.^{1,2}, Artyushenko P.V.^{2,3}, Shchugoreva I.A.^{2,3}, Rogova, A.V.^{2,3}, Moryachkov R.V.^{2,3}, Zablude V.N.^{2,3}, Kichkailo A.S.^{2,3}

1 – Kirensky Institute of Physics, Federal Research Center KSC SB RAS, Krasnoyarsk, Russia

2 – Laboratory for Digital Controlled Drugs and Theranostics, Federal Research Center KSC SB RAS, Krasnoyarsk, Russia

3 – Prof. V.F. Voino-Yasenetsky Krasnoyarsk State Medical University, Krasnoyarsk, Russia
felixnt@gmail.com

This work presents the results of the simulated atomic structure of aptamers in solution based on small-angle X-ray scattering (SAXS) and comparison with X-ray diffraction (XRD) data. The possibility of applying the technique of atomic structure reconstruction from the SAXS experiment is demonstrated, and the peculiarities of the molecular structure of aptamers in solution are established. Computer modelling based on SAXS gives adequate results, so this direction is promising for structure reconstruction from SAXS and design of new aptamers. A specific methodology has been developed for the development of this approach. The first step is to simulate secondary structures based on nucleotide sequences. This step gives a general idea of what the main structural elements of the aptamer will look like, where there will be complementary and non-complementary sites, loops, quadruplexes, single strands of nucleotides, and so on. Then there is a real full-atom simulation of the 3D structure based on the secondary structure. This provides an initial understanding of the atomic structure of the aptamer and the position in space of the main structural elements. Molecular dynamics calculations of the obtained aptamer are then performed under real conditions. This provides information on the conformational changes of the aptamer in solution with explicit consideration of the solvent, temperature, and pressure. Quantum chemical calculations using the FMO2/DFTB3-3ob/PCM method [1] are then performed to clarify the atomic structure obtained in the previous step. Finally, the theoretical scattering curves obtained from the theoretical atomic models are compared with the experimental scattering curve of the SAXS. This step helps to select only those aptamer conformations that have the least deviation from the experiment.

Acknowledgement: This work was supported by Project FWES-2022-0005 of the Russian Ministry of Science and Education. The authors thank the JCSS Joint Super Computer Centre of the Russian Academy of Sciences for providing supercomputers for computer simulations

References:

[1] Nishimoto Y., Fedorov D.G. PCCP. 18 (2016) 22047.

New Class of Supersoft Adaptive Materials Based on Copolymers: Structural Studies with Synchrotron Radiation

Umarov A.Z.¹, Nikitina E.A.², Ivanov D.A.^{1,2}

1 – Faculty of Fundamental Physical and Chemical Engineering, Moscow State University, Moscow, Russia

2 – Department of Chemistry, Moscow State University, Moscow, Russia
umarovakmalum@gmail.com

Bottlebrush elastomers are biomimetic materials considered to be promising for biomedicine. They imitate biological tissues, which exhibit a unique combination of two opposite properties – softness and elasticity under relatively small stress values, but intense strain-stiffening with increase in deformation [1]. These features of mechanical behavior allow to apply bottlebrush elastomers as bioimplants. Another useful property of bottlebrush networks is their ability to change volume manyfold when exposed to an appropriate solvent [2]. Linear-brush-linear (LBL) architecture is applied for getting injectability. Investigation of swelling and gelation processes and mechanisms in such systems is an important task of gel physics.

Small Angle X-Ray Scattering (SAXS) studies were conducted to investigate changes in supramolecular structure during swelling and gelation processes for a series of samples with the same chemical compound (brush blocks from polyethylene glycol and linear blocks from poly(N-isopropylacrylamide)), but different LBL architecture, which determines the structure of system: side chain (PEG) length (n_{sc}), linear blocks chain (PNIPAM) length (n_L) and backbone degree of polymerization between linear (PNIPAM) blocks (n_{bb}). To study the structure as the function of the swelling ratio a unique measurement device was developed. The kit consisted of weighing scale, placed between synchrotron radiation source (European Synchrotron Radiation Facility) and detector. The samples were penetrated by x-ray beam during swelling and drying processes, i.e. mass changes, which were recorded by the kit. Thus, we obtained a series of scattering curves depending on the masses of the samples.

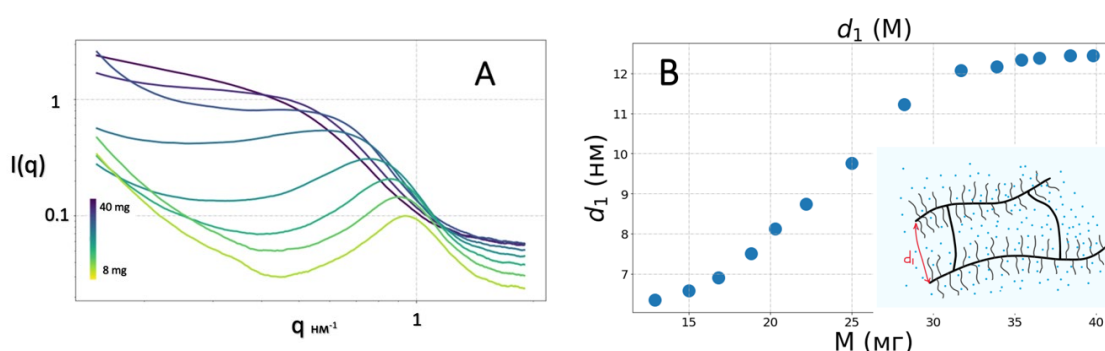


Fig. 1. A – SAXS curves evolution during swelling, B – obtained dependence between the distance d_1 and mass of the sample

For bottlebrush elastomers the scattering peak appears in SAXS curves ($q^* \approx 1 - 3 \text{ nm}^{-1}$) (Fig.1 A). It corresponds to the average distance $d_1 = 2\pi/q^*$ between the

neighboring bottlebrush backbones. During the swelling processes, the peak's location moves to the smaller angle region, i.e. the distance d_1 increases. To analyze this dynamic process, a Python algorithm, which automates the process of choosing an interval and initial data for approximating the experimental data, was built. Thus, we obtained the dependencies between the swelling ratio and the distance d_1 between the neighboring bottlebrush backbones (Fig.1, B). Collected data were compared with models of two-dimensional and three-dimensional swelling.

References:

- [1] Daniel William F.M., Burdynska Joanna, Vatankhah-Varnoosfaderani Mohammad, et al. / Solvent-free, supersoft and superelastic bottlebrush // *Nature Materials*. — 2015. — Nov. — Vol. 15, no. 2. — P. 183–189
- [2] Jacobs, M.; Liang, H.; Dashtimoghadam, E., et al / Nonlinear Elasticity and Swelling of Comb and Bottlebrush Networks. // *Macromolecules* 2019, 52 (14), 5095–5101.

Operating Modes of the UE212M Elliptical Electromagnetic Undulator for Radiation at the Station "Electronic Structure" in the SKIF Project

Gurov D.S., Zolotarev K.V., Zuev V.V., Utkin A.V., Cheskidov V.G.
 Institute of Nuclear Physics. G.I. Budker SB RAS, Novosibirsk, Russia
 a.v.utkin@inp.nsk.su

To generate radiation with different types of polarization for the station of the first stage of "Electronic Structure" in the project of the Siberian Ring Photon Source ("SKIF", [1]), the electromagnetic elliptical undulator UE212M was developed.

The undulator magnetic field was simulated using the "Mermaid" program for magnetostatic calculations [2], and the SR from the undulator was calculated using the Spectra computer program [3].

The UE212M elliptical electromagnetic undulator is the modification of the UE212 undulator manufactured by the Institute of Nuclear Physics for PSI (Switzerland) [4, 5].

In the UE212M undulator, the vertical magnetic field can be changed from 0T to 0.49T, and the horizontal magnetic field from -0.1T to 0.1T in about 1÷5 minutes independently of each other. Since the undulator has iron poles, it has a magnetic hysteresis. When working with an undulator, it is necessary to take into account in which arm (increasing or decreasing of the magnetic field) the undulator is located. For example, if the user needs to reduce the magnetic field in the undulator, when it is on the lift arm, it must pass through the point of the maximal magnetic field.

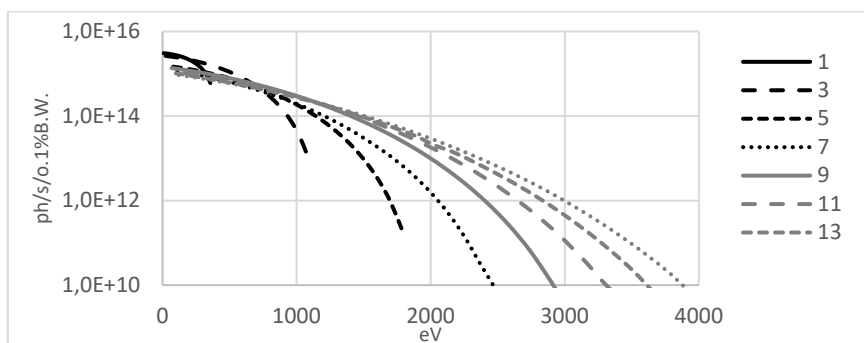


Fig. 1. Radiation of the first eight main harmonics of the UE212M undulator in the 6mm×6mm window at a distance of 25m at elliptical mode.

Figure 1 shows the possible radiation spectra from the UE212M undulator in the elliptical mode, modeled by using the "Spectra" program. When the value of the horizontal magnetic field passes through 0, the chirality of elliptically polarized radiation changes, which is very important for studies in the field of circular magnetic dichroism.

In the planar mode, only the vertical, periodic magnetic field is created. The period of undulator in this mode is $\lambda=212\text{mm}$, and the overall amount of the regular periods is 20. The maximal value of the magnetic field achievable in this mode is $|B_v|=0.49\text{T}$.

In some cases, for the correct operation of equipment with SR from the undulator, it is necessary to suppress the 3rd harmonic of the radiation. This can be achieved, by reducing

the magnitude of the magnetic field in every third regular pole of the undulator by approximately 14%.

In the case of equality of the vertical and horizontal fields in the undulator, the circular mode of operation is created. In this operating mode, the undulator radiates at the basic (fundamental) harmonic, and all higher harmonics are significantly suppressed. Figure 2 is show the possible radiation spectra from the UE212M undulator in the circular mode of operation, simulated using the “Spectra” program.

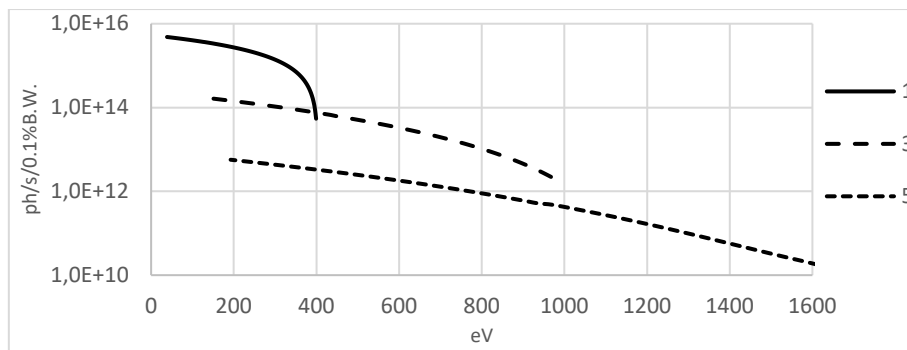


Fig. 2. Radiation of three harmonics of the UE212M undulator in the 6mm×6mm window at the 25m distance in the circular mode of operation.

Acknowledgement: This work was partially supported by the Ministry of Science and Higher Education of the Russian Federation within the governmental order for SRF "SKIF" Boreskov Institute of Catalysis (project 123031300092-4).

References:

- [1] Baranov G. et al. Lattice optimization of the Novosibirsk fourth-generation light source SKIF. arXiv:2107.03081v1, 7 Jul 2021.
- [2] А.Н. Дубровин “Руководство пользователя MERMAID: Магнитный дизайн в двух и трёх измерениях.” Новосибирск, 1994.
- [3] J. Synchrotron Radiation 28, 1267 (2021), URL: <http://spectrax.org/spectra/index.html>
- [4] Schmidt T. et al. FIRST RESULTS OF THE UE212 QUASIPERIODIC ELLIPTICAL ELECTROMAGNETIC UNDULATORS AT SLS. Proceedings of EPAC 2002, Paris, France.
- [5] Д.С. Гуров и др. Эллиптический электромагнитный ондулятор UE212M для станции 1-6 «Электронная структура» источника синхротронного излучения ЦКП «СКИФ». Т. 3: Устройства генерации и фронтенды, системы управления и ИТ-обеспечения экспериментальных станций первой очереди; предварительные проекты экспериментальных станций второй очереди. Новосибирск 2022, ISBN 978-5-906376-43-5. URL: <https://srf-skif.ru/index.php/>

Structure, Morphology, Layered Chemical Composition and Magnetic Properties of Iron (Iron Oxide) Nanocoatings on the Surface of Porous Alumina Obtained by the Annealing of Magnetron Deposited Iron Films

Valeev R.G.¹, Petkov A.A.²

1 – Udmurt Federal Research Center of UB RAS, Izhevsk, Russia

2 – Udmurt State University, Izhevsk, Russia

rishatvaleev@udman.ru

Promising developments in the field of obtaining new nanostructured coatings are more relevant than ever. In particular, the controlled deposition of various materials on the surface of porous media will make it possible to obtain a new class of 2D materials with unique optical, magnetic, catalytic, sensory properties, as well as gas and liquid separation and filtration properties. It should be noted that a large contribution to these properties is made by the surface due to the formation of films with a developed morphology. They are also strongly influenced by chemical purity, structural-phase state, local atomic and electronic structure [1].

This paper presents current results on obtaining and studying the morphology, structural-phase and chemical composition of the surface and magnetic characteristics of iron coatings deposited on the surface of anodic alumina with different porous structures (Fig. 1.). It is shown that the morphological features of the porous matrix affect the structural-phase composition, local atomic and magnetic structure of iron coatings. In particular, on the coordination number of the first coordination sphere of the local atomic environment of iron atoms, the coefficient of rectangularity and the shape of the magnetic hysteresis loop during transverse and longitudinal magnetization.

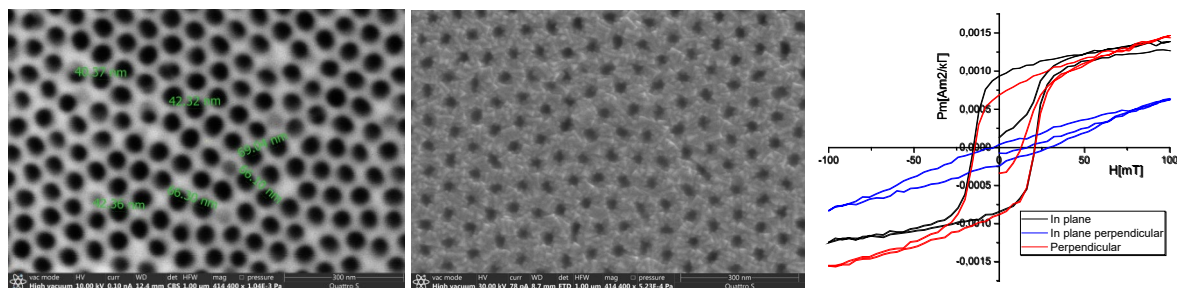


Fig.1. SEM images of the surface of the original matrix and Fe coating on porous Al_2O_3 with a pore diameter of 40 nm and a distance between pore centers of 67 nm, as well as hysteresis loops of the presented sample.

Acknowledgement: This work is supported by the Ministry of Science and Higher Education of Russia under Agreement N 075-15-2021-1351. Investigations were carried out using facilities of shared research center “Surface and novel materials” UdmFRC UB RAS.

References:

[1] R. Valeev, A. Beltiukov, et al. Mater. Res. Express 3 (2016) 015902.

Development Status of the 1-2 Beamline “Structural Diagnostics” at the SRF SKIF

Vinokurov Z.S.¹, Zubavichus Y.V.¹, Shmakov A.N.¹, Mishchenko D.D.¹, Selyutin A.G.¹,
Syrtanov M.S.², Gogolev A.S.², Denisov V.V.³, Teresov A.D.³, Panchenko Y.N.³, Kovalsky S.S.³,
Beskonchin K.V.³, Kiselev V.N.³, Evdokimov A.A.³, Andreev M.V.³

1 – SRF “SKIF” BIC SB RAS, Novosibirsk, Russia

2 – Tomsk Polytechnic University, Russia

3 - Institute of High Current Electronics, Tomsk, Russia

vinokurovzs@catalysis.ru

The progress of the project development and the time schedule of the new synchrotron beamline 1-2 “Structural Diagnostics” at the SRF SKIF dedicated to high-resolution powder diffraction and macromolecular crystallography are to be presented. The beamline uses a cryocooled in-vacuum undulator for photon generation together with refractive optics and a cryocooled double-crystal monochromator to deliver a high brightness focused monochromatic beam to the sample. The development status of each beamline component as well as its key parameters are to be presented. The description of techniques and equipment that will be available at Hi-Res and MX crystallography endstations together with the expected beam performance are to be announced.

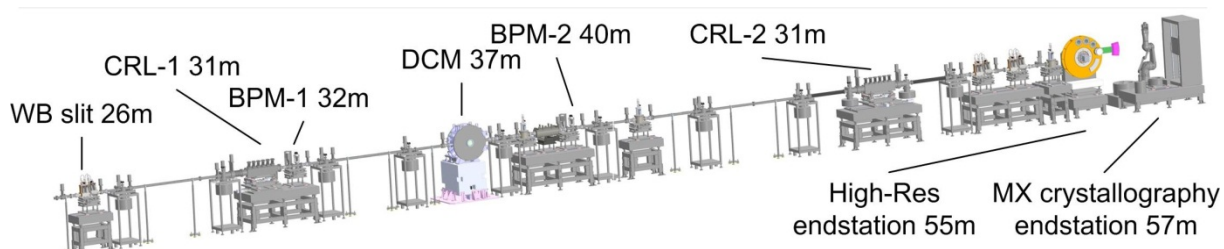


Fig. 1. 1-2 Beamline layout.

Acknowledgement: This work was funded within the framework of budget project for Synchrotron radiation facility SKIF, Boreskov Institute of Catalysis.

Conjugation of the Oxidative Dehydrogenation of Ethylbenzene to Styrene with Steam Conversion of Carbon Monoxide on a 30%Cr₂O₃/1.5%CuO/15%K₂CO₃ /Al₂O₃ Catalyst

Mamedova M.T., Tagiyev D.B., Abasov S.I, Xudiyev A.T., Chelabova K.S.

Y.H. Mammadaliyev Institute of Petrochemical Processes of Ministry of Science and Education of Azerbaijan, Baku, Azerbaijan
memmedova-melahet@mail.ru

In the process of obtaining styrene from the dehydrogenation of ethylbenzene in industry water vapor has a positive effect on the progress of the process of conversion of EB to styrene by accelerating the desorption of conversion products from the surface of the catalyst. At this time, water molecules do not affect the conversion process of EB itself. In the presented work, the effect of water vapor on the oxidative dehydrogenation of ethylbenzene to styrene in the presence of CO₂ was studied. The studies were conducted in a flow-type laboratory setup at atmospheric pressure. A 30%Cr₂O₃/1.5%CuO/15%K₂CO₃ /Al₂O₃ catalyst was synthesized and the studied process was carried out on it. The results of experiments conducted in this direction are given below.

A characteristic feature of the effect of H₂O on the conversion of the EB : CO₂ = 1 : 5 mixture is the expected increase in the stability of the catalyst. By increasing the H₂O : (EB: CO₂ = 1 : 5) ratio (mol) from 0.25 to 2.0, the stability of the catalyst increases monotonically. Increasing the amount of water vapor to the following ratio H₂O:(EB:CO₂=1:5)=2.5 practically does not affect the stability of the process under the studied conditions (120 min.).

The analysis of the conversion products of the EB:CO₂ mixture in the presence of H₂O shows that as the concentration of H₂O vapors increases, the output of CO decreases, while the output of hydrogen increases (fig.1). In general, the change in hydrogen yield is correlated with the change in EB conversion, and the molar sum of CO+H₂ corresponds quantitatively to the molar yield of styrene.

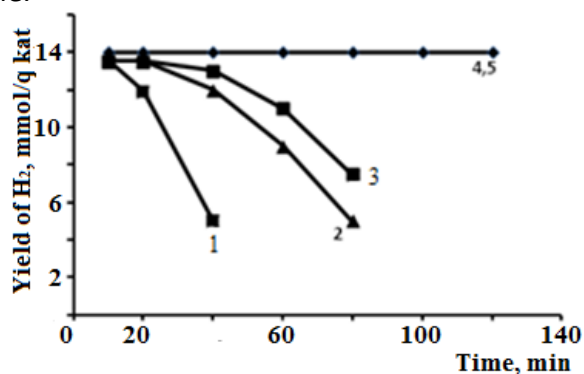
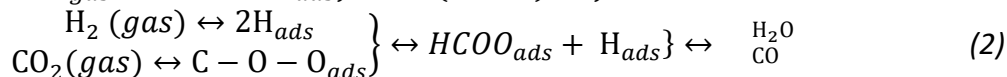


Fig.1. Effect of H₂O on the yield of H₂ in the conversion of EB:CO₂ (1:5 mol/mol) mixture to styrene on a 30%Cr₂O₃/1.5%CuO/15%K₂CO₃/Al₂O₃ catalyst. T = 580°C; WHSV = 2 h⁻¹; selectivity 90-92%; H₂O : (EB : CO₂ = 1 : 5): 1- 0.25; 2 – 0.5; 3 – 1.0; 4 – 2.0; 5 – 2.5.

Thus, the practically absence of CO molecules, the correlation of the yield of hydrogen during the conversion of the mixture of EB and CO₂ with the process of conversion of EB to St indicates that a direct steam conversion reaction of carbon monoxide is taking place. Due to the presence of water vapors, the release of styrene, which is the target product of the reaction, is facilitated, and the passage of the Boudouard reaction, which enables the deactivation of the catalyst, is blocked.

Thus, the conversion of EB to St in the presence of CO₂ can be described by the following scheme, based on the ideas about the mechanism of steam conversion of carbon monoxide:



The absence of CO in the reaction products shows that the reaction (2) in the conversion of EB to St on the catalyst is completely directed towards the formation of CO₂ and H₂ products.

According to the scheme (1), the reaction of dehydrogenation of EB to St proceeds independently, and is directed toward the obtainment of goal product due to the use of the released hydrogen in the reduction of CO₂. On the other hand, the absence of CO in the reaction products and the amount of hydrogen in these products corresponds to the yield of St shows that stage (2) in conditions close to the conditions of obtaining of St from EB in industry is directed towards the formation of steam conversion products of carbon monoxide. The connected nature of forward and reverse directions of steam conversion of carbon monoxide (SCCMO) activated by the 30%Cr₂O₃/1.5%CuO/15%K₂CO₃/Al₂O₃ catalyst allows considering CO₂ as a cyclic carrier of oxygen in the scheme of dehydrogenation of EB to St and conjugation of SCCMO with conversion of ethylbenzene to styrene.

Oxidative conversion of ethylbenzene is naturally accompanied by the formation and accumulation of oxidative condensation products (OCP), resulting in the development of low activity catalyst activity. It is believed that in the initial unstable stage of the process, St is formed in Lewis acid centers, then OCP is formed in the presence of these centers and oxygen. OCP is responsible for the oxidative dehydrogenation of EB. Accumulation of OCP until a monolayer is formed is the beginning of steady-state operation of the catalyst. A possible reason for the catalytic activity of OCP may be the geometric compatibility between EB and the centers located on the surface of OCP. As a result, there is a high concentration of carbon-oxygen centers responsible for the formation of St on the surface. Furthermore, the oxygen contained in the surface oxygenated groups is believed to be active enough to participate in the oxidative dehydrogenation of EB to St. Such a scheme does not involve EB forming any intermediate with oxygen. Therefore, the condensation products (CP) formed before the formation of OCP in oxidative conversion are the same as the CP formed during the direct dehydrogenation of EB. From this point of view, it can be assumed that similar forms of OCP are formed from the interaction of CO₂ with the previously formed CP as a result of the usual dehydrogenation of EB.

Thus, the following scheme of the formation of active centers in CP with the participation of CO₂ in the conversion of EB to St can be proposed:



where \square are carbon defects in CP; $[O...CO-\square] [O...CO... \square]$ shows the interaction of CO₂ with carbon centers (defects) in CP and its dissociation into oxygen atom and CO.

Isomerization of Gas Gasoline on Mordenitecontaining Composite Catalytic Systems

Mamedova M.T., Abasov S.I., Agayeva S.B., Iskenderova A.A., Isayeva Y.S.,
Imanova A.A., Ibrahimzadə S.V.

*Y.H. Mammadaliyev Institute of Petrochemical Processes of Ministry of
Science and Education of Azerbaijan, Baku, Azerbaijan
memmedova-melahet@mail.ru*

In the present study, the isomerization transformation of gas gasoline (GG) from the Garadag Gas Processing Plant (Azerbaijan) (composition: C₄-5.5, i-C₅-25.2, n-C₅-19.2, i-C₆-18, n-C₆8.4, i-C₇-5.4, C₇₊-18.3 wt.%) on composite catalysts consisting of metal-modified (Ni or Co) zeolite HMOR (17) and sulfated zirconia. The studies were carried out at atmospheric pressure, in a flow-type laboratory setup.

Mordenite isomerization catalysts of n-alkanes are the most active medium-temperature zeolite isomerization catalysts. The use of such catalysts for gas gasoline isomerization showed that the C₄- and C₇₊ components of gas gasoline is mainly converted to i-C₅, i-C₆ and n-C₅ on them. The introduction of transition metal (Co), ZrO₂ and sulfate anions into these catalysts allows lowering the process temperature and increasing the isomerization activity of the catalytic system (tab.1).

The results given in the table 1 show that the catalyst M-4 (0.4%Co/HMOR₁₇/10%ZrO₂ - SO₄²⁻ (6%)) has the highest isomerizing activity among these catalysts. For it, the ratio of normal C₅ yield to i-C₅-i-C₆ yield is the lowest (n-C₅/i-C₅-C₆ = 0.02 - 0.08).

Tab. 1. Conversion of GG on modified mordenite catalysts. H₂/CH = 1 : 3; WHSV = 2h⁻¹

T, °C	Conversion of C ₄ - and C ₇₊ components of GG, %	Yield of nC ₅ , wt. %	Yield of iC ₅ -iC ₆ , wt. %	iC ₅ -iC ₆ selectivity,%	nC ₅ /iC ₅ -iC ₆
M-1 (0.4%Co/HMOR ₁₇)					
300	39	11.3	11.4	51	1
320	32.2	10.2	8.6	46.5	1.2
M-2 (0.4%Co/HMOR ₁₇ /10%ZrO ₂)					
160	96	7.4	15.6	69	0.5
180	84.8	6.1	19.2	78.4	0.32
200	94.8	6.2	16.4	73.5	0.4
M-4 (0.4%Co/HMOR ₁₇ /10%ZrO ₂ - SO ₄ ²⁻ (6%))					
180	49	0.8	18.1	97.8	0.02
200	49.7	2	17.1	92.4	0.08

The obtained results show that the main converted components in the conversion of GG in the above catalysts are C₄- and C₇₊ hydrocarbons of GG, and the obtained products are

mainly n-C₅, i-C₅ and i-C₆. Therefore, it can be concluded that during the conversion of GG, first C₄- and C₇₊ hydrocarbons form the bimolecular intermediate [C₄ - C₇₊], and then this intermediate is divided into i-C₅ and n-C₆ or n-C₅ and i-C₆. Thus, high and low molecular weight components of GG are converted into medium molecular weight components. This averaging proceeds with superior formation of isomers on SZ-modified catalysts. Thus, if the ratio of n-C₅/i-C₅-C₆ for M-1 varies from 1 to 1.2, for M-2 and M-4 this ratio is small, that is, it varies from 0.06 to 0.5 (table 1). Thus, mordenite-containing composite catalysts (CC) have the ability to convert n-alkanes of GG into C₅-C₆ alkanes with a high amount of structural isomers at low temperatures. Therefore, it is of interest to study the stability of these systems. The results of the research conducted in this direction show that the stability of the composite catalytic system depends on the modification of the zeolite component with a hydrogenating element and the temperature of the sample treatment with hydrogen (fig.1).

Treatment with hydrogen in the range of 380–500°C of HMOR/10%ZrO₂ - SO₄²⁻ (6%) (M-3) catalyst, which does not contain a hydrogenating element, does not affect its stability (fig.1).

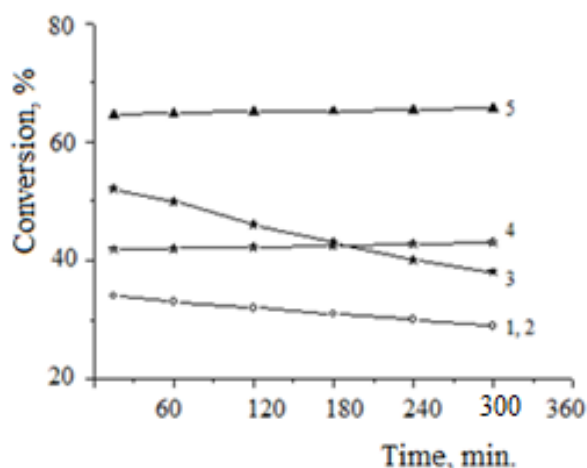


Fig. 1. The influence of the hydrogen reduction temperature of the composite catalysts on their stability in the conversion of GG. 1–M-3(380°C), 2–M-3(500°C), 3–M-4 (380°C), 4–M-4 M(500°C), 5–M-5 (380°C).

The inclusion of cobalt or nickel as a hydrogenating element in the zeolite component of the composite catalytic system has a different effect on the conversion of GG. If the introduction of nickel into the composite catalytic system allows to stabilize the performance of sample 0.4% Ni/HMOR /10%ZrO₂ - SO₄²⁻ (6%) (M-5) after pretreatment with hydrogen at 380°C (fig.1), similar treatment does not affect cobalt-containing M-4. M-4 treated with hydrogen at 380°C is similar in catalytic properties to M-3 (without metal modification). However, increasing the hydrogen treatment temperature of M-4 up to 500°C helps to increase the stability of the catalyst, but in this case its activity decreases (fig.1). Apparently, modification with these elements allows solving the problem of stable operation of CC. Studies show that the rate of CC deactivation is related to the rate of accumulation of bi- or polymolecular intermediates on the catalyst surface and is inversely proportional to their disproportionation by hydrocracking/hydrogenolysis.

List of Participants

ABROSIMOV Sergey

The Smart Materials Research Institute
at the Southern Federal University
Rostov-on-Don, Russia
sergeyabrosimoov@gmail.com

AKHMADEEV Albert

Giredmet JSC
Moscow, Russia
albertakhmadeev1@gmail.com;
t0lpar@yandex.ru

AKIMOV Albert

Institute of Petroleum Chemistry SB RAS
Tomsk, Russia
akimov149@yandex.ru

ALEKSANDROVA Natalia

Novosibirsk State Technical University
Novosibirsk, Russia
aleksandrovanatalie99@gmail.com

ALMAEVA Daria

Boreskov Institute of Catalysis
Novosibirsk, Russia
almaeva@catalysis.ru

ARKHIPOV Sergey

Novosibirsk State University
Novosibirsk, Russia
arksergey@gmail.com

ASYLKAEV Artur

Lavrentyev Institute
of Hydrodynamics of SB RAS
Novosibirsk, Russia
a.asylkaev@g.nsu.ru

AVAKYAN Leon

Southern Federal University
Rostov-on-Don, Russia
laavakyan@sfnu.ru

AYDAKOV Egor

Boreskov Institute of Catalysis
Novosibirsk, Russia
e.ajdakov@g.nsu.ru

BAKSHEEV Evgeny

Ecoalliance LLC
Novouralsk, Russia
rzmatal102@gmail.com

BELENKAYA Svetlana

State Research Center of Virology
and Biotechnology VECTOR
Novosibirsk, Russia
belenkaya.sveta@gmail.com

BOGDANOV Nikita

Boreskov Institute of Catalysis
Novosibirsk, Russia
nebo1329@gmail.com

BORISEVICH Sophia

Synchrotron Radiation Facility SKIF
Koltsovo, Russia
sophiamonrel@gmail.com

BORODIN Nikolai

Ecoalliance LLC
Novouralsk, Russia
borodin.n2000@yandex.ru

BOYKO Konstantin

Research Center of Biotechnology RAS
Moscow, Russia
kmb@inbi.ras.ru

BUKHTIYAROV Andrei

Synchrotron Radiation Facility SKIF
Novosibirsk, Russia
avb@catalysis.ru

BUKHTIYAROV Valerii

Boreskov Institute of Catalysis
Novosibirsk, Russia
vib@catalysis.ru

BULAVCHENKO Olga

Boreskov Institute of Catalysis
Novosibirsk, Russia
isizy@catalysis.ru

BULGAKOV Aleksei

The Smart Materials Research Institute
at the Southern Federal University
Rostov-on-Don, Russia
alexeybulgakov359@gmail.com

BULUSHEV Dmitri

Boreskov Institute of Catalysis
Novosibirsk, Russia
dmitri.bulushev@catalysis.ru

BULUSHEVA Lyubov

Nikolaev Institute
of Inorganic Chemistry SB RAS
Novosibirsk, Russia
bul@che.nsk.su

BURDILOV Aleksandr

Novosibirsk State Technical University
Novosibirsk, Russia
burdilov12@gmail.com

CHEREPANOVA Svetlana

Boreskov Institute of Catalysis
Novosibirsk, Russia
svch@catalysis.ru

CHETYRIN Igor

Boreskov Institute of Catalysis
Novosibirsk, Russia
chia@catalysis.ru

DEVUSHKIN Mikhail

Lavrentyev Institute
of Hydrodynamics of SB RAS
Novosibirsk, Russia
mihaildevuskin0970@gmail.com

DIUSENOVA Sabina

Novosibirsk State University
Novosibirsk, Russia
sabinadyusanova@gmail.com

DOROVATOVSKII Pavel

NRC "Kurchatov institute"
Moscow, Russia
paulgemini@mail.ru

DOVZHENKO Gleb

Synchrotron Radiation Facility SKIF
Novosibirsk, Russia
g.d.dovjenko@srf-srkif.ru

DYBTSEV Danil

Nikolaev Institute
of Inorganic Chemistry SB RAS
Novosibirsk, Russia
dan@niic.nsc.ru

DZHARKINOV Ruslan

Novosibirsk State University
Novosibirsk, Russia
r.dzharkinov@g.nsu.ru

ERMAKOVA Aleksandra

Southern Federal University
Rostov-on-Don, Russia
aleker@sfnu.ru

ESINA Tatiana

State Research Center of Virology and
Biotechnology VECTOR
Koltsovo, Russia
esina_ti@vector.nsc.ru

FEDIN Vladimir

Nikolaev Institute
of Inorganic Chemistry SB RAS
Novosibirsk, Russia
cluster@niic.nsc.ru

FEDORENKO Anastasiya

Nikolaev Institute
of Inorganic Chemistry SB RAS
Novosibirsk, Russia
fedorenko@niic.nsc.ru

FEDOROV Aleksei

Boreskov Institute of Catalysis
Novosibirsk, Russia
alexfed97@yandex.ru

FEDOSEEVA Yuliya

Nikolaev Institute
of Inorganic Chemistry SB RAS
Novosibirsk, Russia
fedoseeva@niic.nsc.ru

FILIMONOV Alexey

Peter the Great St. Petersburg
Polytechnic University
Saint Petersburg, Russia
filalex@inbox.ru

GAYDAMAKA Anna

Boreskov Institute of Catalysis
Novosibirsk, Russia
a.gaidamaka@g.nsu.ru

GERBER Evgeny

Frumkin Institute of Physical Chemistry
and Electrochemistry RAS
Moscow, Russia
chem.gerber@gmail.com

GLADYSHEVA Anastasia

State Research Center
of Virology and Biotechnology VECTOR
Koltsovo, Russia
gladysheva_av@vector.nsc.ru

GLUSHAK Anastasia

Budker Institute
of Nuclear Physics of SB RAS
Novosibirsk, Russia
aaglushak@mail.ru

GOLDENBERG Boris

Synchrotron Radiation Facility SKIF
Novosibirsk, Russia
b.g.goldenberg@srf-skif.ru

GORKUSHA Aleksandr

Novosibirsk State University
Novosibirsk, Russia
a.gorkusha@g.nsu.ru;
deepforesttt922@gmail.com

GREBENNIKOV Vladimir

M.N. Miheev Institute
of Metal Physics UB RAS
Ekaterinburg, Russia
vgrebennikov@list.ru

GUDA Alexander

The Smart Materials Research Institute
at the Southern Federal University
Rostov-on-Don, Russia
guda@sfedu.ru

GUROV Denis

Budker Institute
of Nuclear Physics of SB RAS Novosibirsk,
Russia

GUROVA Olga

Nikolaev Institute of Inorganic Chemistry SB
RAS
Novosibirsk, Russia
gurova@niic.nsc.ru

GUTOROVA Svetlana

Lomonosov Moscow State University
Moscow, Russia
svetlana.gutorova@chemistry.msu.ru

IBRAHIM Ibrahim

Novosibirsk State University
Novosibirsk, Russia
i.ibragim@g.nsu.ru

IGNATOV Mark

Novosibirsk State University
Novosibirsk, Russia
m.ignatov@g.nsu.ru

IGNATOVA Nina

Siberian Federal University
Krasnoyarsk, Russia
nyignatova@sfu-kras.ru

ILYINA Margarita

Synchrotron Radiation Facility SKIF
Novosibirsk, Russia
margarita.kondrova@yandex.ru

ISHTEEV Arthur

National University
of Science and Technology MISiS
Moscow, Russia
arturishteev@misis.ru

KAICHEV Vasily

Boreskov Institute of Catalysis
Novosibirsk, Russia
vvk@catalysis.ru

KALININA Polina

Novosibirsk State University
Novosibirsk, Russia
P.kalinina@g.nsu.ru

KARDASH Tatyana

Boreskov Institute of Catalysis
Novosibirsk, Russia
kardash@catalysis.ru

KHAINOVSKY Mark

Novosibirsk State University
Novosibirsk, Russia
interstellar.ocean@gmail.com

KHALEMENCHUK Vyacheslav

Laurentyev Institute
of Hydrodynamics of SB RAS
Novosibirsk, Russia
slava.khalemenchuk@mail.ru

KHAMETOVA Elina

Udmurt Federal Research Center UB RAS
Izhevsk, Russia
elinaphanilevna851@gmail.com

KHARCHENKO Nadezhda

Novosibirsk State University
Novosibirsk, Russia
n.kharchenko@g.nsu.ru

KHOMYAKOV Yuri

Budker Institute
of Nuclear Physics of SB RAS
Novosibirsk, Russia

KHRUSTALEV Victor

RUDN University
Moscow, Russia
khrustalev-vn@rudn.ru

KICHKAILO Anna

Federal Research Center
"Krasnoyarsk Science Center SB RAS"
Krasnoyarsk, Russia
annazamay@yandex.ru

KNYAZEV Yuriy

Kirensky Institute of Physics SB RAS
Krasnoyarsk, Russia
yuk@iph.krasn.ru

KOLOSOV Petr

Altai State University
Barnaul, Russia
petro.kolosov@gmail.com

KONDRANOVA Anastasia

Novosibirsk State University
Novosibirsk, Russia
a.kondranova@gmail.com

KONOPKINA Ekaterina

Lomonosov Moscow State University
Moscow, Russia
konopkina.kate@gmail.com;
Spinmozg-mladshiy2@list.ru

KONOVALOVA Anna

Synchrotron Radiation Facility SKIF
Novosibirsk, Russia
eliminator400@ya.ru

KONOVALOVA Valeria

Boreskov Institute of Catalysis
Novosibirsk, Russia
lekorux@gmail.com

KORNEEV Stepan

Tomsk Polytechnic University
Tomsk, Russia
stepan20019@yandex.ru

KOROTAEV Evgeniy

Nikolaev Institute
of Inorganic Chemistry SB RAS
Novosibirsk, Russia
Jodow@rambler.ru

KRASNIAKOVA Irina

The Smart Materials Research Institute
at the Southern Federal University
Rostov-on-Don, Russia
adjirina@yandex.ru

KRASNOV Pavel

Siberian Federal University
Krasnoyarsk, Russia
kpo1980@gmail.com

KRIVENTSOV Vladimir

Boreskov Institute of Catalysis
Novosibirsk, Russia
kriven@mail.ru

KROT Anna

Lomonosov Moscow State University
Moscow, Russia
Anna.d.krot@gmail.com

KUPER Konstantin

Synchrotron Radiation Facility SKIF
Novosibirsk, Russia
k.e.kuper72@gmail.com

KUZNETSOV Sergey

Prokhorov General Physics Institute RAS
Moscow, Russia
kouznetzovsv@gmail.com

KUZNETSOVA Tatyana

M.N. Miheev Institute
of Metal Physics UB RAS
Ekaterinburg, Russia
kuznetsovaups@mail.ru

LARICHEV Yurii

Boreskov Institute of Catalysis
Novosibirsk, Russia
ylarichev@gmail.com

LAVRUKHINA Svetlana

Nikolaev Institute
of Inorganic Chemistry SB RAS
Novosibirsk, Russia
x-rayspectroscopy@mail.ru

LAZARENKO Vladimir

NRC "Kurchatov institute"
Moscow, Russia
vladimir.a.lazarenko@gmail.com

LAZURENKO Daria

Novosibirsk State Technical University
Novosibirsk, Russia
pavlyukova_87@mail.ru

LEVICHEV Eugene

Synchrotron Radiation Facility SKIF
Koltsovo, Russia
e.b.levichev@inp.nsk.su

LITVINTSEVA Kseniya

Boreskov Institute of Catalysis
Novosibirsk, Russia
k.litvintseva@g.nsu.ru

LOGUNOVA Svetlana

Boreskov Institute of Catalysis
Novosibirsk, Russia
logunova@catalysis.ru

LOSEV Evgeniy

Boreskov Institute of Catalysis
Novosibirsk, Russia
losev.88@mail.ru

MALYGINA Aleksandra

Synchrotron Radiation Facility SKIF
Novosibirsk, Russia
a.b.malygina@srf-skif.ru

MAMEDOVA Malahat

Institute of Petrochemical Processes named
after Academician Yusif Mammadaliyev
Baku, Azerbaijan
memmedova-melahet@mail.ru

MARCHENKO Mikhail

Institute of Computational Mathematics and
Mathematical Geophysics SB RAS
Novosibirsk, Russia
marchenko@sscc.ru

MARCHUK Aleksandr

Boreskov Institute of Catalysis
Novosibirsk, Russia
alexander.s.marchuk@gmail.com

MARTYANOV Oleg

Boreskov Institute of Catalysis
Novosibirsk, Russia
oleg@catalysis.ru

MASS Anna

Novosibirsk State Technical University
Novosibirsk, Russia
annmass@mail.ru

MAXIMOVA Anna

Kurnakov Institute
of General and Inorganic Chemistry RAS
Moscow, Russia
mr.albatroz@yandex.ru

MIKHENKO Maxim

Boreskov Institute of Catalysis
Novosibirsk, Russia
m.mikhnenko@catalysis.ru

MISHCHENKO Denis

Synchrotron Radiation Facility SKIF
Novosibirsk, Russia
q14999@yandex.ru

MURZINA Anastasiya

Budker Institute
of Nuclear Physics of SB RAS
Novosibirsk, Russia
a.murzina@g.nsu.ru

NARANOV Evgeny

Topchiev Institute
of Petrochemical Synthesis RAS
Moscow, Russia
xek.off@gmail.com

NASENNIK Igor

Novosibirsk State Technical University
Novosibirsk, Russia
goga.mer@mail.ru

NAUMKIN Viktor

Kutateladze Institute
of Thermophysics of SB RAS
Novosibirsk, Russia
vsnaumkin@itp.nsc.ru

NESTERENKO Maria

N.S. Kurnakov Institute
of General and Inorganic Chemistry RAS
Moscow, Russia
alena.gaverment@gmail.com

NEVOLIN Iurii

Frumkin Institute of Physical Chemistry
and Electrochemistry RAS
Moscow, Russia
somonka1@gmail.com

NIKULIN Vasily

Novosibirsk State University
Novosibirsk, Russia

NISHCHAKOVA Alina

Nikolaev Institute
of Inorganic Chemistry SB RAS
Novosibirsk, Russia
nishchakova@niic.nsc.ru

NIZOVSKII Aleksandr

Boreskov Institute of Catalysis
Novosibirsk, Russia
alexniz@inbox.ru

OGNEVA Tatiana

Novosibirsk State Technical University
Novosibirsk, Russia
pandorra.06@mail.ru

PAKHARUKOVA Vera

Boreskov Institute of Catalysis
Novosibirsk, Russia
verapakh@catalysis.ru

PANAFIDIN Maxim

Synchrotron Radiation Facility SKIF
Novosibirsk, Russia
mpanafidin@catalysis.ru

PANINA Maria

N.S. Kurnakov Institute
of General and Inorganic Chemistry RAS
Moscow, Russia
maaria381@gmail.com

PENYAZKOV Oleg

A.V. Luikov Heat and Mass Transfer
Institute of NAS of Belarus
Minsk, Belarus
penyaz@dnp.itmo.by

PIROZHKOVA Aleksey

Tomsk Polytechnic University
Tomsk, Russia
alpir11260@gmail.com

PLATUNOV Mikhail

Synchrotron Radiation Facility SKIF
Koltsovo, Russia
m.s.platunov@srf-skif.ru

PLUMAN Aleksei

Lavrentyev Institute
of Hydrodynamics of SB RAS
Novosibirsk, Russia, pluman@bk.ru

POPOVA Anna

Federal Research Center
of Coal and Coal-Chemistry SB RAS
Kemerovo, Russia
h991@yandex.ru

PRIANICHNIKOV Stepan

Institute of Metallurgy UB RAS
Ekaterinburg, Russia
stepian@yandex.ru

ROLDUGIN Victor

Southern Federal University
Rostov-on-Don, Russia
roldugin.victor@gmail.com

RUBANIK Darya

Southern Federal University
Rostov-on-Don, Russia
missdare.dr@gmail.com

RUBTSOV Ivan

Synchrotron Radiation Facility SKIF
Novosibirsk, Russia
rubtsov@hydro.nsc.ru

RUD Polina

Southern Federal University
Rostov-on-Don, Russia
prud@sfedu.ru

SADOVNIKOV Aleksey

Topchiev Institute
of Petrochemical Synthesis RAS
Moscow, Russia
sadovnikov@ips.ac.ru

SARAEV Andrei

Boreskov Institute of Catalysis
Novosibirsk, Russia
asaraev@catalysis.ru

SELIVANOVA Aleksandra

Boreskov Institute of Catalysis
Novosibirsk, Russia
avselivanova@catalysis.ru

SELYUTIN Aleksandr

Boreskov Institute of Catalysis
Novosibirsk, Russia
saga111a@gmail.com

SEMUSHKINA Galina

Nikolaev Institute
of Inorganic Chemistry SB RAS
Novosibirsk, Russia
spectroscopy@mail.ru

SHARAYA Svetlana

Novosibirsk State University
Novosibirsk, Russia
s.sharaya@g.nsu.ru

SHCHERBAKOV Dmitriy

State Research Center
of Virology and Biotechnology VECTOR
Koltsovo, Russia
dshcherbakov@gmail.com

SHCHERBAKOVA Valentina

A.V. Luikov Heat and Mass Transfer
Institute of NAS of Belarus
Minsk, Belarus
valya1998@mail.ru

SHEFER Kristina

Boreskov Institute of Catalysis
Novosibirsk, Russia
shefer@catalysis.ru

SHEVTSOV Mikhail

Moscow Institute of Physics and Technology
Dolgoprudnyy, Russia
mishevtsov@googlemail.com

SNETKOV Petr

ITMO University
Saint Petersburg, Russia
ppsnetkov@itmo.ru

SNIGIREV Anatoly

Immanuel Kant Baltic
Federal University
Kaliningrad, Russia
ASnigirev@kantiana.ru

SOLOVOVA Nadezhda

Novosibirsk State University
Novosibirsk, Russia
n.solovova@g.nsu.ru

STUDENNIKOV Alexey

Synchrotron Radiation Facility SKIF
Novosibirsk, Russia
aleksei.studennikov@mail.ru

SUKHANOV Andrei

Federal Research Center
"Crystallography and Photonics" of the RAS
Moscow, Russia
sukhanov.ae15@physics.msu.ru

SUKHARINA Galina

Southern Federal University
Rostov-on-Don, Russia
gbsukharina@sfnu.ru

SUVOROVA Marina

Boreskov Institute of Catalysis
Novosibirsk, Russia
ms-suvorova@yandex.ru

SVETOGOROV Roman

NRC "Kurchatov institute"
Moscow, Russia
rdsvetov@gmail.com

SYROKVASHIN Mikhail

Nikolaev Institute
of Inorganic Chemistry SB RAS
Novosibirsk, Russia
syrokvashin@niic.nsc.ru

TITOVA Svetlana

Institute of Metallurgy UB RAS
Ekaterinburg, Russia
sgtitova@mail.ru

TOMILIN Felix

Kirensky Institute of Physics SB RAS
Krasnoyarsk, Russia
felixnt@gmail.com

TSYBULYA Sergey

Boreskov Institute of Catalysis
Novosibirsk, Russia
tsybulya@catalysis.ru

UMAROV Akmal

Lomonosov Moscow State University
Moscow, Russia
umarovakmalum@gmail.com

UTKIN Anatoly

Budker Institute of Nuclear Physics of SB RAS
Novosibirsk, Russia
a.v.utkin@inp.nsk.su

VAKHRUSHEV Sergey

Ioffe Institute
Saint Petersburg, Russia
s.vakhrushev@mail.ioffe.ru

VALEEV Rishat

Udmurt Federal Research Center UB RAS
Izhevsk, Russia
rishatvaleev@mail.ru

VANIN Konstantin

Novosibirsk State Technical University
Novosibirsk, Russia
kostell595@gmail.com

VINOKUROV Zakhar

Synchrotron Radiation Facility SKIF
Koltsovo, Russia
vinzux@mail.ru

VITOSHKIN Igor

Khristianovich Institute of Theoretical
and Applied Mechanics of SB RAS
Novosibirsk, Russia
ghatu0oosj37@mail.ru

VOLOSNIKOVA Ekaterina

State Research Center
of Virology and Biotechnology VECTOR
Koltsovo, Russia
kulenok84@mail.ru

VORFOLOMEEVA Anna

Nikolaev Institute
of Inorganic Chemistry SB RAS
Novosibirsk, Russia
vorfolomeeva@niic.nsc.ru

YAKUSHEV Ilya

N.S. Kurnakov Institute
of General and Inorganic Chemistry RAS
Moscow, Russia
cs68@mail.ru

ZABLUDA Vladimir

Kirensky Institute of Physics SB RAS
Krasnoyarsk, Russia
zvn@iph.krasn.ru

ZAGUZIN Alexander

Nikolaev Institute
of Inorganic Chemistry SB RAS
Novosibirsk, Russia
zaguzin@niic.nsc.ru

ZAKHAROV Boris

Boreskov Institute of Catalysis
Novosibirsk, Russia
b.zakharov@yahoo.com

ZAKHAROV Nikita

Federal Research Center of Coal
and Coal-Chemistry SB RAS
Kemerovo, Russia
2metil4@gmail.com

ZHARKOV Dmitry

Institute of Chemical Biology
and Fundamental Medicine
Novosibirsk, Russia
dzharkov@niboch.nsc.ru

ZHDANKIN Grigory

Novosibirsk State University
Novosibirsk, Russia
g.zhdankin@g.nsu.ru

ZOLOTAREV Konstantin

Synchrotron Radiation Facility SKIF
Koltsovo, Russia
k.v.zolotarev@srf-skif.ru

ZUBAVICHUS Yan

Synchrotron Radiation Facility SKIF
Koltsovo, Russia
yzubav@gmail.com

ZUEV Vitalii

Budker Institute
of Nuclear Physics of SB RAS
Novosibirsk, Russia

ZYURKALOVA Darya

Institute of Protein Research RAS
Puschino, Russia
dzyurkalova@yandex.ru

Content

Plenary Lectures	5
PL-1 Fedin V. Metal-Organic Frameworks: From Synthesis and Structure to Porous Materials for Separation of Hydrocarbons	7
PL-2 Svetogorov R.D. Kurchatov Synchrotron Radiation Source: Current Status, Research and Development Prospects	9
PL-3 Marchenko M. Digital Twin of the Siberian Ring Source of Photons - a Modern Tool to Support the Life Cycle of a Mega-Science Facility and Manage Big Scientific Data	11
PL-4 <u>Bukhtiyarov A.</u> , Zubavichus Y.V., Levichev E.B., Bukhtiyarov V.I. Current Status of SRF "SKIF" Project	12
PL-5 Platunov M.S. Magnetism as Seen with X-Rays	13
PL-6 Khrustalev V.N. Art in Chemistry: Cage-Like Metallasilsesquioxanes	14
PL-7 Snigirev A. Coherent X-Ray Optics and Microscopy for Advanced Material Research Applications	15
PL-8 Kuper K. Synchrotron Radiation Station "Diagnostics in the High-Energy X-Ray Range" Present and Future	17
PL-9 Zharkov D. Structural Biology in the Study of Enzymatic Catalysis: An Example of DNA Glycosylases	18
PL-10 Boyko K.M. Structure Guided Assistance in Biological Tasks	19

Oral Presentations	21
OP-1	
<u>Yakushev I.A., Smirnova N.S., Vargaftik M.N.</u> Combined Studies of Crystal Structure and Catalytic Properties of Pt and Pd-Based Heterometallics	23
OP-2	
<u>Rud P.A., Burachevskaya O.A., Gritsai M.A., Soldatov M.A.</u> XANES Investigation of Oxaliplatin Loaded Zr-MOFs for Targeted Drug Delivery	24
OP-3	
<u>Zakharov B.A.</u> Single-Crystal X-Ray Diffraction for Molecular Crystals at Synchrotron vs. Laboratory Source	26
OP-4	
<u>Bulavchenko O.A., Vinokurov Z.S., Konovalova V.P., Mishchenko D.D.</u> Application of <i>In Situ</i> XRD to Study of MnOx-CeO₂-ZrO₂ Catalysts Formation	27
OP-5	
<u>Avakyan L.A., Alexeev R.O., Firsova J.A., Shakhgildyan G.Yu., Sukharina G.B., Sigaev V.N., Bugaev L.A.</u> Middle-Range Atomic Order in Glasses of La₂O₃-Nb₂O₅-B₂O₃ and BaO-Nb₂O₅-P₂O₅ Systems	28
OP-6	
<u>Grebennikov V.I., Kuznetsova T.V.</u> Interatomic Auger Transitions End Excitations in Photoemission from Cu₂SnS₃	30
OP-7	
<u>Vakhrushev S.B., Bronwald Iu.A., Petroukhno K.A., Filimonov A.V., Raevski I.P.</u> Improper Ferrielectric Phase Transitions in the PMN-PSN Solid Solutions	32
OP-8	
<u>Pakharukova V., Kharchenko N., Vinokurov Z., Stonkus O., Saraev A., Gorlova A., Rogozhnikov V., Potemkin D.</u> Application of High-Energy X-Rays and Atomic Pair Distribution Function Analysis to Structural Diagnostics of Ni/Ce_{0.75}Zr_{0.25}O₂ Catalysts for Methanation of Carbon Oxides	33
OP-09	
<u>Lazarenko D.V., Lozanov V.V., Dovzhenko G.D.</u> Influence of Alloying Elements on the Retention of Al₁₁Ti₅ at Room Temperature	34
OP-10	
<u>Lazarenko V.A., Dorovatovskii P.V., Svetogorov R.D.</u> Current Experimental Capabilities of the “XSA/Belok” Beamline of the Kurchatov Synchrotron Radiation Source for Single Crystals X-Ray Diffraction Analysis and 2022/2023 Highlight Results	36

OP-11	
<u>Kuznetsova T.V., Grebennikov V.I., Ponomareva E.A.</u>	
Application of Resonant X-Ray Photoemission Spectroscopy for Studying the Local Electronic Characteristics of Multicomponent Functional Materials, Including Localized and Itinerant Aspects of the Behavior of f- and d-Electrons.....	37
OP-12	
<u>Gaydamaka A.A., Arkhipov S.G., Zakharov B.A., Bogdanov N.E., Rashchenko S.V., Semerikova A.I., Smirnova E.S., Ivanova A.G., Boldyreva E.V.</u>	
High Pressure and Low Temperature Study of Purine Nucleobases Salt Crystals.....	38
OP-13	
<u>Gerber E., Krot A., Chernyshev V., Trigub A., Sobolev N., Averin A., Maksimov S., Svetogorov R., Nevolin I.</u>	
Structural Investigation of Layered Ammonia Polyuranates	39
OP-14	
<u>Fedorenko A.D., Asanov I.P., Asanova T.I., Nikolenko A.D.</u>	
X-ray Absorption Spectroscopy Study on Spin-Orbit Interaction in Osmium Compounds.....	41
OP-15	
<u>Titova S.G., Yi-Ying Chin, Pei-Ci Lai, Shu lun Chang, Kuzhetsova T.V., Grebennikov V.I., Sterkhov E.V., Trigub A.L.</u>	
XMCD and XANES Study of Double Manganite NdBaMn₂O₆	42
OP-16	
<u>Gutorova S.V., Trigub A.L., Novichkov D.A., Matveev P.I.</u>	
EXAFS Study of Actinide Complexes with N,O-Donor Polydentate Ligands.....	43
OP-17	
<u>Syrovkashin M.M., Korotaev E.V.</u>	
Lanthanide-Doped Solid Solutions Based on α-MnS with Thermoelectric Properties: XANES Investigation	45
OP-18	
<u>Abrosimov S.V., Guda A.A., Guda S.A., Shapovalova S.O.</u>	
Wavelet Analysis and Machine Learning. New Methodology for XAS Spectrum Analysis.....	46
OP-19	
<u>Kardash T.Yu., Cherepanova S.V., Stonkus O.A., Ivanova A.S., Bondareva V.M.</u>	
PDF and XRD Analysis of Promoted Layered Double Ni-Al-O Catalysts for Oxidative Dehydrogenation of Propane	47
OP-20	
<u>Bulushev D.A., Golub F.S., Trubina S.V., Zvereva V.V.</u>	
Nature of Pd Sites Supported on Covalent Triazine Frameworks.....	48
OP-21	
<u>Dovzhenko G.D., Emurlaev K.I., Kutkin O.M., Burdilov A.A., Nasyrova A.K., Zverev D.A., Snigirev A.A., Bataev I.A.</u>	
2-1 “High Energy for Structural Materials Research” Beamline Concept for the Synchrotron Radiation Facility “SKIF”	50

OP-22

Kuznetsov S.V., Ermakova Yu.A., Sedov V.S., Boldyrev K.N., Batygov S.Ch., Alexandrov A.A., Drobysheva A.R., Martyanov A.K., Rezaeva A.D., Voronov V.V., Tiazhelov I.A., Tarala V.A., Vakalov D.S.

Radiation-Resistant Luminescent Diamond Composites Based on Polycrystalline Diamond with Embedded Oxide and Fluoride Nanoparticles..... 52

OP-23

Knyazev Yu.V., Kuznetsov S.V., Sedov V.S., Martyanov A.K., Tyazhelov I.A., Nikolenko A.D., Platunov M.S., Semenov S.V., Shestakov N.P.

Composite Diamond Thin Film with Embedded Fe-Based Nanoparticles 53

OP-24

Fedoseeva Yu.V., Vorfolomeeva A.A., Shlyakhova E.V., Sysoev V.I., Makarova A.A., Smirnov D.A., Bulusheva L.G., Okotrub A.V.

In situ XPS and NEXAFS Study of Halogenated Carbon for Accumulation of Alkali Metals..... 54

OP-25

Aulchenko V.M., Glushak A.A., Zhulanov V.V., Titov V.M., Shekhtman L.I.

Current Status of the Development of a One-Coordinate X-Ray Counting Detector..... 55

OP-26

Guda A., Shapovalov V., Chapek S., Bulgakov A., Soldatov A.V.

Microfluidic Systems for the In Situ X-Ray Spectral Diagnostics and Screening of Synthesis Parameters..... 56

OP-27

Borisevich S.S., Ilyina M.G., Khamitov E.M., Diusenova S.E., Belenkaya S.V., Shevtsov M.B., Borshchevskiy V.I., Kolosov P.V., Volosnikova E.A., Elchaninov V.V., Kolybalov D.S., Arkhipov S.G., Shcherbakov D.N.

Characterization of Altai Wapiti Chymosin Interaction with the Chymosin-Sensitive Region of Three Different κ -Caseins: Experimental and Modelling Studies 58

OP-28

Kichkailo A.S., Zabluda V.N., Moryachkov R.V., Tomilin F.N.

The Role of Small-Angle X-Ray Scattering and Molecular Simulations in Elucidation of Aptamers 3D Structure..... 60

OP-29

Bulgakov A.N., Krasnyakova I.O., Guda A.A., Soldatov A.V.

Microfluidic Synthesis of Vinyl Iodide..... 62

OP-30

Dorovatovskii P.V., Lazarenko V.A., Svetogorov R.D.

Experimental Beamline “Serial Macromolecular Crystallography” at 4th- Generation Synchrotron Radiation Source “SILA”..... 63

Poster Presentations	65
PP-01 <u>Akimov A.I.S.</u> , Petrenko T.V., Akimov A.S. X-Ray Studies of Nanocluster Polyoxometalate Molybdenum Compounds	67
PP-02 Aleksandrova N.S. Investigation of the Formation of a Ti-Al-Based Metal-Intermetallic Laminated (MIL) Composite during Heating Using Synchrotron Radiation	68
PP-03 Asylkaev A.M. Restoration of the Density Distribution behind the Front of a Strong Shock Wave in a Porous Medium	70
PP-04 <u>Aydakov E.E.</u> , Saraev A.A. Features of X-ray Photoelectron Spectra of Cobalt and Cobalt Oxides	71
PP-05 <u>Bogdanov N.E.</u> , Zakharov B.A., Boldyreva E.V. Effect of Hydrostatic Compression on the Structural Changes of δ-Chloropropamide	73
PP-06 <u>Bulusheva L.G.</u> , Fedoseeva Yu.V., Kotsun A.A., Okotrub A.V. Synchrotron Spectroscopy Study of the Effect of Carbon Support on the Transformation of Molybdenum Sulfides under Annealing	74
PP-07 <u>Krasniakova I.O.</u> , Nikitenko D.V., Krasnyakova T.V., Guda A.A., Mitchenko S.A. The XAS Magic to Prove Solvent-Specific Reduction of Pt^{IV} into Pt^{II} with NaI in Acetone Solution	75
PP-08 <u>Goldenberg B.G.</u> , Gusev I.S., Krupovich E.S., Legkodymov A.A., Kolmogorov Yu.P. Detection of Low-Z Elements by SR-XRF Method on the VEPP-4M Storage Ring	76
PP-09 <u>Gorkusha A.S.</u> , Cherepanova S.V., Shmakov A.N., Tsybulya S.V. Method for Estimating the Content of Planar Defects in Structures of the A_2BO_4 Type from Diffraction Data	78
PP-10 <u>Ignatova N.Y.</u> , Polyutov S.P., Kimberg V.V., Krasnov P.O., Gel'mukhanov F. Kh. A New Method for Studying Inter-Atomic Interactions Based on the Non-Linear Dispersion of the Resonances in Resonant inelastic X-Ray Scattering Map	80
PP-11 <u>Ishteev A.</u> , Konstantinova K., Saranin D. Ionizing Detectors Based on Perovskite Absorbers	81

PP-12 <u>Kalinina P.P., Zakharov B.A.</u> Effect of Temperature, Hydrostatic Pressure and Irradiation on Photosensitive Complexes [Co(NH₃)₅NO₂]XNO₃, X = Br, I and [Co(NH₃)₅NO₂]₂I₃Cl	82
PP-13 <u>Khainovsky M.A.</u> DFT-Modeling of Structural Evolution in Crystals of Organic Piezoelectrics on the Example of γ-Glycine	83
PP-14 <u>Konopkina E.A., Novichkov D.A., Trigub A.L., Matveev P.I., Borisova N.E.</u> EXAFS Spectroscopy for Establishing the Structure of Eu(III) Complexes in Solution: Advantages, Limitations, Supporting Methods	84
PP-15 <u>Korneev S.P., Syrtanov M.S.</u> In Situ XRD Synchrotron Investigation of Cr/Ta-Coated Zr-1Nb Alloy under High-Temperature Oxidation	86
PP-16 <u>Korotaev E.V., Syrokvashin M.M., Nikolenko A.D.</u> The Lanthanide Doped Chromium Disulfides CuCr_{0.99}Ln_{0.01}S₂ (Ln=La...Lu): XANES Investigation	88
PP-17 <u>Blinov S.N., Kimberg V.V., Krasnov P.O., Gelmukhanov F.Kh., Polyutov S.P.</u> Pump-Probe Spectroscopy of Vibrational Wave Packet Revival for Mapping Molecular Potentials	89
PP-18 <u>Krot A.D., Trigub A.L., Yapaskurt V.O., Tolpeshta I.I., Vlasova I.E.</u> XAS Investigation of U Local Structure in Nuclear Legacy Sites	91
PP-19 <u>Lavrukhina S.A., Fedorenko A.D., Sysoev V.I., Semushkina G.I., Okotrub A.V.</u> Study of CA(TCA)/SWCNTs Hybrid Sensor Materials by XES, NEXAFS, XPS, and Quantum Chemistry Methods.....	92
PP-20 <u>Litvintseva K.A., Chesalov Yu.A., Selivanova A.V., Saraev A.A., Kaichev V.V.</u> Mechanistic Study of Methanol Oxidation over Monolayer V₂O₅/CeO₂ and V₂O₅/TiO₂ Catalysts.....	94
PP-21 <u>Losev E.A., Zheltikova D.Ya., Boldyreva E.V.</u> Investigation of Polymorphic Transition in Carbamazepine Induced by Mechanical Treatment	95
PP-22 <u>Maximova A.D., Yakushev I.A.</u> X-Ray and Computational Studies of Platinum Acetate Polymorphs and Solvatomorphs.....	96

PP-23	
<u>Mishchenko D.D., Vinokurov Z.S., Shmakov A.N.</u>	
Unusual Lattice Parameters Behavior for $\text{La}_{1.9}\text{Ca}_{0.1}\text{NiO}_{4+\delta}$ at the Temperatures below Oxygen Loss	97
PP-24	
<u>Naranov E., Sadovnikov A., Arapova O., Guda A.</u>	
Determination of Active Sites of Ru- and Ir-Catalysts during Hydrogenation of Bio-Oils and Aromatics	99
PP-25	
<u>Nasennik I.E.</u>	
Evolution of the Structure of a Metal Wire under Tension, Observed by Synchrotron X-Ray Diffraction	101
PP-26	
<u>Nesterenko M.Yu., Panina M.V., Yakushev I.A.</u>	
Synthesis and Structural Investigation of Carboxylic Platinum-Based Complexes for Catalytical and Biological Application	102
PP-27	
<u>Nizovskii A.I., Shmakov A.N., Ligkodymov A.A., Bukhtiyarov V.I.</u>	
Phase Composition of Biomineral Objects by HARD X-Ray Diffracton Data	104
PP-28	
<u>Ogneva T.S., Emurlaev K.S., Malyutina Yu.N., Kuper K.E.</u>	
In-Situ X-Ray Synchrotron Diffraction Study of Solid–Liquid Transitions in the Structure of Al-Co-Cr-Fe-Ni High-Entropy Alloys during Heating	105
PP-29	
<u>Pirozhkov A.V., Sidelev D.V.</u>	
In Situ XRD Study of TiC Coating for HfH_x Neutron Control Rods	107
PP-30	
<u>Popova A.N., Sozinov S.A.</u>	
Structure Investigation of Carbon Materials by Synchrotron Radiation	109
PP-31	
<u>Pryanichnikov S.V., Likhacheva A.Yu., Sterkhov E.V., Sidorov V.A., Titova S.G.</u>	
High Pressure Synchrotron Study of Double Manganite $\text{NdBaMn}_2\text{O}_6$	110
PP-32	
<u>Roldugin V.A., Medvedev P.V., Gritsai M.A., Soldatov M.A.</u>	
Transition Metal Nanocomposites as a Catalyst for Hydrogen Production: Structure and Evolution Synchrotron Study	111
PP-33	
<u>Rubanik D.S., Srabionyan V.V., Vetchinnikov M.V., Durymanov V.A., Viklenko I.A., Avakyan L.A., Shakhgildyan G.Yu., Sigaev V.N., Bugaev L.A.</u>	
Local Electric Field Enhancement Around Ag Nanoparticles and their Agglomerates in Silicate and Zinc-Phosphate Glasses	113

PP-34	
<u>Rubtsov I.A., Bukhtiyarov A.V., Zubavichus Y.V., Kazantsev S.R., Kashkarov A.O., Kuper K.E., Pruel E.R., Studennikov A.A., Ten K.A., Tolochko B.P., Halemenchuk V.P., Shekhtman L.I.</u>	
Beamline for Studying Fast-Flowing Processes at the Synchrotron Radiation Facility SKIF	114
PP-35	
<u>Sadovnikov A., Naranov E., Guda A.</u>	
The <i>In-Situ</i> XAS and <i>Ex-Situ</i> XPS Studies of the Oxidation State on a RuO₂-Based Catalyst after Hydrogenation of Oxygen Containing Substances.....	115
PP-36	
<u>Semushkina G.I., Fedoseeva Y.V., Makarova A.A., Pinakov D.V., Chekhova G.N., Okotrub A.V., Bulusheva L.G.</u>	
Photochemical Degradation of Fluorinated Graphite with Embedded Nitrogen Oxides under White-Beam Synchrotron Radiation	117
PP-37	
<u>Sharaya S.S., Zakharov B.A., Boldyreva E.V.</u>	
Structural Changes in Rochelle Salt on Cooling Across the Ferroelectric Phase Transition Points.....	118
PP-38	
<u>Snetkov P.P., Morozkina S.N., Romanov A.E.</u>	
Synchrotron and X-Ray Techniques for Hyaluronic Acid-Based Nanomaterials	119
PP-39	
<u>Solovova N.Yu., Golyashov V.A., Tereshenko O.E.</u>	
ARPES Study of the Bismuth Thin Films Electronic Structure on the InAs(111)A-(2x2) Surface.....	120
PP-40	
<u>Sukharina G.B., Ermakova A.M., Ponosova E.E., Gladchenko-Jevelekis J. N., Shemetova E.I., Pryadchenko V.V., Srabionyan V.V., Avakyan L.A., Bugaev L.A.</u>	
XAFS Study of the Local Atomic Structure of Copper Centers in Cu-MOR	122
PP-41	
<u>Tomilin F.N., Artyushenko P.V., Shchugoreva I.A., Rogova, A.V., Moryachkov R.V., Zabluda V.N., Kichkailo A.S.</u>	
Molecular Simulations and Restoration of the Atomic Structure of DNA-Aptamers from SAXS Data.....	123
PP-42	
<u>Umarov A.Z., Nikitina E.A., Ivanov D.A.</u>	
New Class of Supersoft Adaptive Materials Based on Copolymers: Structural Studies with Synchrotron Radiation	124
PP-43	
<u>Gurov D.S., Zolotarev K.V., Zuev V.V., Utkin A.V., Cheskidov V.G.</u>	
Operating Modes of the UE212M Elliptical Electromagnetic Undulator for Radiation at the Station "Electronic Structure" in the SKIF Project	126

PP-44

Valeev R.G., Petkov A.A.

Structure, Morphology, Layered Chemical Composition and Magnetic Properties of Iron (Iron Oxide) Nanocoatings on the Surface of Porous Alumina Obtained by the Annealing of Magnetron Deposited Iron Films 128

PP-45

Vinokurov Z.S., Zubavichus Y.V., Shmakov A.N., Mishchenko D.D., Selyutin A.G.,
Syrtnov M.S., Gogolev A.S., Denisov V.V., Teresov A.D., Panchenko Y.N.,
Kovalsky S.S., Beskonchin K.V., Kiselev V.N., Evdokimov A.A., Andreev M.V.

**Development Status of the 1-2 Beamline “Structural Diagnostics”
at the SRF SKIF 129**

PP-46

Mamedova M.T., Tagiyev D.B., Abasov S.I., Xudiyev A.T., Chelabova K.S.

**Conjugation of the Oxidative Dehydrogenation of Ethylbenzene to Styrene with
Steam Conversion of Carbon Monoxide on a 30%Cr₂O₃/1.5%CuO/15%K₂CO₃ /Al₂O₃ Catalyst 130**

PP-47

Mamedova M.T., Abasov S.I., Agayeva S.B., Iskenderova A.A., Isayeva Y.S.,
Imanova A.A., Ibrahimzade S.V.

Isomerization of Gas Gasoline on Mordenitecontaining Composite Catalytic Systems 132

List of participants 134

Content 143

Scientific edition

**«Synchrotron Radiation Techniques for Catalysts and Functional
Materials»**

II International Conference

October 23-27, 2023, Novosibirsk, Russia

Abstracts

Editors: Prof. V.I. Bukhtiyarov, Prof. O.N. Martyanov, Ya.V. Zubavichus

Научное издание

**Использование синхротронного излучения для исследования
катализаторов и функциональных материалов**

23-27 октября 2023 года, Новосибирск, Россия

Сборник тезисов докладов

Под общей редакцией: академика В.И. Бухтиярова, д.х.н. О.Н. Мартянова,
д.х.н. Я.В. Зубавичуса

Составители: М.С. Суворова, С.С. Логунова

Компьютерная обработка: Ю.В. Климова, Т.О. Барсуков

Обложка: Е.К. Казакова

Издатель:

Федеральное государственное бюджетное учреждение науки
«Федеральный исследовательский центр «Институт катализа им. Г.К. Борескова
Сибирского отделения Российской академии наук»

630090, Новосибирск, пр-т Академика Лаврентьева, 5, ИК СО РАН

<http://catalysis.ru>

E-mail: bic@catalysis.ru Тел.: +7 383 330 67 71

Электронная версия:

Издательский отдел Института катализа СО РАН

E-mail: pub@catalysis.ru Тел.: +7 383 326 97 15

Объём: 13 МБ. Подписано к размещению: 19.10.2023.

Адрес размещения: <http://conf.nsc.ru/SRTCfM-2023/en>

Системные требования: i486; Adobe® Reader® (чтение формата PDF)

ISBN 978-5-906376-54-1



2023